Nagra
Nationale
Genossenschaft
für die Lagerung
radioaktiver Abfälle

Cédra
Société coopérative
nationale
pour l'entreposage
de déchets radioactifs

Cisra
Società cooperativa
nazionale
per l'immagazzinamento
di scorie radioattive

TECHNICAL REPORT 87-27

Final Report of the Borehole, Shaft, and Tunnel Sealing Test – Volume III: Tunnel plugging

R. Pusch
L. Börgesson
Swedish Geological Co, Sweden
G. Ramqvist
El-Tekno Co, Sweden

February 1987

Parkstrasse 23 5401 Baden/Schweiz Telephon 056/20 55 11

Nagra
Nationale
Genossenschaft
für die Lagerung
radioaktiver Abfälle

Cédra
Société coopérative
nationale
pour l'entreposage
de déchets radioactifs

Cisra
Società cooperativa
nazionale
per l'immagazzinamento
di scorie radioattive

TECHNICAL REPORT 87-27

Final Report of the Borehole, Shaft, and Tunnel Sealing Test – Volume III: Tunnel plugging

R. Pusch
L. Börgesson
Swedish Geological Co, Sweden
G. Ramqvist
El-Tekno Co, Sweden

February 1987

Parkstrasse 23 5401 Baden/Schweiz Telephon 056/20 55 11

Der vorliegende Bericht betrifft eine Studie, die für das Stripa-Projekt ausgeführt wurde. Die Autoren haben ihre eigenen Ansichten und Schlussfolgerungen dargestellt.Diese müssen nicht unbedingt mit denjenigen des Auftraggebers übereinstimmen.

Le présent rapport a été préparé pour le projet de Stripa. Les opinions et conclusions présentées sont celles des auteurs et ne correspondent pas nécessairement à ceux du client.

This report concerns a study which was conducted for the Stripa Project. The conclusions and viewpoints presented in the report are those of the authors and do not necessarily coincide with those of the client.

Das Stripa-Projekt ist ein Projekt der Nuklearagentur der OECD. Unter internationaler Beteiligung werden von 1980-86 Forschungsarbeiten in einem unterirdischen Felslabor in Schweden durchgeführt. Diese sollen die Kenntnisse auf folgenden Gebieten erweitern:
- hydrogeologische und geochemische Messungen in Bohrlöchern
- Ausbreitung des Grundwassers und Transport von Radionukliden durch Klüfte im Gestein
- Verhalten von Materialien, welche zur Verfüllung und Versiegelung von Endlagern eingesetzt werden sollen
- Methoden zur zerstörungsfreien Ortung von Störzonen im Fels

Seitens der Schweiz beteiligt sich die Nagra an diesen Untersuchungen. Die technischen Berichte aus dem Stripa-Projekt erscheinen gleichzeitig in der NTB-Serie der Nagra.

The Stripa Project is organised as an autonomous project of the Nuclear Energy Agency of the OECD. In the period from 1980-86, an international cooperative programme of investigations is being carried out in an underground rock laboratory in Sweden. The aim of the work is to improve our knowledge in the following areas:
- hydrogeological and geochemical measurement methods in boreholes
- flow of groundwater and transport of radionuclides in fissured rock
- behaviour of backfilling and sealing materials in a real geological environment
- non-destructive methods for location of disturbed zones in the rock

Switzerland is represented in the Stripa Project by Nagra and the Stripa Project technical reports appear in the Nagra NTB series.

Le projet Stripa est un projet autonome de l'Agence de l'OCDE pour l'Energie Nucléaire. Il s'agit d'un programme de recherche avec participation internationale, qui sera réalisé entre 1980 et 1986 dans un laboratoire souterrain, en Suède. Le but de ces travaux est d'améliorer et d'étendre les connaissances dans les domaines suivants:
- mesures hydrogéologiques et géochimiques dans les puits de forage
- chimie des eaux souterraines à grande profondeur
- écoulement des eaux souterraines et transport des radionucléides dans les roches fracturées
- comportement des matériaux de colmatage et de scellement des dépôt finals
- méthodes de localisation non destructive des zones de perturbation de la roche

La Suisse est représentée dans le projet Stripa par la Cédra. Les rapports techniques du projet Stripa sont publiés dans la série des rapports techniques de la Cédra (NTB).

ABSTRACT

Like the Borehole and Shaft plugging tests, the Tunnel test gave evidence of the very effective sealing power of Na bentonite. The test arrangement consisted of a 9 m long 1.5 m diameter steel tube surrounded by sand and cast in concrete plugs at each end. These plugs contained bentonite forming "O-ring" sealings at the concrete/rock interface. The test had the form of injecting water into the sand and measuring the leakage that took place through the adjacent rock and along the plug. It was concluded that the drop in leakage from more than 200 l/hour at 100 kPa water pressure early in the test to 75 l/hour at 3 MPa pressure at the end was due partly to the swelling pressure exerted by the bentonite on the rock and by penetration of bentonite into water-bearing rock fractures. The major sealing process appears to be the establishment of a very tight bentonite/rock interface.

RESUME

L'essai en tunnel, comme les essais d'obturation de trous de forage et de puits de mine, a mis en évidence les qualités d'étanchement très efficaces de la bentonite au sodium. Le dispositif d'essai consistait en un tube d'acier, d'un diamètre de 1.5 m et long de 9 m, entouré de sable et scellé à chaque extrémité par un bouchon en béton. Ces bouchons contenaient de la bentonite constituant des "joints toriques" (O-ring) destinés à assurer l'étanchéité entre le béton et la roche. L'essai consistait à injecter de l'eau dans le sable et à mesurer les fuites au travers de la roche avoisinante et le long du bouchon. On a conclu que la diminution du débit des fuites, de plus de 200 l/heure sous une pression d'eau de 100 kPa en début d'essai à 75 l/heure sous 3 MPa à la fin, était due en partie à la pression exercée sur la roche par le gonflage de la bentonite et à sa pénétration dans les fissures aquifères de la roche. Le mécanisme d'étanchement semble être dû à la formation d'une interface bentonite/roche très compacte.

ZUSAMMENFASSUNG

Aehnlich wie bei den Versiegelungsversuchen für Bohrlöcher und Schächte, zeigte auch der Tunnelversiegelungsversuch, dass Na-Bentonit sehr wirksame abdichtende Eigenschaften besitzt.

In einem Stollen wurde ein 9 m langes, im Durchmesser 1.5 m messendes Stahlrohr zentrisch installiert, mit Sand umhüllt und beidseitig mit Betonverschlüssen abgeschlossen. An der Grenzfläche Beton/Gestein wurden ringförmige Dichtungen aus Bentonit angebracht.

Während des Versuches wurde Wasser in den Sand injiziert, um die Durchlässigkeit der Bentonit-Dichtung und des Nebengesteins zu bestimmen.

Die Abnahme der abpressbaren Wassermenge von mehr als 200 l/Stunde bei 0.1 MPa bei Versuchsbeginn auf 75 l/Stunde bei 3 MPa am Versuchsende wird zum Teil auf die zunehmende Abdichtung des quellenden Bentonits, zum Teil auch auf das Eindringen des Bentonits in wasserführende Klüfte zurückgeführt.

Die beobachtete Wirksamkeit der Versiegelung ist auch auf die sehr gute Abdichtung der Grenzfläche zwischen Bentonit und Gestein zurückzuführen.

CONTENTS

SUMMARY

The presently reported test is the last one in a series of three field experiments with highly compacted bentonite as sealing component, the two earlier tests being related to borehole and shaft plugging. These experiments had already given evidence of the very effective sealing power of Na bentonite and the purpose of the Tunnel plugging test was therefore mainly to find out whether it is a practical technique also on a large scale. Also, the experiment involved exposure of the maturing bentonite to very high gradients with the aim to determine the possible risk of erosion and washing out of the clay.

The test arrangement consisted of a 9 m long and 1.5 m diameter steel tube surrounded by sand and cast in concrete plugs at each end. These plugs hosted bentonite blocks arranged in the form of "O-ring" sealings at the rock/concrete interface. This simulated a temporary sealing of a water-bearing rock zone penetrated by a tunnel in a repository, allowing for transports through the plug construction while minimizing the water inflow into the tunnel. The water pressure in the sand fill could be raised to 3 MPa and the associated leakage was accurately measured by flow meters and by collecting water that leaked from the plug. The swelling pressure exerted on the rock and on the sand fill by the expanding bentonite was measured by Gloetzl cells, and the deformation and displacement of the plug components were recorded by use of extensometers.

Predictions indicated that the leakage from the plug construction would have been about 1000 l/hour if no bentonite sealings had been applied, and that these sealings would reduce the flow to 60-600 l/hour at 3 MPa water pressure at the end of the test.

The leakage turned out to be about 200 l/hour at the application of 100 kPa water pressure early in the test but it dropped considerably in the course of the test and became 75 l/hour at 3 MPa pressure at the end of the about 20 months long test. During the 3 MPa pressure period, which lasted for about 10 months, the leakage dropped from about 200 l/hour to 75 l/hour and this very significant reduction was found to be caused by three effects. The major one was the establishment of a very tight contact between the rock surface and the bentonite,

while the flow-reducing influence of the swelling pressure on certain rock fractures and the penetration of bentonite into fractures were less important but still of some significance.

1 SCOPE OF TEST

1.1 INTRODUCTION

Long-lasting sealing is required of boreholes and shafts, which would otherwise serve as short-circuits between the biosphere and deeply located repositories. Drifts and tunnels for transportation and deposition of high level waste canisters may also require such sealings, which can suitably be constructed in the way represented by the lower bentonite plug that was investigated in the Shaft Sealing Test (1). In addition to this type of long-term plugging facilities, temporary sealing is required for those parts of tunnels and drifts which intersect richly water-bearing rock zones. If these are left open or become only partially sealed they may cause considerable flooding problems by letting much water in, and large, unwanted changes in groundwater chemistry in the construction and operative periods can also take place at these stages since the hydraulic gradients are high. The problem is to arrange the sealing so that the radial inflow from the rock is eliminated while still leaving a passage that is wide enough to permit traffic etc through the sealed section. A possible design principle would be that indicated in Fig 1-1, i.e. one with an inner casing of steel, or possibly concrete, forming the required passage, with its ends sealed off so that the clay seal is confined laterally. Such an arrangement, termed "tunnel plug", was constructed and tested in Stripa, a full report being given in this document. The size of the plug was approximately 50 % of those in real repositories, which makes the "Tunnel Sealing Test" a practically oriented study of an almost full-scaled plug version.

The sealing component of the tunnel plug was the same as that used in the Borehole and Shaft Plugging Tests, i.e. sodium-saturated dense bentonite in the form of Wyoming "Volclay MX-80" bentonite. Its mineral composition and basic physical and rheological properties have been fully described in earlier Stripa Project reports (2), to which the reader is referred for detailed information.

As in the preceding Stripa sealing tests the present study involved application of the sealing component in the form of relatively tightly arranged dense blocks of bentonite. Such blocks can be produced by compacting finely granulated Na

bentonite powder under high pressure. The bulk density of such blocks will be 2.00-2.15 t/m^3 if the compaction pressure is in the range of 50-120 MPa. The water content of the blocks will be the same as that of the powder, which is in turn determined by the humidity of the atmosphere in which it has been stored. Usually, the water content is in the interval 8-15 %, which means that the highly compacted blocks are water saturated to a degree of at least 40-50 % from the start. The huge swelling capacity of Na bentonite that is associated with water uptake means that plugs that are built up to form stacks of discrete blocks will become homogeneous and fill up a confined space completely after a sufficiently long time.

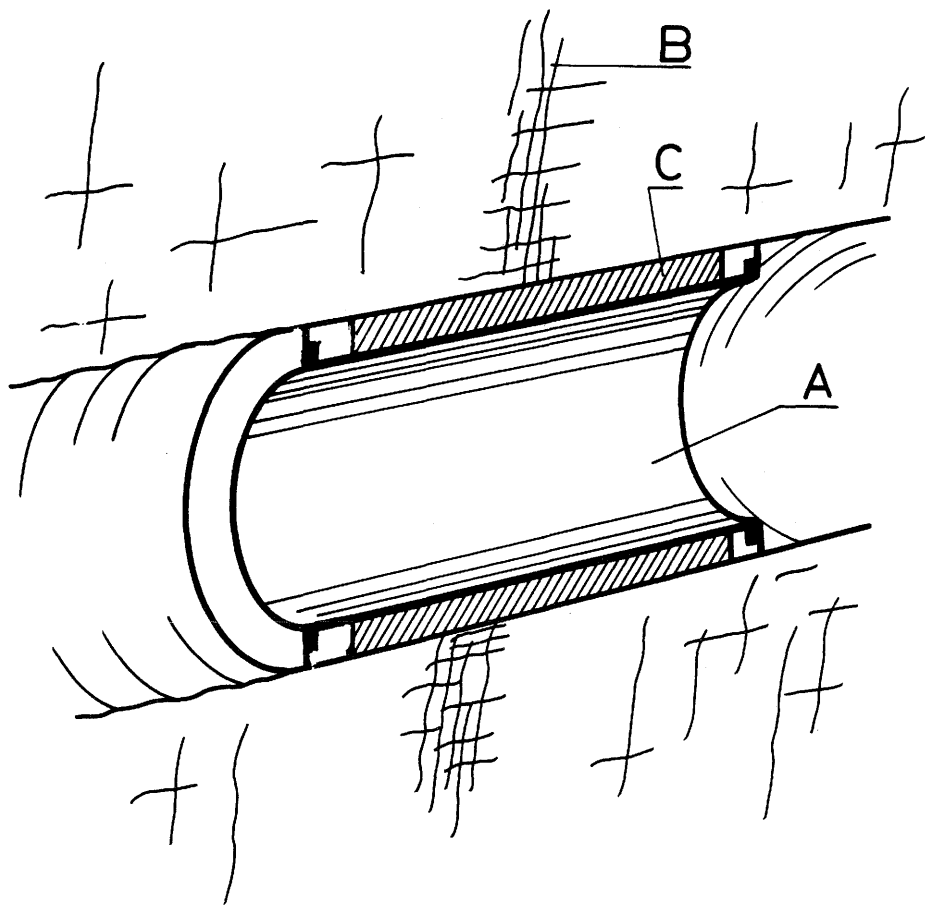

Figure 1-1. Schematic picture of tunnel plug. A) Casing, B) Strongly water-bearing rock zone, C) Dense bentonite

1.2 PLUGGING OPERATION AND FUNCTION OF THE APPLIED PLUG

In practice, the excavation of tunnels and drifts in repositories will be preceded by pilot drilling holes in the direction of the planned excavation, by which strongly water-bearing rock structures can be identified well in time to prepare for the sealing operation. When approaching such structures it may be suitable to grout the rock with smectite clay, which is sufficiently flexible to fill up fractures that may be widened as a consequence of the altered stress conditions caused by the excavation (Fig 1-2). This latter operation is preferably made by full-face drilling or very careful blasting so that the cylindrical space is produced with minimum extension of the fissured zone that is unavoidable when the latter technique is applied.

After application of the casing, which must be sufficiently long to extend into low-pervious rock, bentonite blocks are inserted to fill the space between the casing and the rock (Fig 1-3). Concrete is finally cast at the ends of the casing to support the bentonite.

The function of such a plug is that the bentonite between the casing and the rock eliminates axial flow along the plug and exerts a swelling pressure that will partly restore the initial rock stress state, thereby tending to close some of the widened fractures. It also feeds and thereby seals wide fractures with expansive clay.

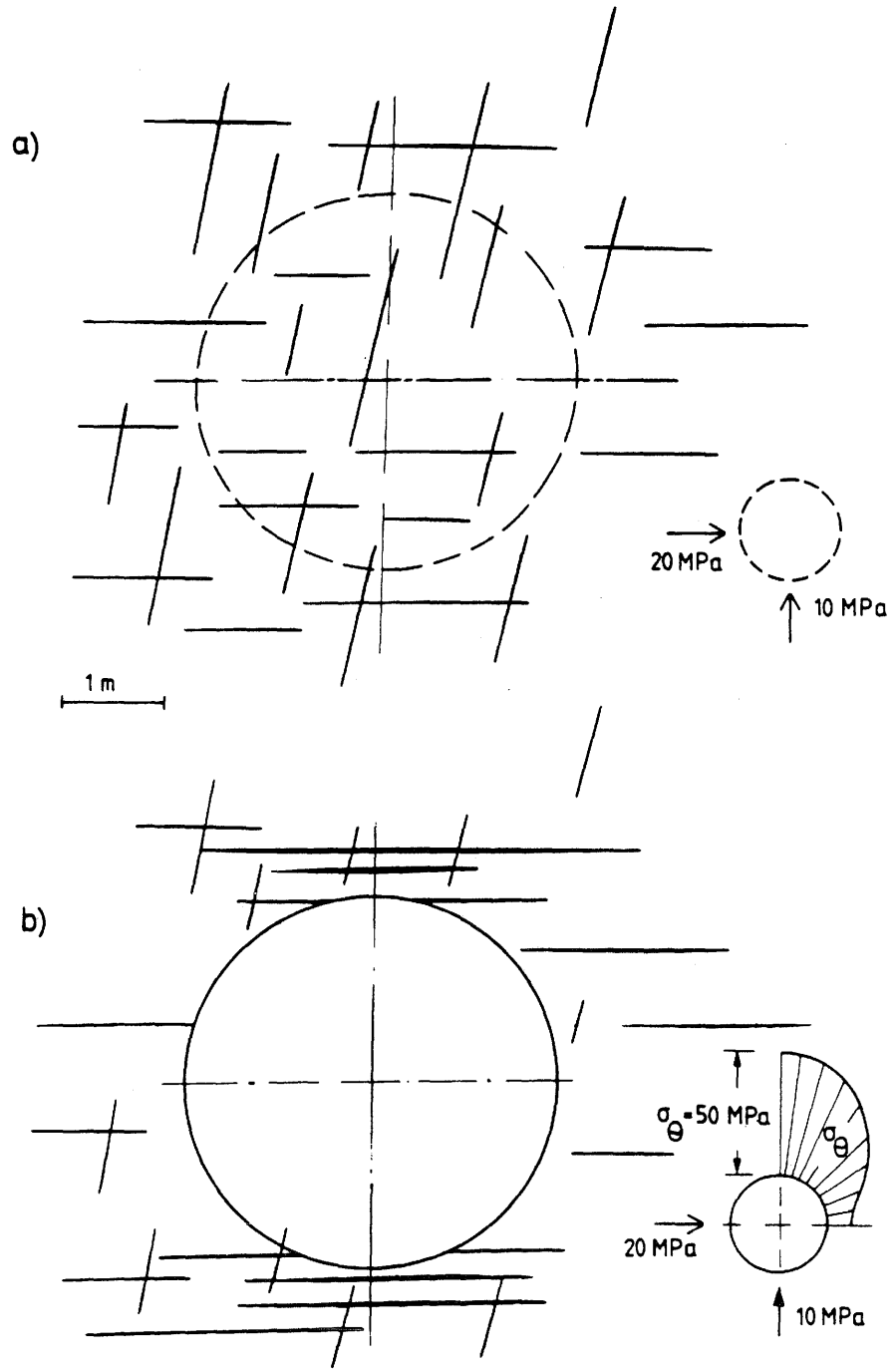

Figure 1-2. Schematic stress-induced alteration of fracture geometry. a) Initial pattern. b) Altered geometry. Notice propagation and generation of subhorizontal fractures at crown and base when the primary horizontal stress is high

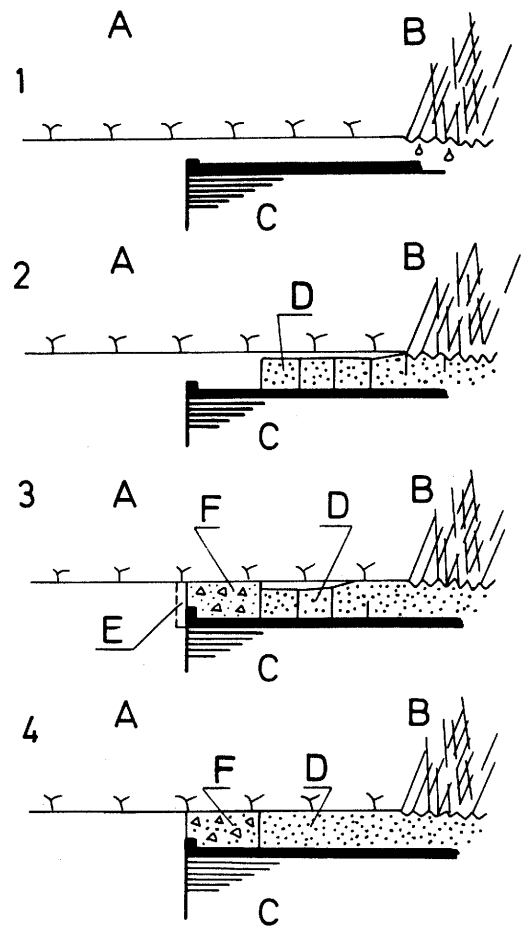

Procedure:

1 Suitable positions of plug ends are selected (fracture-poor rock, A)

2 Bentonite blocks, fragments and powder are applied between casing and rock (rapid swelling at the water-bearing zone)

3 Casting of concrete support

4 Ultimate condition with matured bentonite

Figure 1-3. Axial section of tunnel illustrating a possible procedure in plugging tunnels so that passage-through is allowed for. A) Fracture-poor rock, B) Water-bearing rock zone, C) Steel casing, D) Bentonite E) Temporary steel form, F) Concrete

1.3. SCOPE OF TESTING

In practice, tunnel plugs designed in the described way will be exposed to significant hydraulic gradients soon after their application and one of the initial objects was therefore to find a zone of strongly water-bearing rock in Stripa where the corresponding test conditions could be obtained. It turned out, however, that structures of this sort

were not available and the test was therefore conducted in tight rock where an artificial, richly water-bearing zone could be arranged around the plug. This made it possible to control the water pressure and accurately record the leakage, which was the primary object of the test.

Although the suitability of Na bentonite as sealing substance was known from preceding laboratory and field tests, a number of fundamental questions remained to be answered. Some of them can be recognized from the Shaft Plugging Test, but since the present study concerned sealing on a much larger scale, they have quite different implications. The questions are:

- Is it practical to install plugs consisting of blocks in a large tunnel with the typical irregular rock surface shape that is caused by normal blasting?

- Is the general model of uniform water uptake over the rock/clay interface that was derived from the Buffer Mass Test valid also when there is no thermal gradient?

- Will the bentonite interact with the rock so effectively that no preferential flow passages are formed at their interface also when the hydraulic gradient becomes very high soon after the construction?

- Will erosion take place and clay material be transported away from the plug by water that flows along it?

- There are at least two sealing effects that may be induced by the bentonite but it is not known whether they have any significant influence in practice. They are:

    * The swelling pressure tends to compress fractures in the rock that are subparallel to the tunnel

    * Bentonite tends to penetrate rapidly and deeply into fractures which are wider than about 1 mm, by which they become sealed

In addition to these questions, which were all answered by the test, there is also a major point concerning the chemical longevity. This matter has been dealt with in a number of earlier Stripa Project reports (cf. 1) and will not be considered here since the sealing effect is primarily intended to be of short duration.

2 DESCRIPTION OF TEST

2.1 GENERAL FEATURES

The test involved a construction phase, which served to demonstrate the practicality of the method of preparing and applying bentonite blocks on a large scale, and a testing phase which comprised measurement of the outflow of water from a central sand-filled chamber located between two ring-shaped concrete plugs with bentonite as sealing components. The plugs, which were united by a central steel casing and a number of tie-rods, confined the sand-filled, water saturated chamber into which water was injected at pressures up to 3 MPa (Fig 2-1). The plugs were equipped with pressure cells for recording the total pressures (sum of swelling pressure and water pressure) at the clay/rock, clay/sand, and clay/concrete interfaces. Strong acrylate plastic tubes extended through the plugs into the sand fill to make it possible to identify the successive displacement of the clay/sand interface caused by the expansion of the dense bentonite. At the termination of the test a very comprehensive clay sampling operation gave a detailed picture of the water uptake, thus offering a possibility of comparing the predicted water absorption and the actual one.

2.2 SITE CHARACTERIZATION

2.2.1 Location

The test was conducted in a 35 m long drift with about 11 m^2 cross section, which was blasted in March 1983 from the ramp leading down to the 410 m level (Fig 2-2). The test drift is W/E-oriented and located approximately on the 380 m level. It was given a slight dip towards the ramp for drainage purposes.

The length of the drift was determined by the requirement that the major part of the approximately 9 m long plug should be located in homogeneous, fracture-poor rock. This led to a final length of the drift of about 35 m because it was intersected by several diabase intrusions which were assumed to have an imperfect contact with the host rock. The test site was found to be suitable after making inflow tests in a 37 m long, centrally located Ø 76 mm pilot hole.

The shape and geometry of the blasted drift was carefully determined by laser-based measuring techniques so that accurate calculation of the volume of the tested part of the drift could be made, and so that a basis for detailed design of the plug arrangement was obtained. A characteristic cross section is shown in Fig 2-3.

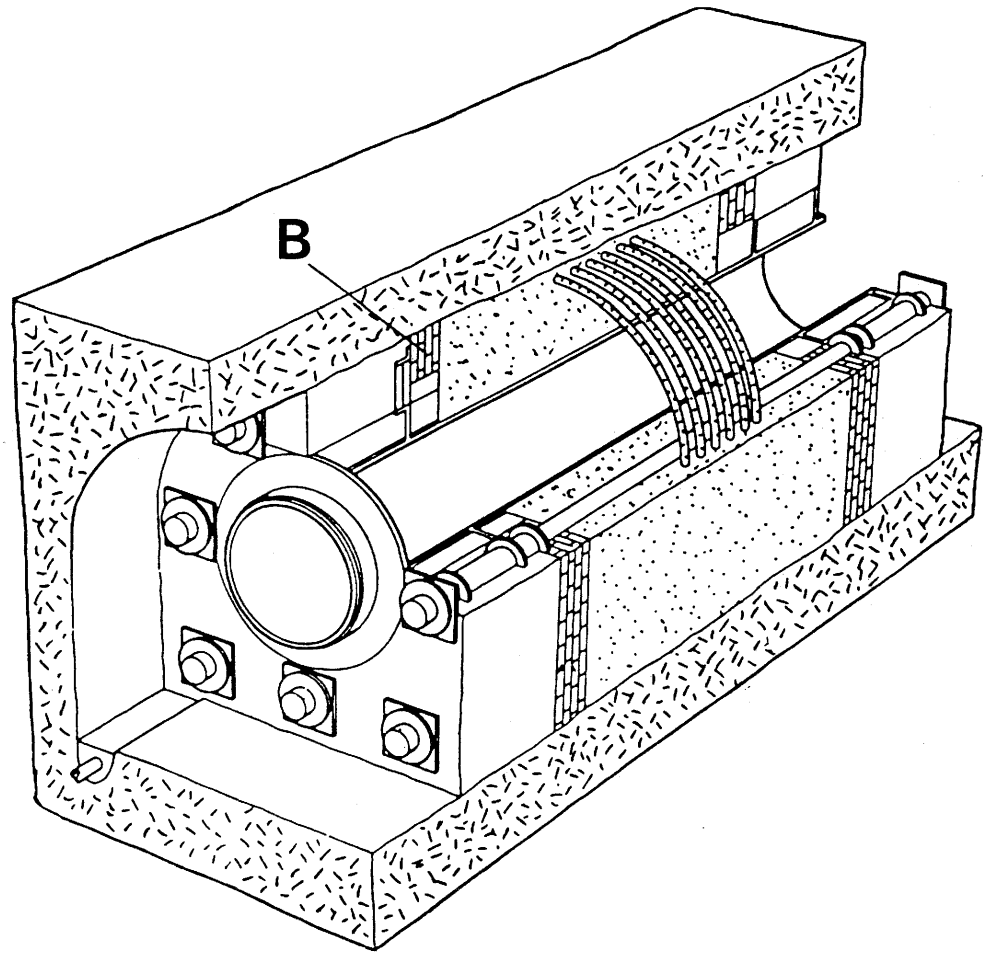

Figure 2-1. General view of the test arrangement with the central steel casing and tie-rods passing through the concrete plugs with bentonite sealings (B) at the ends, and the sand-filled chamber, which simulates a richly water-bearing rock zone

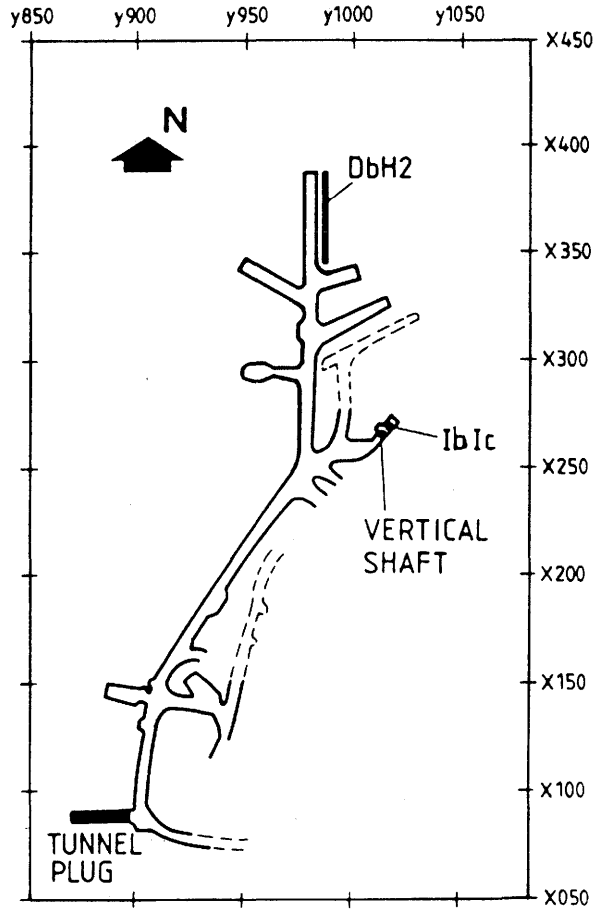

Figure 2-2. Location of the Tunnel Plug Test in relation to the Vertical Plug Test and the Borehole Plugging Tests (DbH2 and Ib and Ic)

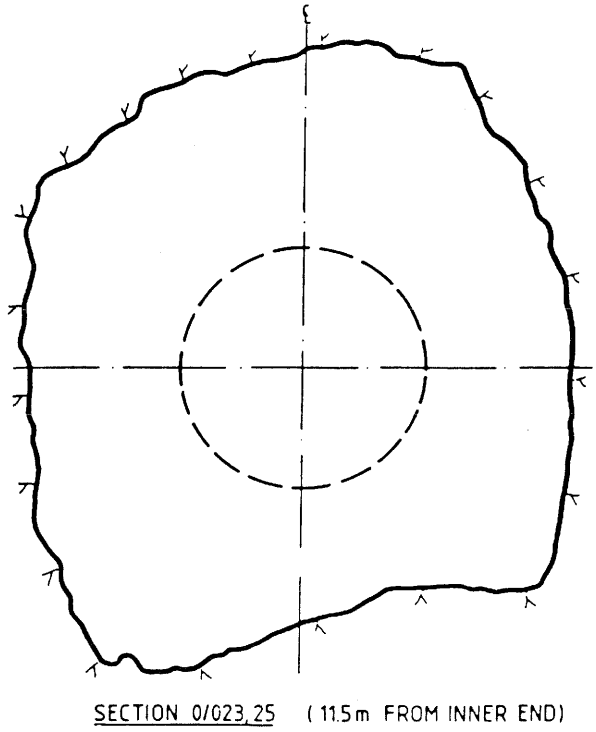

Figure 2-3. Characteristic cross section of the drift where the experiment took place

2.3 ROCK CONDITIONS

2.3.1 Fracture characteristics, major structures

The core from the Ø 76 mm pilot hole drilled axially through the center of the planned test drift illustrated the general character of the rock at the test site (Fig 2-4). The fracture log showed the presence of a set of diabase intrusions and rather wide pegmatite dikes, and these features were essential for the location of the tunnel plug. Thus, the granite/diabase contacts were assumed to represent potential leaks of major importance and so were the pegmatite dikes, which appeared to be rather porous. In the excavated tunnel the contact between the diabase dikes and the host rock appeared to be relatively tight, with the possible exception of the inner, wide diabase structure, while the pegmatite zones turned out to leak significant amounts of water. Positions adjacent to the inner diabase dike and the outer, largest pegmatite structure were therefore selected as suitable positions of the plug units, in order to create conditions for critical evaluation of the sealing ability of the bentonite.

The granite was of the type that is common in the whole northern part of the mine, i.e. a relatively fine-grained grey/reddish matrix with quartz, microcline and plagioclase as major constituents, and chlorite, muscovite, biotite and epidote as accessory minerals.

The exposed rock at the plug site was mapped with respect to the appearance of joints and fractures. Their frequency was found to be low and their apertures small indicating a characteristically high quality of the granite and minimum damage by the blasting. The major sets are the following:

- Strike N60° - N90°W, Dip 80° to the north
- Strike N20° - N40°E, Dip 80° to the east
- Strike N-S, Vertical

Fracture fillings are mainly calcite, chlorite and quartz.

The topography of the blasted rock surface became very irregular, which is characteristic of homogeneous granitic rock with fractures of limited extension. It was assumed and later confirmed by coring that the blasting had caused considerable disturbance in the form of a significantly increased frequency of fissures and slightly widened apertures of preexisting fractures in a zone which is estimated to extend a few decimeters from the rock surface (cf Fig 2-5).

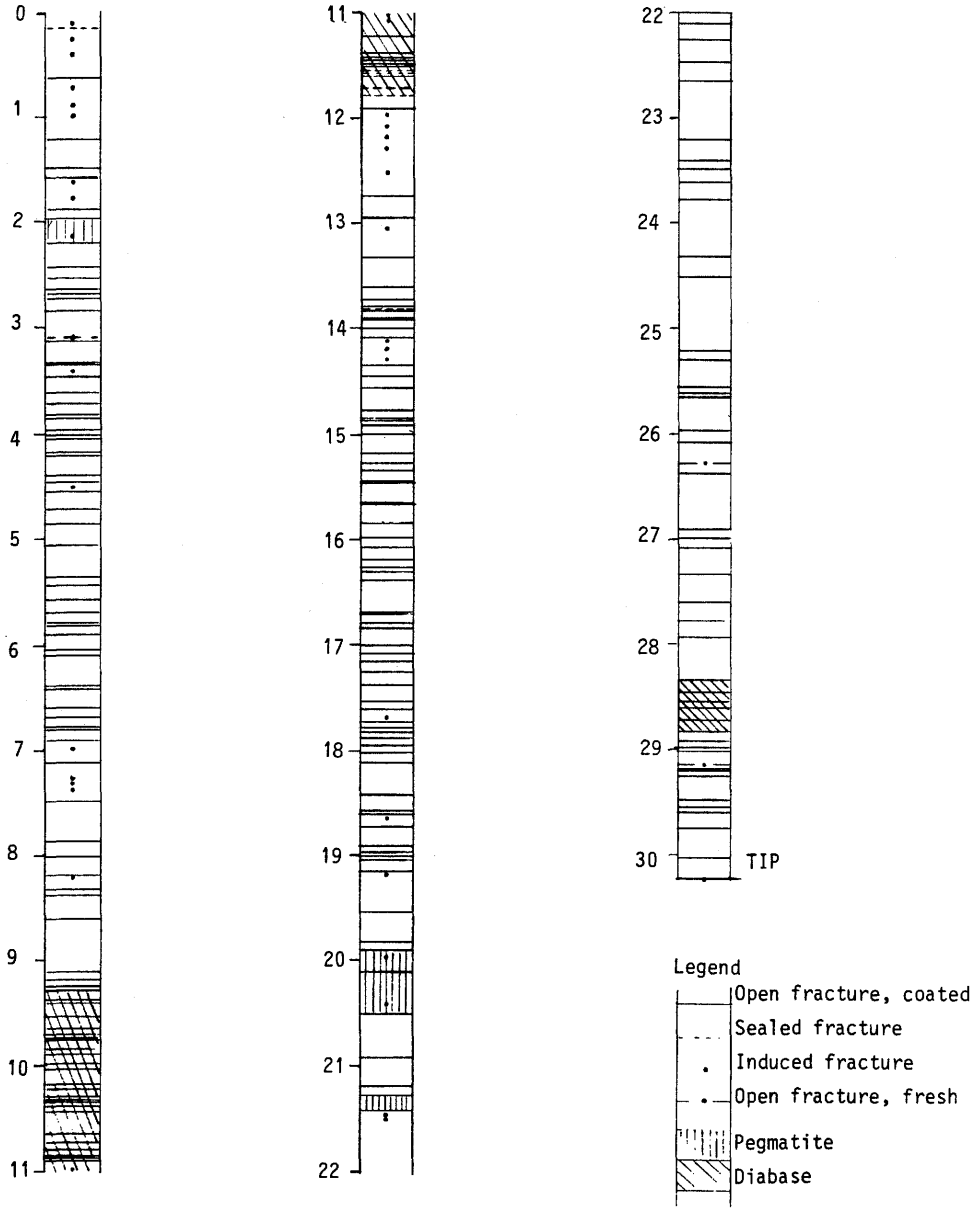

Figure 2-4. Core log of the Ø 76 mm pilot hole. Figures denote the distance from the outer end

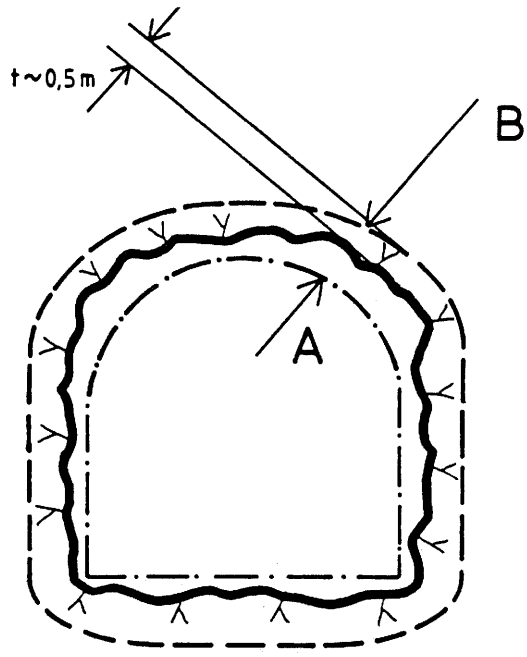

Figure 2-5. Schematic cross section of the drift with estimated zone of disturbance by blasting. A denotes theoretical section, B the outer boundary of the zone which is structurally affected by the blasting

The previously mentioned diabase and pegmatic dikes were assumed to represent potential leaching structures of particular interest for the present test and they were therefore carefully mapped. The location of the tunnel plug was chosen so as to interfere with the major pegmatite zone and the inner diabase dike in the way shown in Figs 2-6 and 2-7.

2.3.2 Rock stresses

Rock stresses were not measured at this test site but the rather large distance to neighboring drifts and shafts would suggest that the local primary stress field is not very different from the general conditions in the granite mass of which the values in the Buffer Mass Test area are taken to be representative:

- Major principal stress oriented W/E, about 20 MPa
- Intermediate principal stress, oriented N/S, about 10 MPa
- Minor principal stress, oriented vertically, about 4 MPa

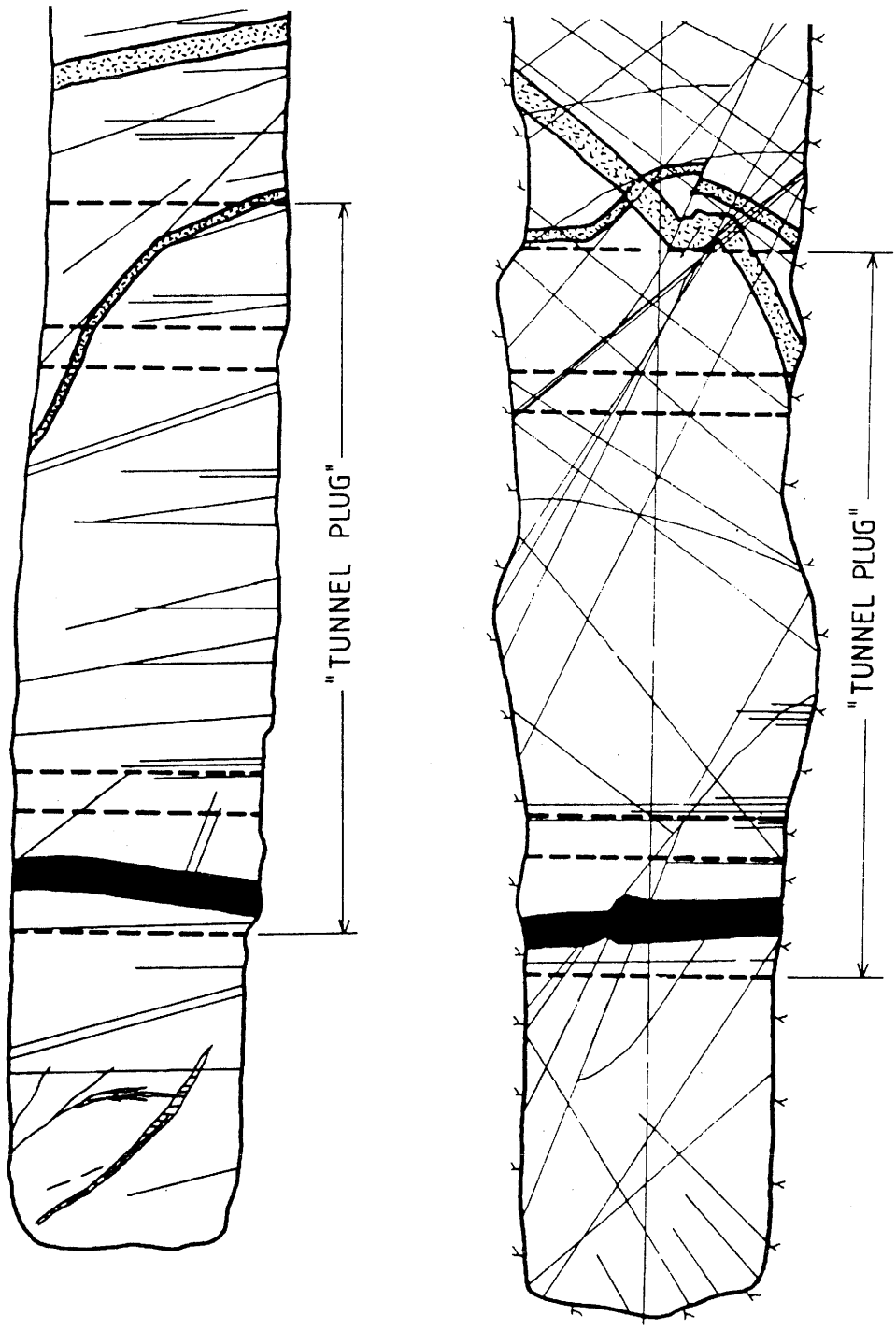

Figure 2-6. Joints and fractures in the northern wall (left) and the floor (right) of the plugged part of the drift. Dark areas represent diabase, dotted areas are pegmatite. The finally selected position of the plug construction is indicated

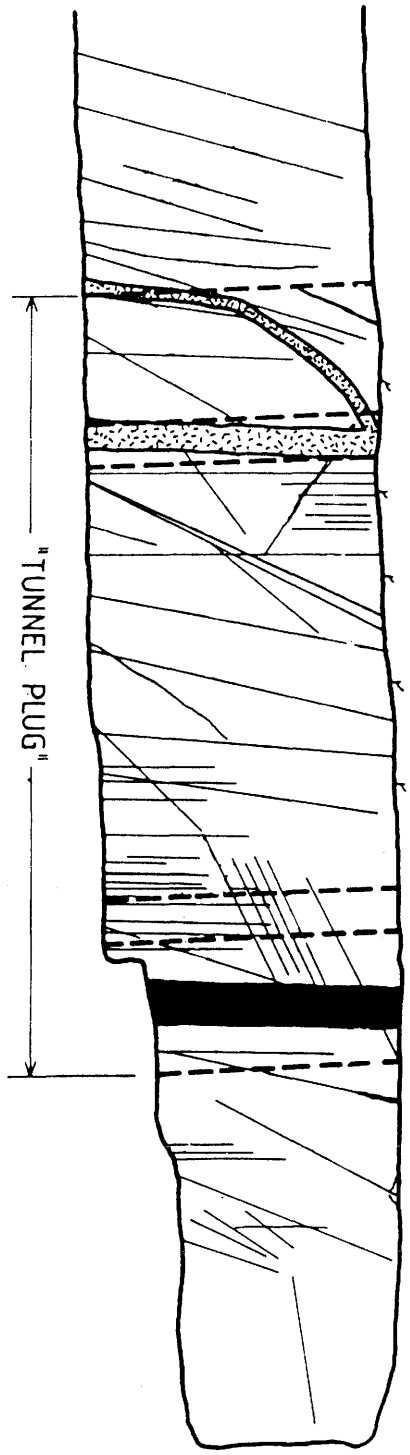

Figure 2-7. Joints and fractures in the southern wall of the plugged part of the drift

It is probable, however, that the minor principal stress is higher by at least 30-50 % because of the significant distance to disturbing excavations and because of the set of stiff, stress-absorbing diabase dikes. This yields a relatively isotropic stress field resulting in effective tangential compressive stresses on the order of 10-20 MPa at 1 to 2 meters distance from the rock surface at the crown and floor of the tunnel. Closer to the free surface of the tunnel the stresses are considerably lower.

2.3.3 Hydrological conditions

The piezometric head at the test site was estimated at 1-1.5 MPa before the excavation started and these initial pressure conditions were assumed to be preserved at more than 3-5 m distance from the tunnel periphery throughout the test. Within about 1 m distance the pressure had probably dropped to less than 500 kPa before the test started, as concluded from the Buffer Mass Test and the DbH2 borehole sealing test (3).

Before deciding the exact location of the tunnel plug components, a detailed fracture mapping was made with special respect to the main water-bearing structures, the result being shown in Figs 2-8--2-14. It was concluded that the major pegmatite zone was the dominant pervious rock structure, but that a relatively small number of discrete fractures did also transfer much water into the tunnel. With the location of the plugs indicated in the fracture maps, strong leakage from the injection chamber was expected to take place through the outer pegmatite zone along the upper part of the outer plug, and through the major fractures in the floor and walls of the rock. Fig 2-15 gives a detailed picture of the latter potential flow paths with the indicated position of the outer plug. No strongly water-bearing structures were identified at the inner plug with the exception of the non-complete contact between the inner diabase dike and the granite. At least 70-80 % of the outflow from the injection chamber was therefore assumed to take place at the outer plug.

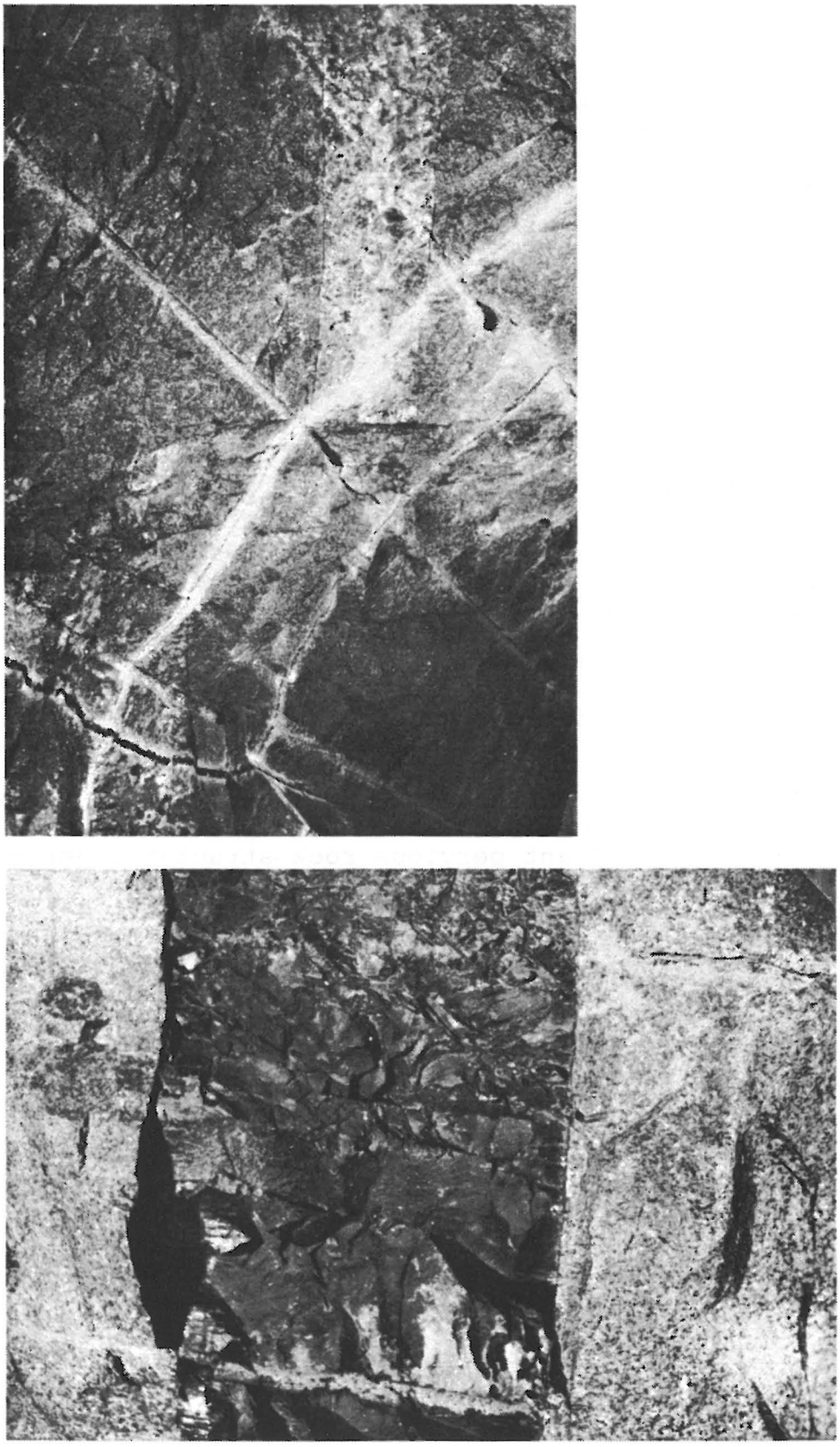

Figure 2-8. The major potential seeping structures were the coarse-grained pegmatite at the outer end of the tunnel plug (upper) and the diabase/granite contact at the inner end

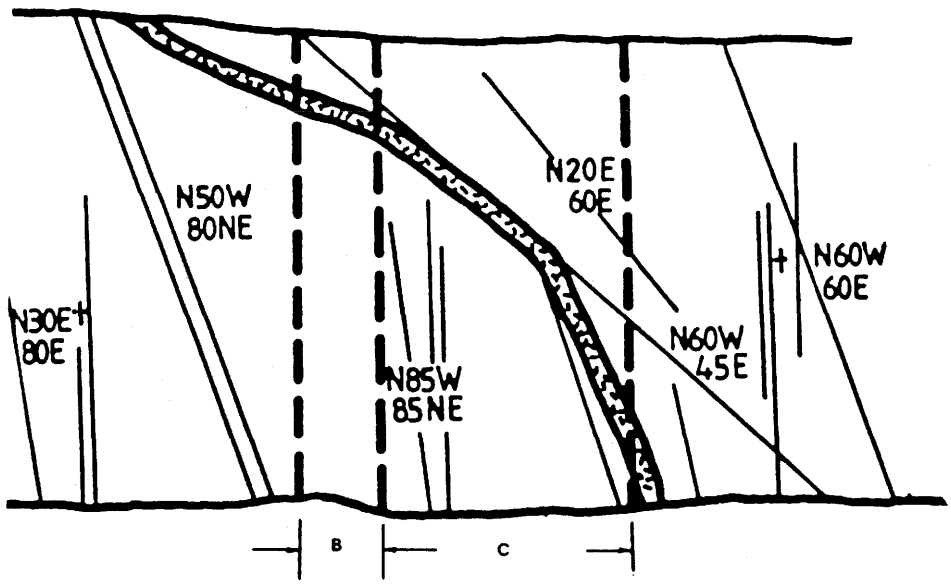

Figure 2-9 Water-bearing rock structures of the northern wall at the outer plug. Dotted area is pegmatite. B denotes position of bentonite sealing. C denotes concrete part of the plug

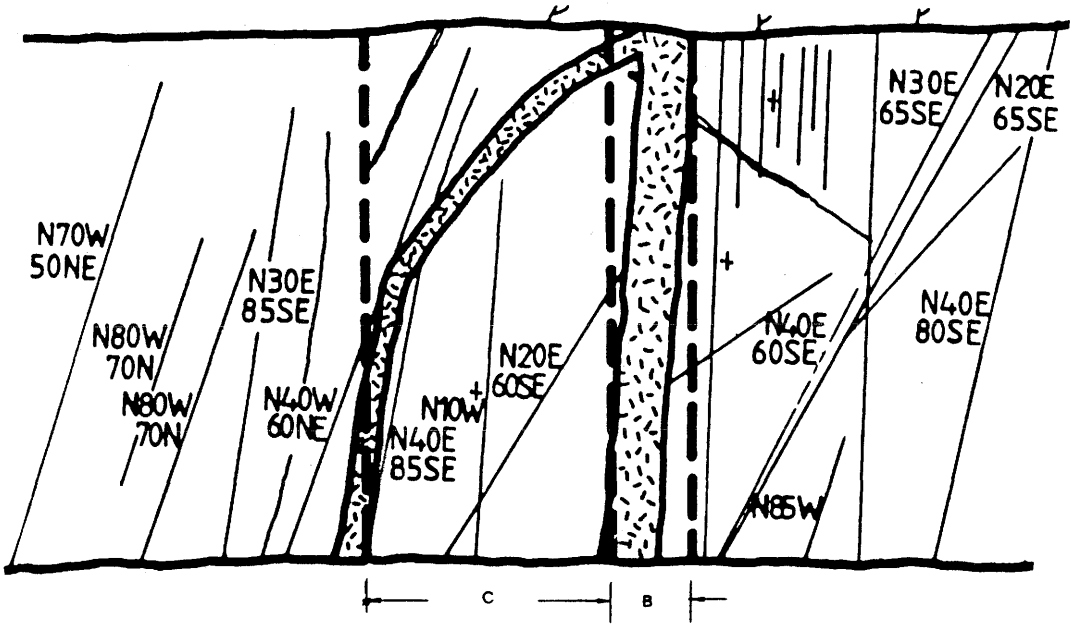

Figure 2-10. Water-bearing rock structures of the southern wall at the outer plug. Symbols same as in Fig 2-9

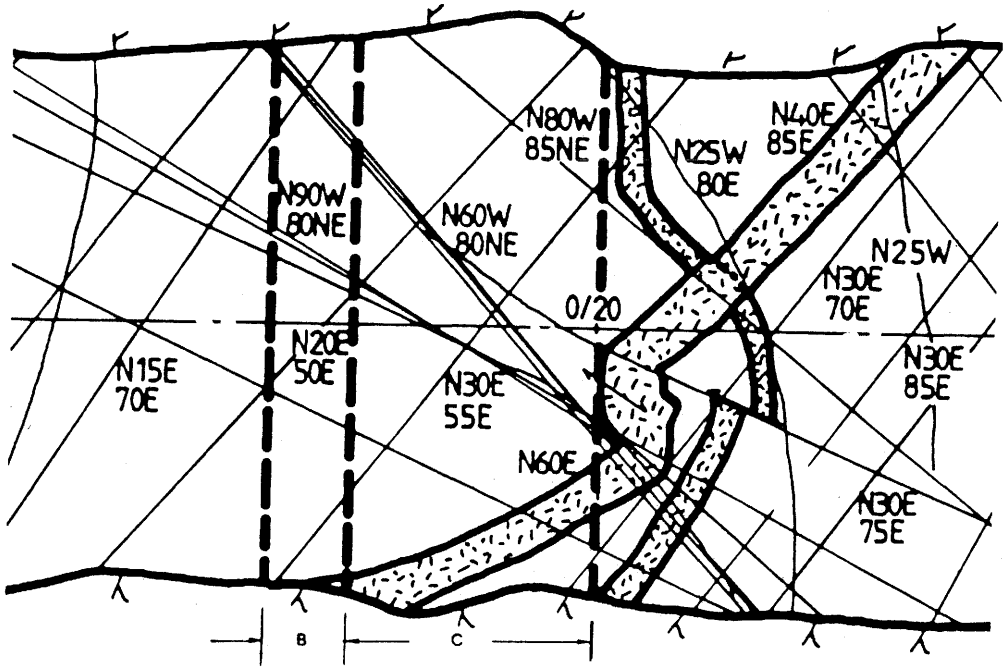

Figure 2-11. Water-bearing rock structures of the floor at the outer plug. Symbols same as in Fig 2-9

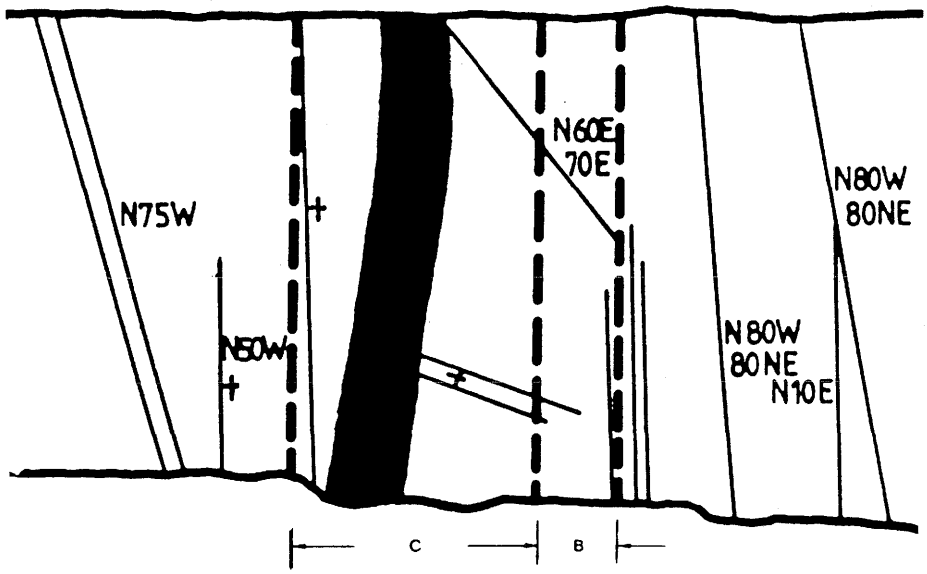

Figure 2-12. Water-bearing rock structures of the northern wall at the inner plug. Dark area is diabase, other symbols being those in Fig 2-9

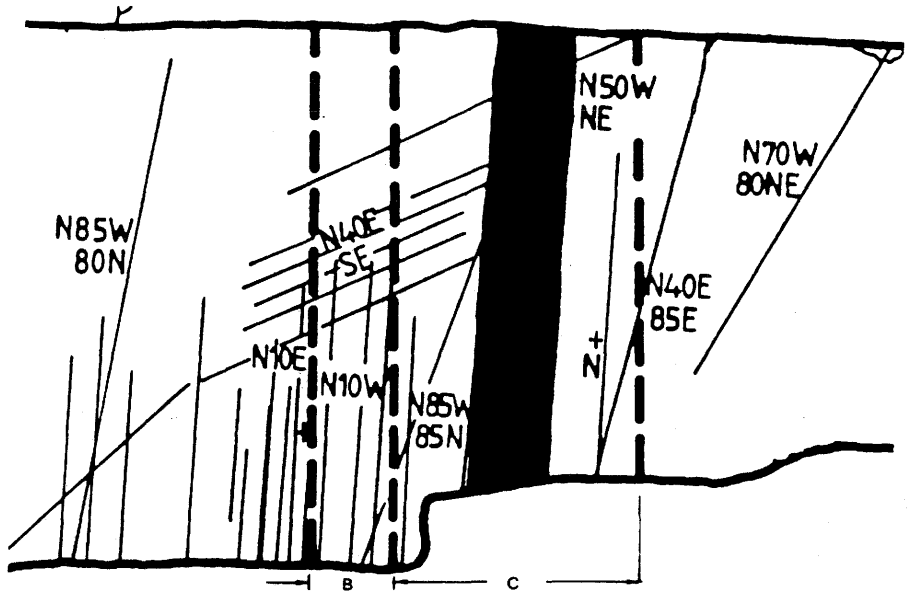

Figure 2-13. Water-bearing rock structures of the southern wall at the inner plug. Symbols same as in Fig 2-12

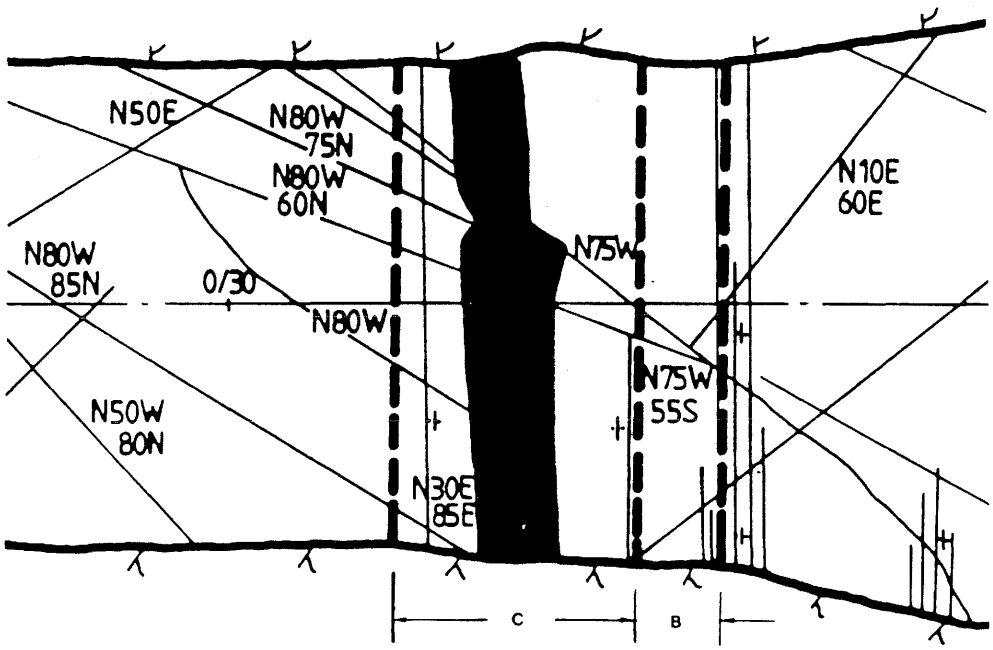

Figure 2-14. Water-bearing rock structures of the floor at the inner plug. Symbols same as in Fig 2-12

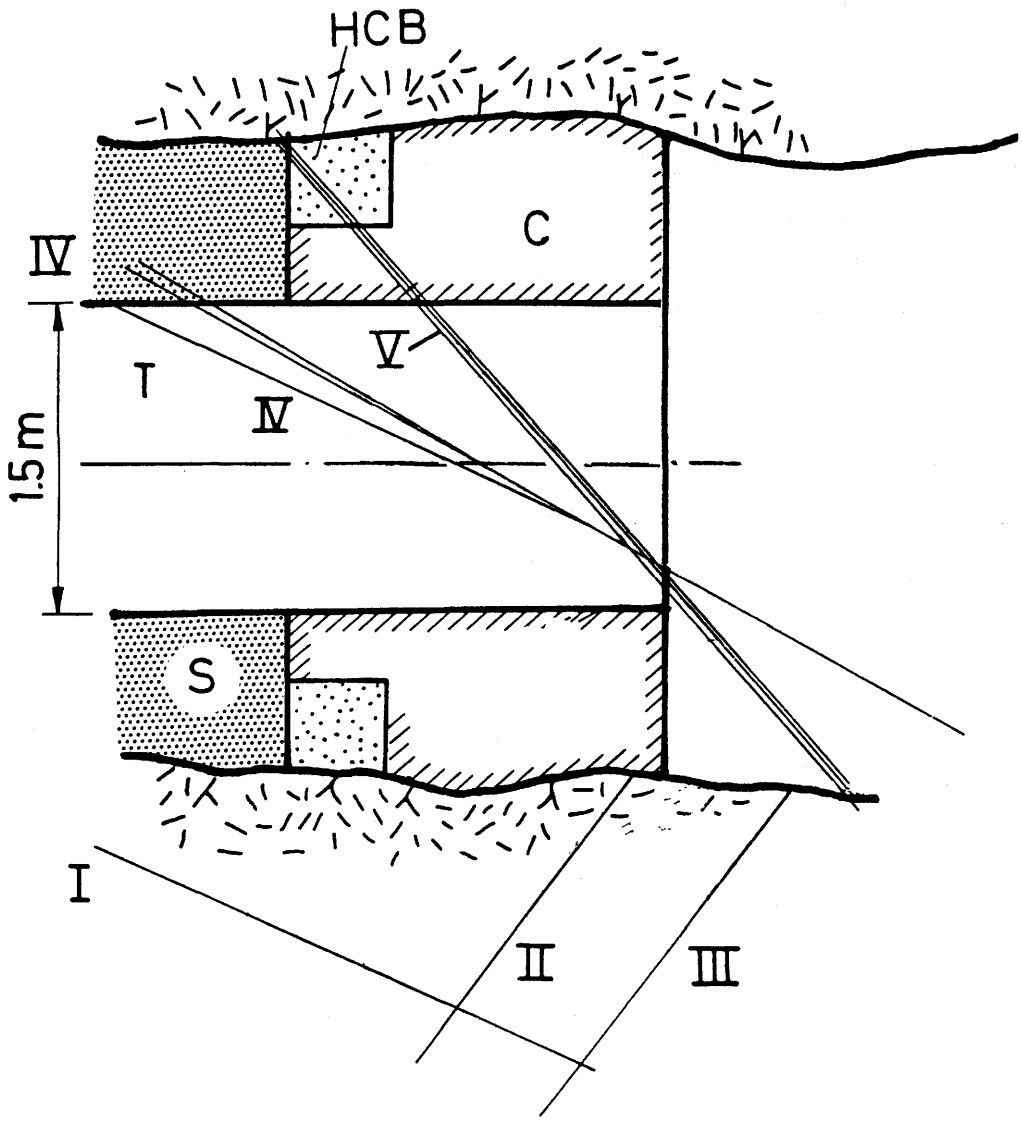

Figure 2-15. Dominant water-bearing fractures at the outer end of the tunnel plug, all being steeply oriented. C represents concrete, HCB highly compacted bentonite and T the steel casing. S is the sand-filled injection chamber

2.4 TEST ARRANGEMENT

2.4.1 General

The test required quite comprehensive construction operations to arrive at the arrangement with two 1.5 m thick concrete plugs with bentonite blocks inserted in recesses to form "O-ring" sealings, and with the almost 10 tons heavy central steel casing and the seven tie-rods that kept the plugs together (Fig 2-1). Like in the Buffer Mass Test, the transportation of building materials down in the mine and from the main shaft to the test site required careful planning and considerable time. However, no significant delay was caused and no unforeseen difficulties appeared. The construction part of the test set-up took about one half year and, as had been foreseen, required most of the budgeted money. The involved activities are specified in Table 1-1. A set of major drawings used in the construction work are shown in Appendices 1-4.

Table 1-1. Major operations in the plug construction

Activity	Start	End
Planning, design	Nov 1982	Feb 1983
Pilote drilling, inflow measurements, location of plugs	Feb 1983	Feb 1983
Blasting of drift	Mar 1983	May 1983
Form, reinforcement and casting of inner wall	Nov 1983	Jan 1984
Form, reinforcement and casting of outer wall	Jan 1984	Feb 1984
Construction of casing	Dec 1983	Mar 1984
Preparation of bentonite blocks	Nov 1983	Mar 1984
Sand filling	Mar 1984	Apr 1984
1:st prestressing of tie-rods	Apr 1984	Apr 1984
2:nd prestressing of tie-rods	Oct 1984	Oct 1984

The water injection system had to be designed so that the pressure could be controlled and kept constant at any level up to 3 MPa, with a pump capacity of at least 50 liters per minute and with precision flow measurement facilities. Since the injection and flow measurement were the key

operations that had to be very reliable, much effort was put in selecting safe techniques and durable components. The ones used in the tests turned out to operate well and can be recommended for this kind of test installations.

The cross section of the plug site was given asymmetric shape (cf. Fig 2-3) to permit drainage from the inner space during the sand-filling operation in which much water was infiltrated. The drainage had the form of a ditch that was discharged through a pipe which passed through the outer plug and which was equipped with a valve. During the test, drainage of water from the saturated sandfill through the tube was of course prevented.

The finally selected position and general features of the plug construction are shown in Fig 2-16.

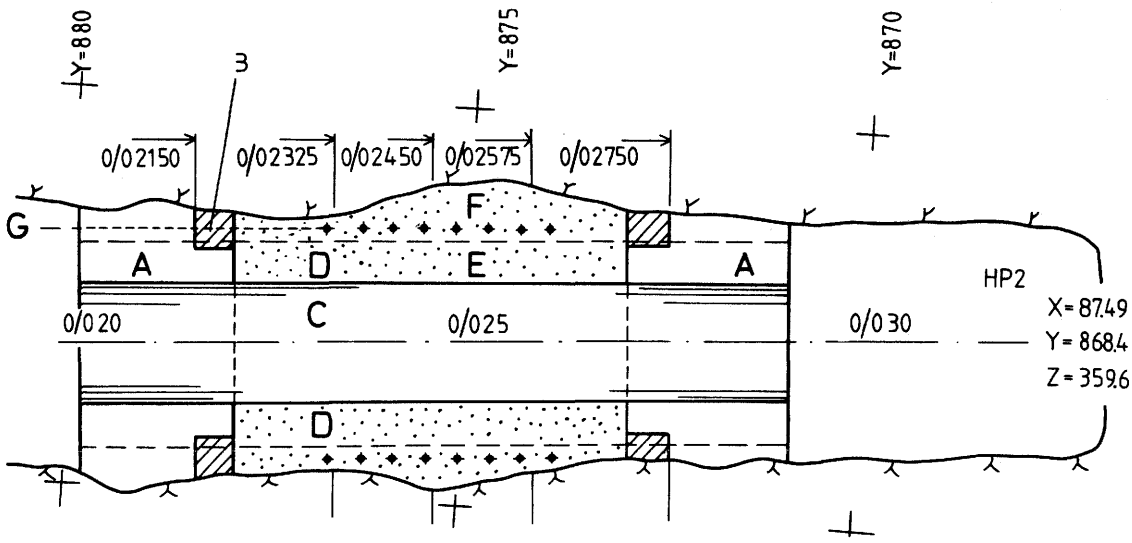

Figure 2-16. Layout of plug construction. A) concrete plugs, B) bentonite blocks placed in recesses, C) Steel casing, D) Tie-rods, E) Sand-filled injection chamber, F) Pipe gallery, G) Injected water from pump installation

2.4.2 Plug design and construction

The design of the steel components was based on the assumption that the water pressure in the injection chamber could be as high as 3 MPa in certain test phases and that the expected swelling pressure would rise to about 3 MPa in the approximately 20 months long testing period. This would yield pressures producing a total axial force of about 7000 tons tending to separate the two plug members.

The applied statical operation principle was to minimize the axial displacement of the concrete plugs during the pressure build-up by mobilizing tension in the central casing and the tie-rods, so that the rock contacting the concrete would not be exposed to significant stress changes. This was considered to be essential to the flow test because large plug movements would induce rock strain and changes in fracture apertures which could alter the hydraulic conductivity of the rock adjacent to the plugs in a way that might mask the sealing effect of the bentonite and be totally irrelevant to the study. Relatively fixed plug positions were expected by prestressing tie-rods located in casings that passed through the plugs and the sandfill.

The seven tie-rods consisted of 37 Ø15 mm units which were individually prestressed by a hydraulic jack so that each tie-rod was loaded to 200 ton tension force in a first sequence and later to 450 tons. At the end of the first prestressing the water pressure would only be 1 MPa and the swelling pressure insignificant, meaning that the prestressing force would almost balance the expansive force caused by the water pressure. For the later part of the test with fully developed internal pressure, it was assumed that the steel casing would take the net load of the prestressed tie-rods and the water and swelling pressures,i.e. about 3850 tons. The calculated maximum axial deformation of the casing was estimated at about ±9 mm in the course of the test, the plus and minus signs referring to the contraction caused by the second prestressing, and to the expansion caused by complete build-up of internal pressures, respectively. Taking the strain to occur symmetrically, the outer ends of the casing would be displaced by ±4.5 mm at maximum. This strain represents the maximum possible displacement of the concrete plugs provided that the plugs would behave as perfectly rigid bodies with slip at the rock/concrete interface. The expected shrinkage of the hardening concrete was assumed to result in relatively poor interaction between rock and concrete, and thus in easy slip. Changes in axial loads of the plug construction and associated strain were therefore not assumed to affect the hydraulic conductivity of the rock adjacent to the plug.

Despite the fact that the compressive stress in the steel rose to almost 150 MPa in certain test phases, there was no risk of buckling of the casing because of its insignificant excentricity.

It was essential to avoid leakage through the concrete and along the interface between the casing and the concrete. The concrete, which had a cube compressive strength of at least 40 MPa, was therefore heavily reinforced to make the plugs so strong that significant fractures would not be produced (cf. Fig 2-17), and the casing was equipped with flanges extending into the concrete in order to increase the flow path length and thereby to minimize leakage along the steel/concrete interface.

The irregular rock surface made the form-work difficult and tedious and the application of all the extra components for testing purposes, like tie-rod casings and observation tubes, made the construction period much longer than under similar conditions in a repository.

The large central casing, which had a thickness of 35 mm, was constructed down in the mine and applied in one piece. Certain weldings were checked by X-ray testing and appeared to be homogeneous. Late in the test it turned out, however, that slight leakage took place through four of them.

The detailed design of the concrete and steel components of the plugs was made by Jacobson & Widmark, Luleå and Stockholm. The construction of the steel units was made by Gävle Varv AB, Gävle, while the construction and prestressing of the tie-rods was made by Stabilator AB, Stockholm.

2.4.3 Bentonite sealing

Bentonite blocks with cubical shape and 200 mm side length were applied to form a relatively tight pattern in the recesses of the concrete plugs. This space was design so as to give the bentonite annulus a quadratic cross section with a side length of 0.5 m. Small bentonite fragments from crushed blocks and bentonite powder were used to fill the space between the regular sets of blocks and the irregular rock surface. This led to local variations in homogeneity in the early part of the test, as would also be characteristic of this kind of plugs in real repositories with blasted tunnels.

The bentonite blocks were prepared from larger units that were left over from the Buffer Mass Test. They had been produced by compacting Volclay MX-80 bentonite powder with an initial water content of 10-13 %, which yielded a bulk density of

2.07-2.14 t/m^3. The blocks appeared to have retained their physical state due to tightly fitting plastic covers but a slight reduction of the water content down to about 8-9 % had taken place in a few instances.

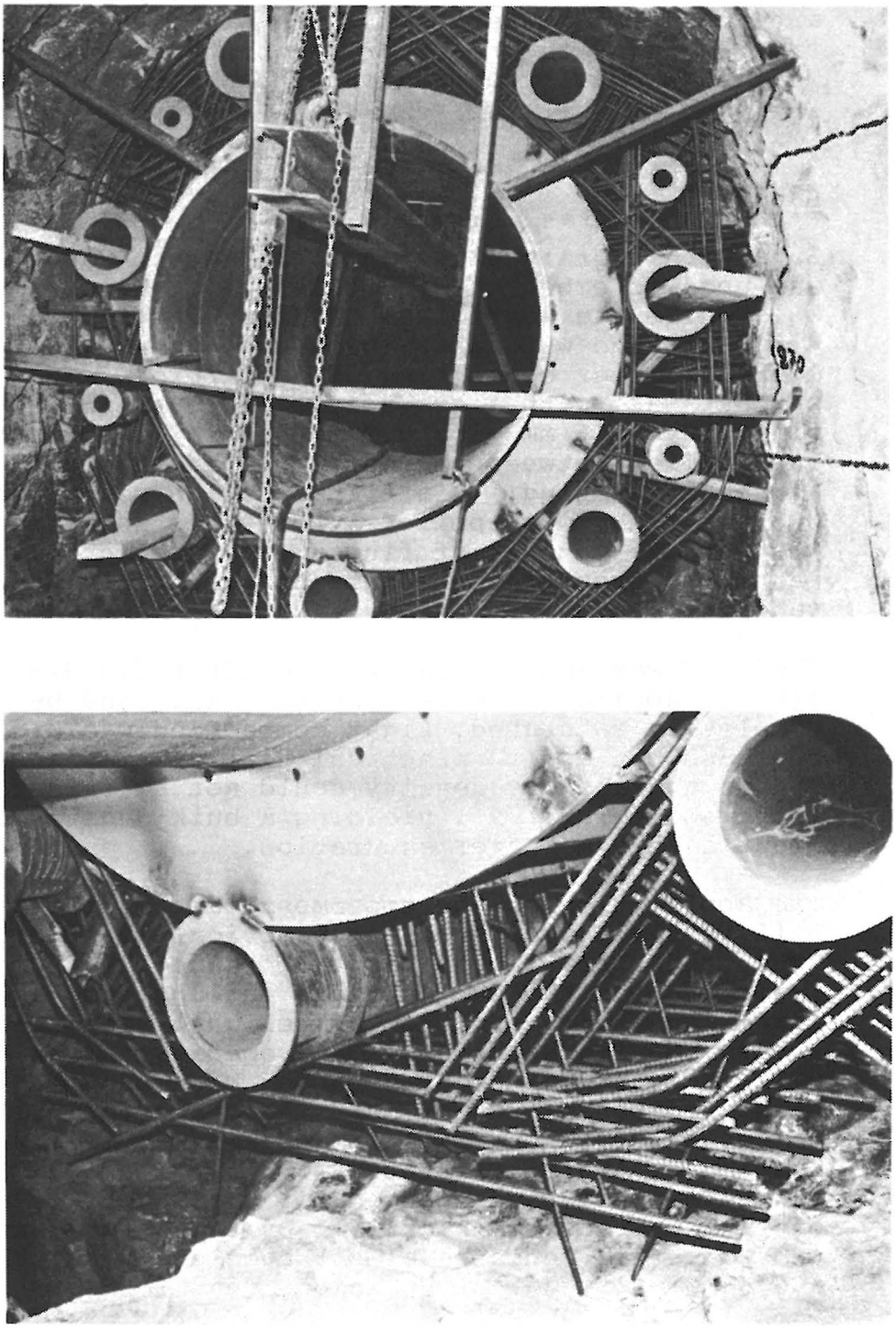

Figure 2-17. Photographs illustrating the reinforcement of the concrete plugs as it appeared before the form was applied

The total amount of bentonite blocks at the outer plug was 5515 kg and 5710 kg at the inner plug, while the amount of bentonite block fragments and powder was 1140 kg at the outer and 1055 kg at the inner plug. The total amount of bentonite was about 13400 kg.

It was estimated that the average net bulk density after complete water saturation would be about 2.0 t/m^3 in the larger part of the bentonite sealing. This bulk density corresponds to a water content of 26 %.

2.4.4 Sandfill

Sand with a grain size ranging between 4 and 8 mm was used to embed the injection pipe gallery (13965 kg), while the rest of the chamber was filled with 47800 kg sand with a grain sand of 0.6-2 mm. A 0.3 m thick filter consisting of a mixture of 78 weight percent sand with a grain size of 0.6-2 mm and 22 % finer than 0.6 mm with 0.2 mm as minimum diameter, was applied between the bentonite and the sand fill at the inner plug. This filter, which contained 3680 kg sand, was applied in order to investigate whether the content of fines would prevent clay particles from the bentonite to penetrate into the sandfill.

The sand was applied layer-wise after flooding the already applied material, so that the sand became completely saturated. Light compaction was made of the sand but due to practical difficulties in doing so the average dry density could not be raised above about 1.2 t/m^3, yielding a bulk density of about 1.75 t/m^3 after saturation.

The application of the uppermost part of the sandfill involved some foreseen practical difficulties. Thus, this backfilling had to be made by one man lying flat on the wet sand and putting chunks of almost saturated sand to form slightly inclined layers. Moving back to a small opening in the outer wall, through which the sand had been brought in, he had reasonable control of the degree of filling up the space. The very last part was formed by casting a plug of reinforced concrete through which valve-equipped pipes passed for complete saturation of this part of the backfill. By this procedure the sand backfill could be almost completely saturated and no significant air cushions were formed.

Figures 2-18--2-21 show characteristic sections through the plugs and the injection chamber with the casing for the tie-rods and the acrylate tubes used for inspection of the displacement of the bentonite/sand interface. The complex irregular

shape of the recesses for the bentonite was chosen in order to get approximately the same net density of the matured bentonite around the entire tunnel periphery.

The detailed design including careful planning of application of the bentonite and sand was made in cooperation with Jacobson & Widmark, Luleå. Gustavsson & Ericsson AB, Storå, was the construction company.

2.4.5 Water injection system

Safely operating water injection and flow measurement systems were of course essential to the test and much effort was put in the design of accurate pressure control facilities. Fig 2-22 shows the circuit diagram of the pump system. The function was, in principle, that pressurized water was pumped at a constant rate through the circuit to which the injection chamber was connected. Thereby, the excess water, i.e. the amount of water that was not injected in the sandfill, flowed through the circuit and thereby cooled the pumps. The pumps were fed with ordinary mine water that was stored in a small concrete pool, the excess water being discharged back to the pool, which was continuously percolated by fresh mine water to keep the temperature low and constant (10-12°C). In the first stage of the test when pressures lower than about 1 MPa were required, the tap water system of the mine was used. Fig 2-23 illustrates the water injection system.

The pressure of the injected water was controlled by a transducer-operated valve of type Micro Pak PN 250 (Nordiska Armaturfabriken, Stockholm), which also recorded the pressure in digital form. A precision manometer was used as a backup, the current recording of the water pressure being obtained through Gloetzl pressure cells which were located in the sand fill (see below). The system was programmed to log and store the recorded pressure values at time intervals ranging from a few hours to 1 day using the data acquisition system that was established for the Buffer Mass Test (BMT), (4).

The high pressure pumps were of type KSB MOVI v 32/6, driven by 11 kW 1EC 160 M 380/660 V electric engines. They had a capacity of 1 liter per second at 1.5 MPa differential pressure and 2910 r/m (C.A. Mörck, Gothenburg).

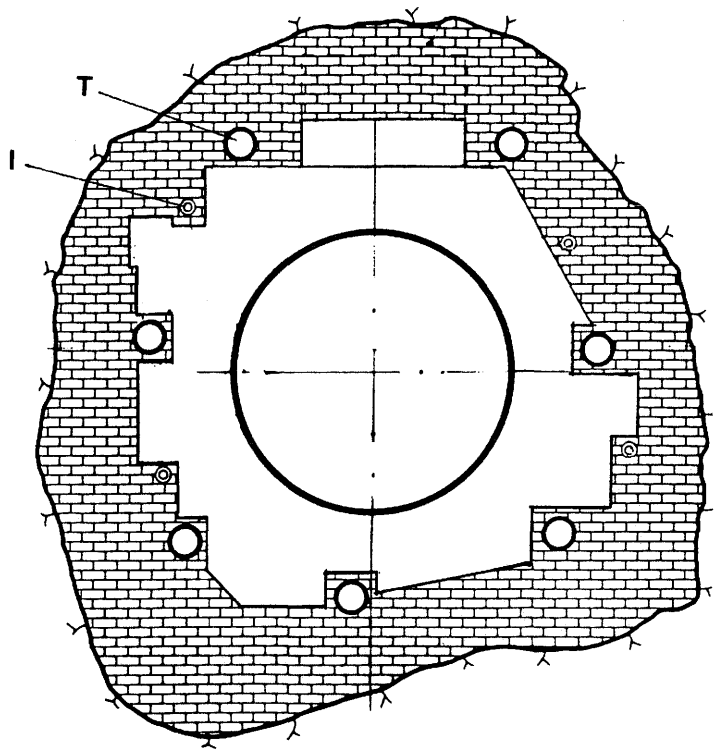

Figure 2-18. Actual shape of the cross section through the bentonite (brickwork) at the outer plug. T indicate the casings of the tie-rods, while I represent the plexiglass inspection tubes

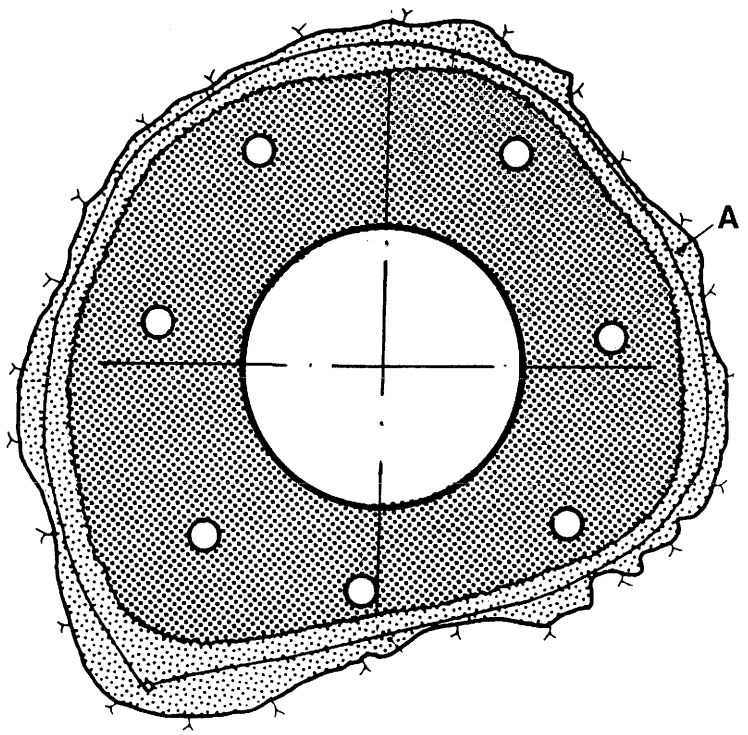

Figure 2-19. Actual shape of the cross section through the injection pipe gallery with the coarse sand (A) surrounding the pipes

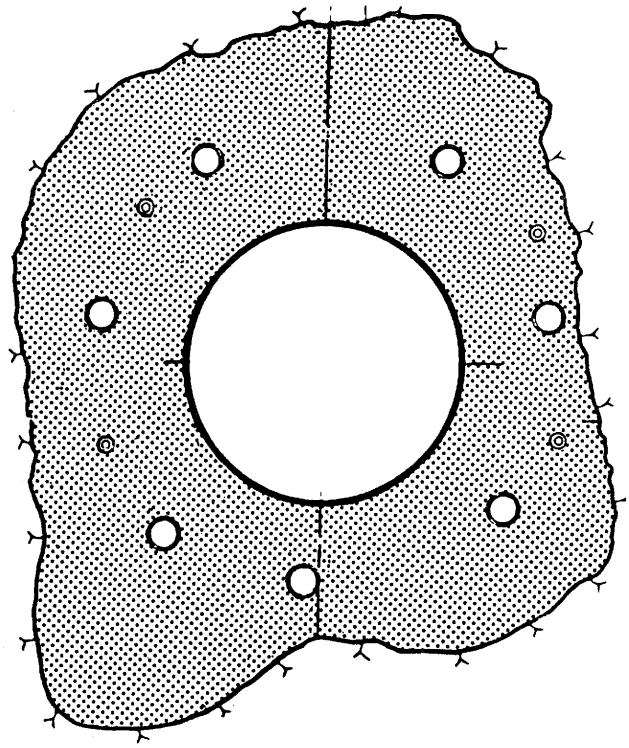

Figure 2-20. Actual shape of the cross section through the sand just outside the inner plug

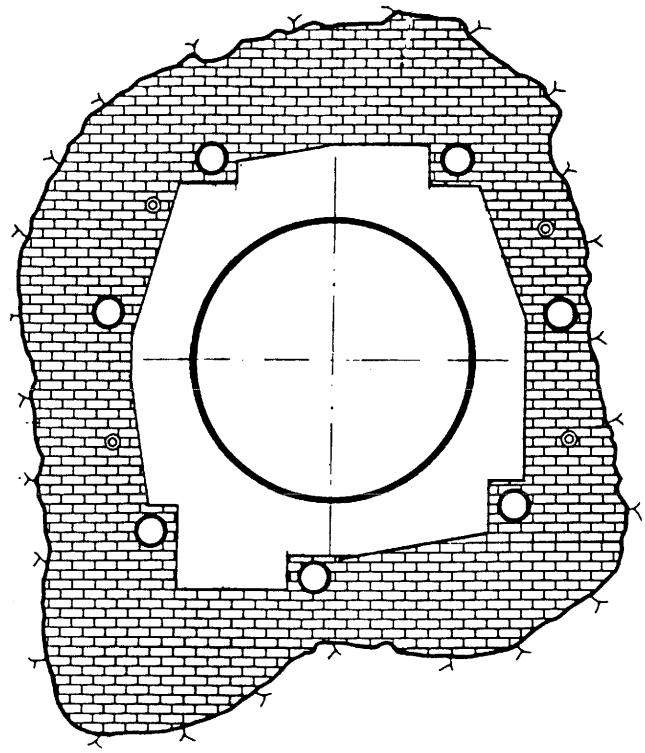

Figure 2-21. Actual shape of the cross section through the bentonite at the inner plug

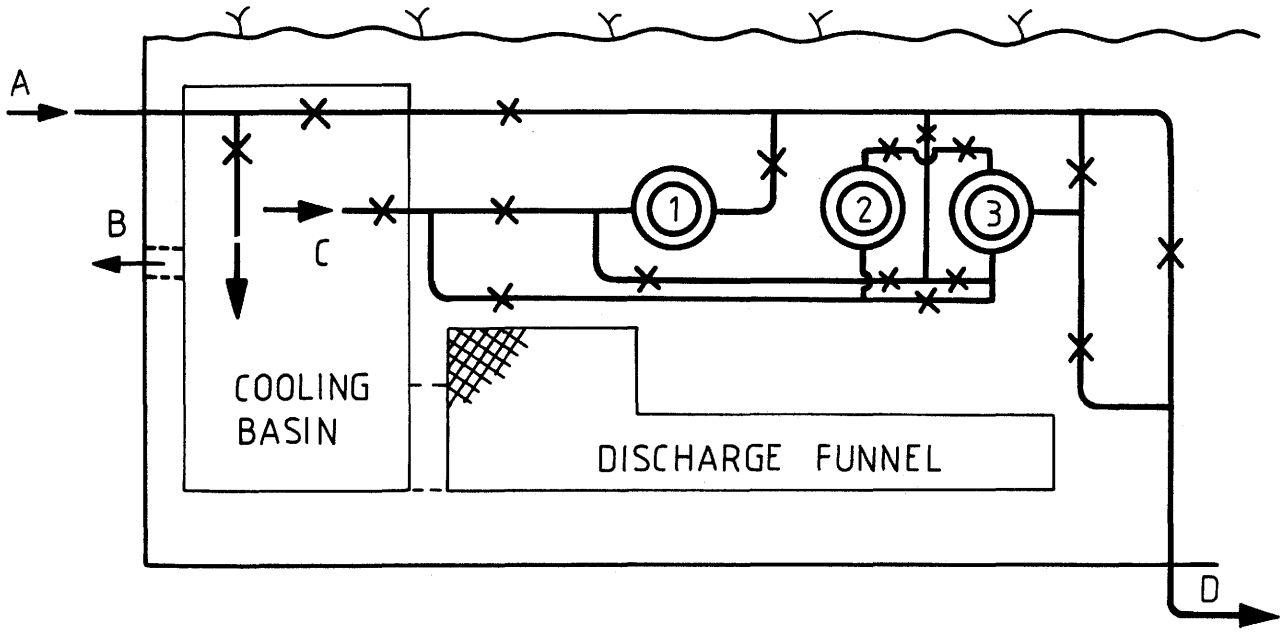

Legend:

1, 2, 3 Pumps
A Inlet from tap water system
B Spillway
C Inlet to pumps from cooling basin
D Outlet to tunnel plug via pressure control and flow recording units

x denotes valves

Figure 2-22. Pump circuit diagram

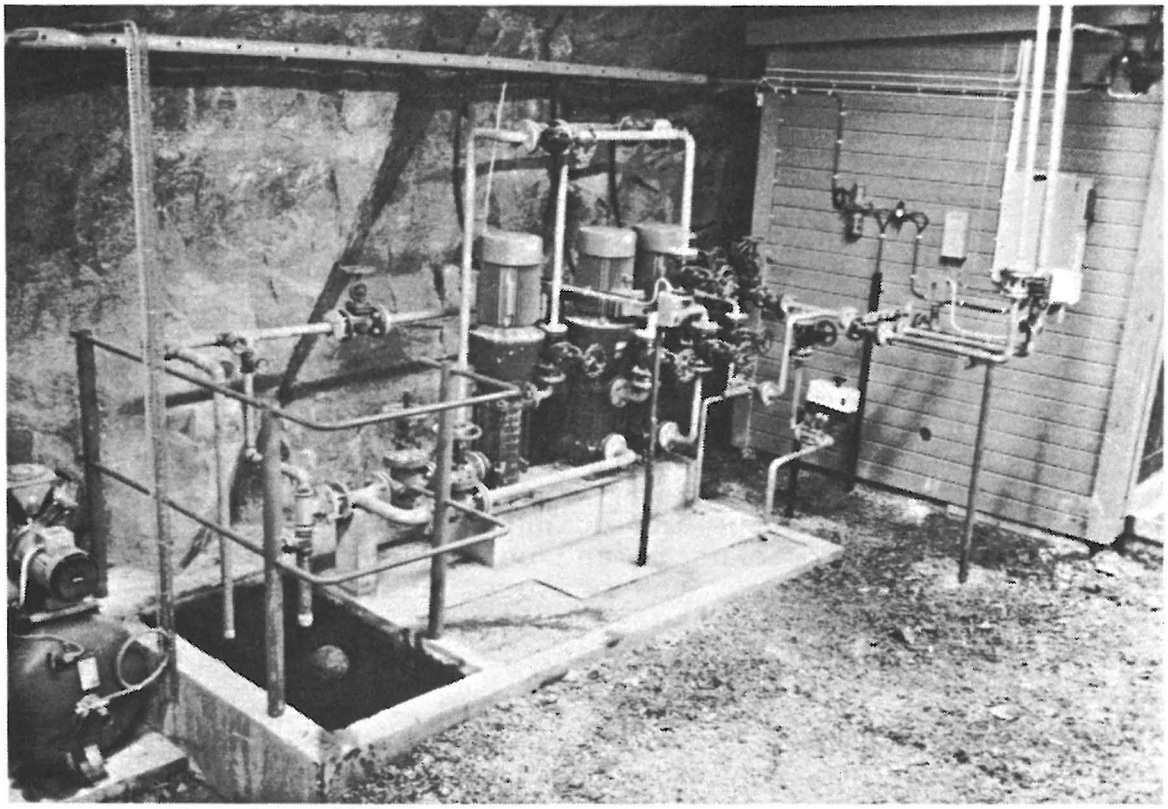

Figure 2-23. Photograph of the pump installation. The three pumps mounted with their axes oriented vertically are located in the center of the picture. In the far back, the flow recording and pressure control units are seen mounted on the wall of the shed in which the Gloetzl recording units were located.

2.4.6 Instrumentation

Flow recording

At injection pressures below 1 MPa in the initial test phase when the flow was expected to be very high, a simple turbine flow meter of type PN10 was used (Nordiska Armaturfabriken, Stockholm). The current recording of the flow of injected water at high pressures was made by use of a precision Fischer & Porter inductive flowmeter type 1001475 BCXC21SXAB. This gauge, which recorded the flow with an accuracy of ±1 %, delivered an output signal of 4-20 mA DC, which made it possible to use the available BMT data acquisition system for regular, automatic measurement and plotting. Fig 2-24 shows the entire arrangement for pressure control and recording of the flow of injected water.

An arrangement for measuring the outflow of water at the ends of the plug was also made. For this purpose, shallow excavations were blasted in the tunnel floor immediately outside the concrete walls and automatically operating pumps were applied for collecting inflowing water. Naturally, this arrangement could not catch all the water that leached from the interior of the plug, nor did it prevent water that could move in from other sources from being recorded. Applying the philosophy that most of the leaking water would follow the shortest paths from the injection chamber along and around the concrete units and consequently be collected and pumped up, the measurements should give approximately the same figure for the outflowing as for the injected water. This also turned out to be the case.

At the start of the test the intention was to determine the flow from the injection chamber into the tunnel immediately outside the plugs by applying the simple method of estimating flow of water into tunnels that was tried in the Buffer Mass Test and seemingly gave adequate results (6). It was based on the use of commercial air-drying devices of the simple water-collecting type which tend to yield a constant value of the flux provided that the hydraulic gradient of the inflowing water is constant and can be measured or estimated. The decision was to install units of this type in the inner space and outside the outer end of the plug construction. In order to create defined, closed tunnel sections, a light wall was built a couple of meters from the outer plug and the ends of the central casing were sealed off to prevent air from flowing through it. It would thereby be possible to estimate how much of the injected water that passed through the rock around the plugs into the isolated sections of the drift. This was actually done and

measurements were made for a few weeks, but it was then realized that the induced temperature increase, i.e. from about 10-11°C to about 30°C, caused expansion of the shallow rock by which the fractures tended to be closed and the water outflow from the injection chamber to be decreased. When the driers were removed, the outflow increased considerably indicating that this method of determining the leakage from the chamber could not be applied.

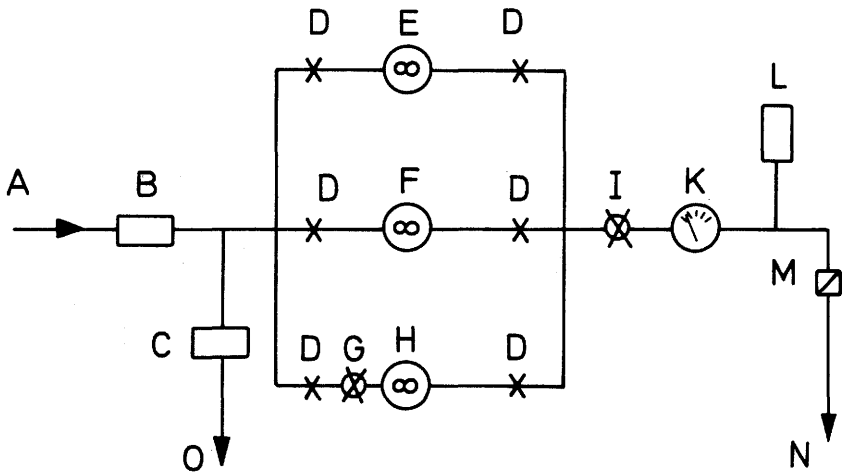

LEGEND:

A From pumps
B Filter
C Pressure control PN 250
D Valves
E Turbine flow meter M 40750/30
F Inductive flow meter
G Safety valve (1.05 MPa)
H Flow meter PN 10
I Adjustable safety valve (1.5-3.0 MPa)
K Manometer
L Pressure transducer (control unit)
M Back-valve
N Injection in pipe gallery
O Overflow to pool

Figure 2-24. Diagram showing the pressure control and flow recording units

Swelling pressure recording

Gloetzl pressure cells of type B 15/25 QM 100 F with pads and pressure tubings of stainless steel, type Werkstoff 1.4571, with injection tubings of the same material and return flow tubings of stiff nylon, were used for measuring the total pressures (sum of water and swelling pressures). The same recording equipment was used as in the Buffer Mass Test, i.e. the pump and read-out units operated in two different pressure intervals (0-4 MPa, and 0-16 MPa), and digital reading and printing was made at programmed time intervals through the data acquisition system (2). As in the BMT the measuring operation was rather slow. Thus, the time for measuring and recording was about 1-10 minutes for each individual circuit.

The total number of cells was 46, the location being shown in Figs 2-25--2-29 (cf. Fig 2-16). The intention was to measure not only the pressure at the sand/bentonite (section 0/0220 - and 0/02700) and at the rock/bentonite interfaces (sections 0/02175 and 0/02725) but also to record the swelling pressure transferred to the concrete (sections 0/02150 and 0/02750) as well as to the sand fill at 1.5 m distance (sections 0.02325 and 0/02575) from the bentonite surface and at 2.75 m distance from the sand/concrete interface (Central section 0/02450). Table 2-2 summarizes the location of the cells, giving also the full identification codes and the reference numbers used in the following text. The table describes the location of the respective cell as 1 o'clock, 2 o'clock etc, assuming the sections to be viewed in the direction towards the inner end of the drift.

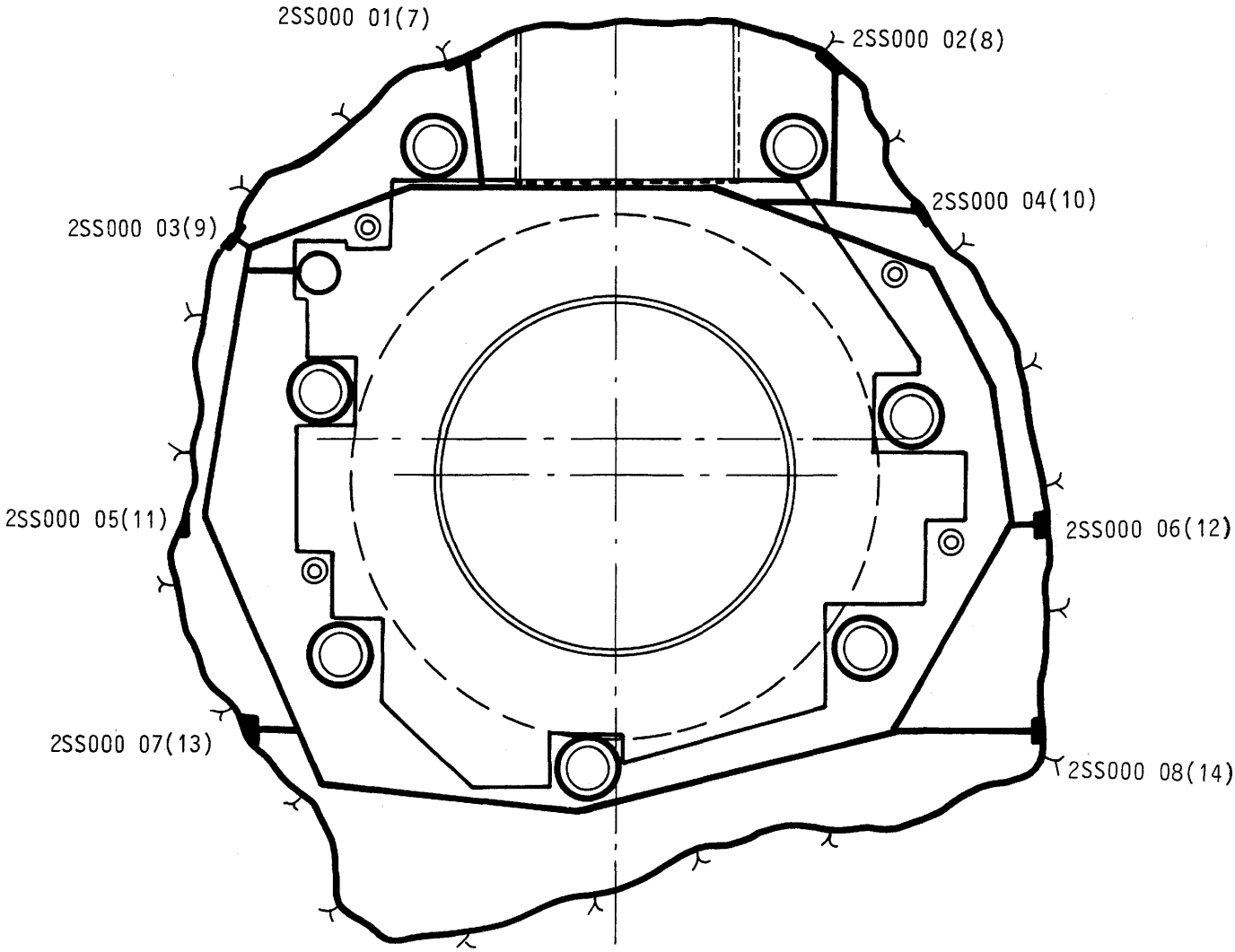

Figure 2-25. Location of Gloetzl cells Ref no 7-14 (total pressure) at the rock/bentonite contact of the outer plug (section 0/02175). T denotes casing for the tubings leading to the logging units outside the plug

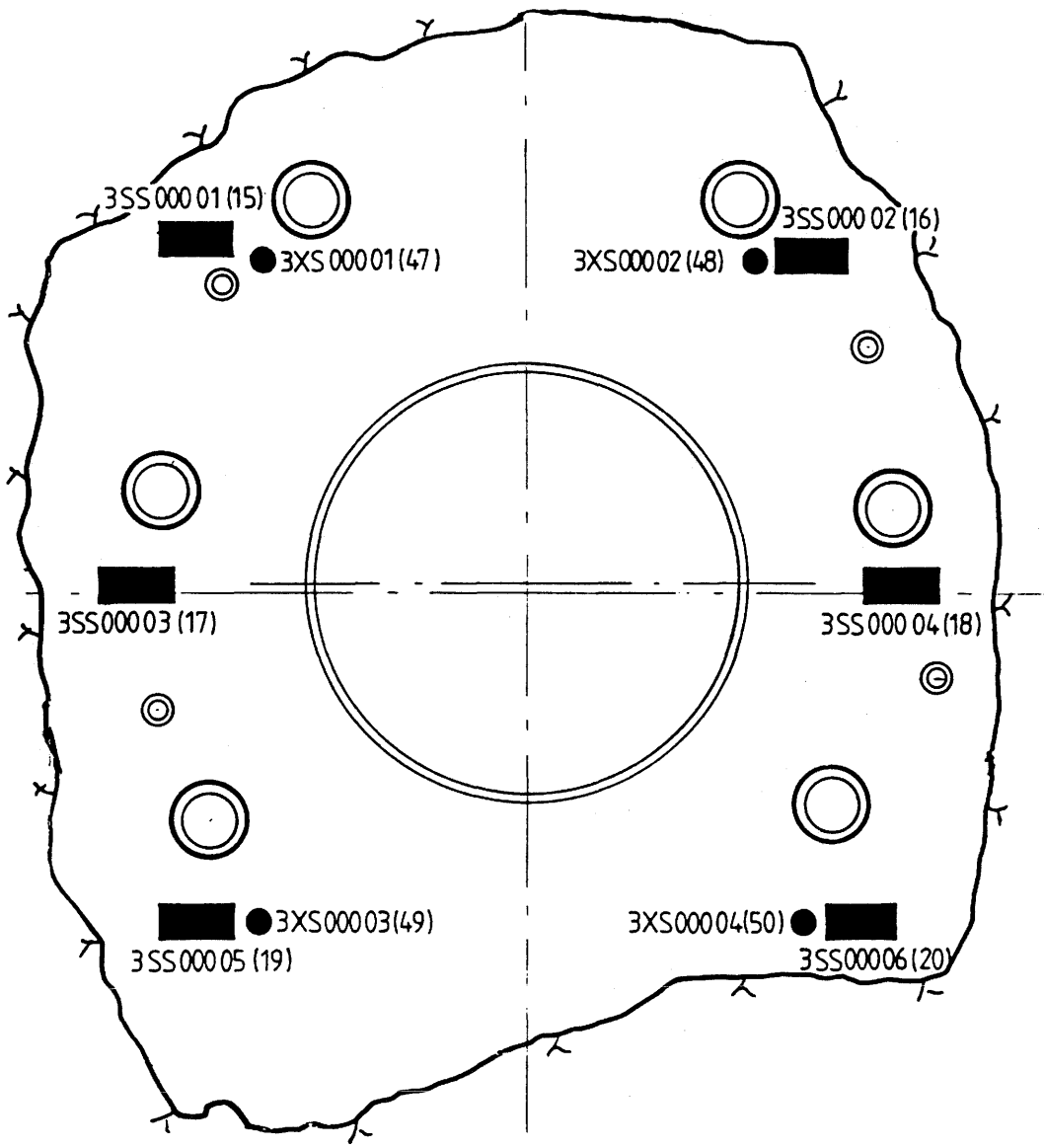

Figure 2-26. Location of Gloetzl cells Ref no 15-20 (total pressure) at sand/bentonite interface (section 0/02200). Also, the positions of piezometers Ref no 47-50 are given (section 0/02325)

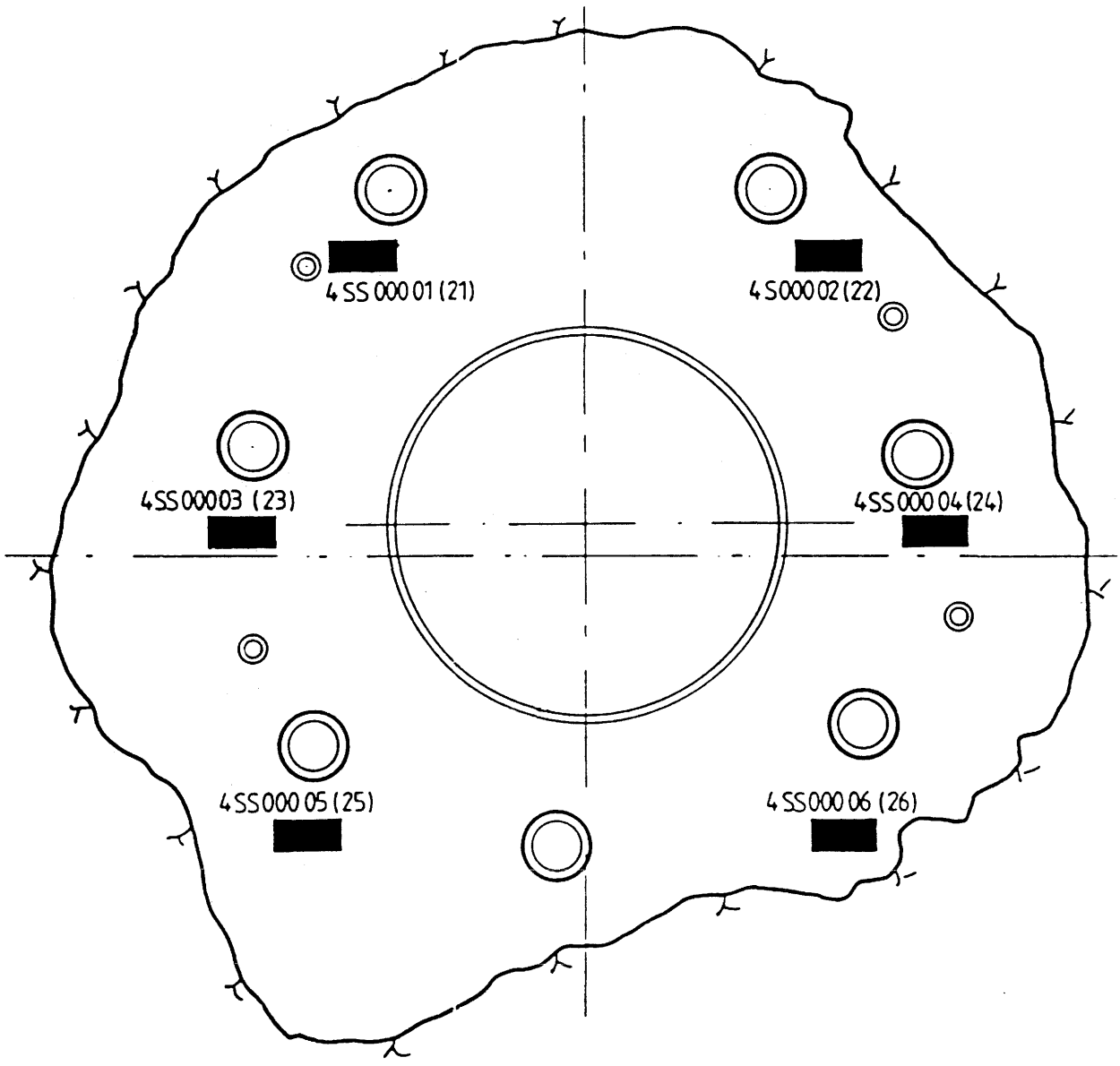

Figure 2-27. Gloetzl cells Ref no 21-26 (total pressure) in the sand, (section 0/02450)

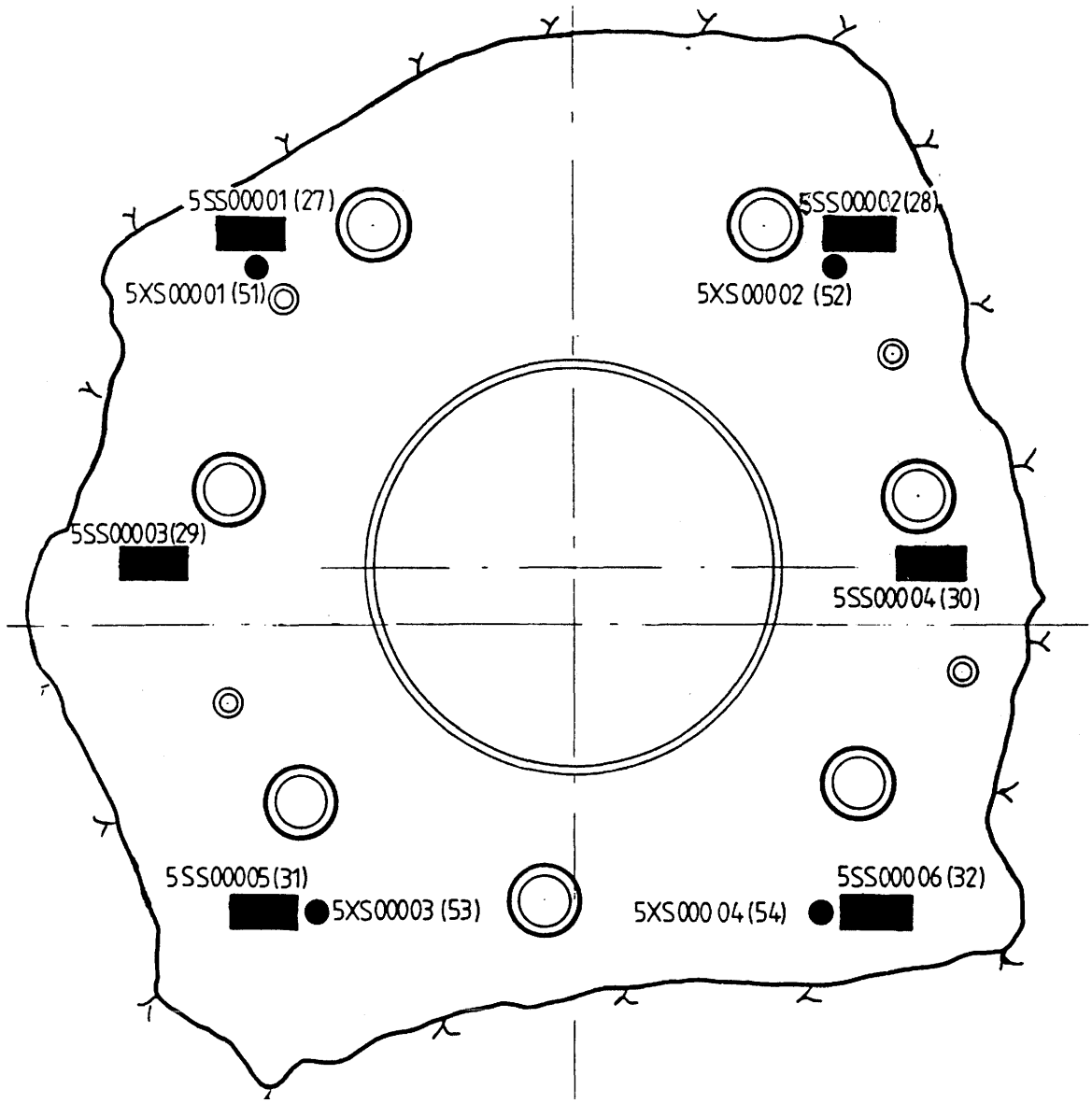

Figure 2-28. Location Gloetzl cells Ref no 27-32 (total pressure) at the sand/bentonite interface (section 0/02700). The positions of piezometers Ref no 51-54 are also given (section 0/02575)

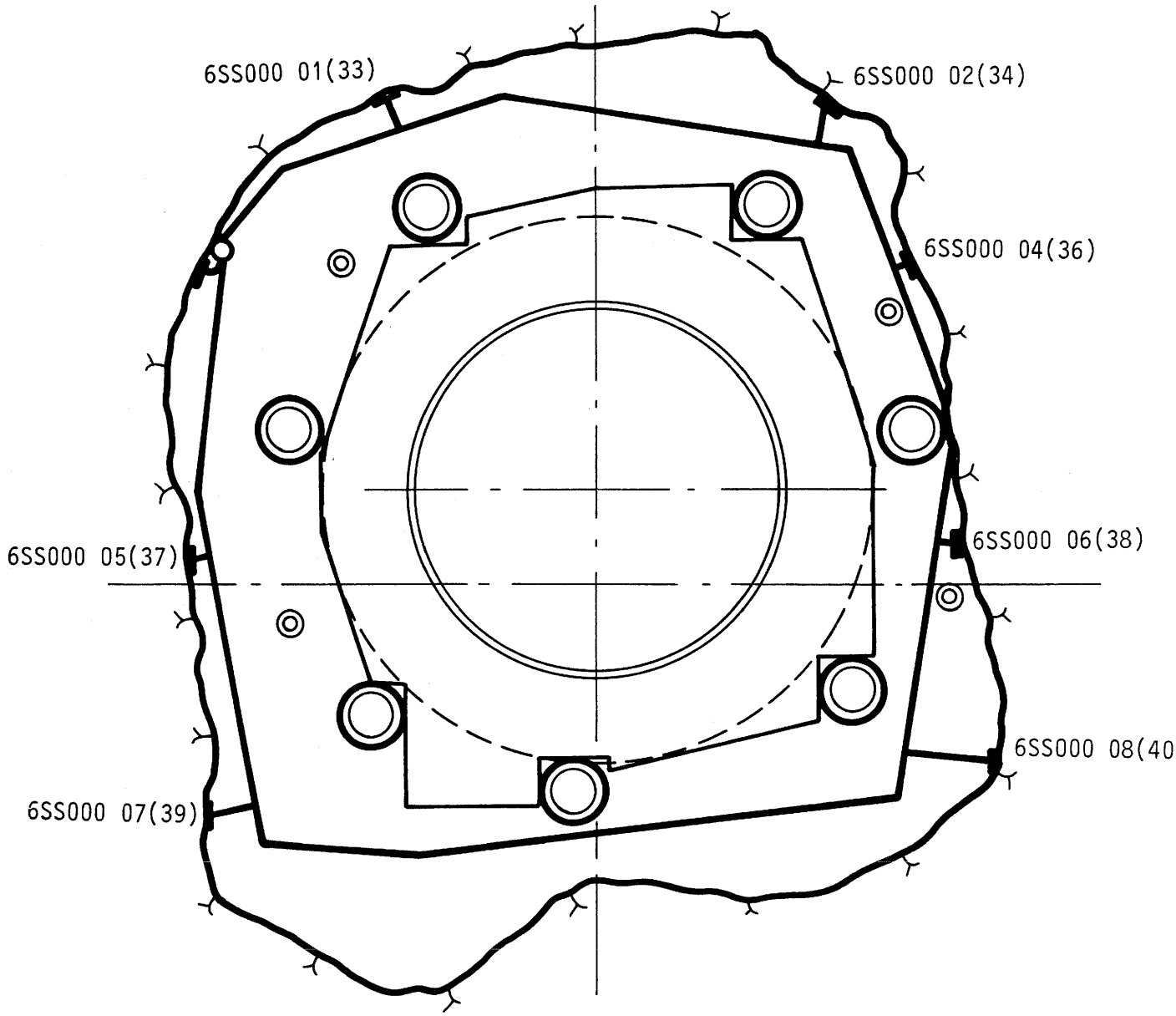

Figure 2-29. Location of Gloetzl cells Ref no 33-40 (total pressure) at the rock/bentonite contact of the inner plug (section 0/02725)

Table 2-2. Gloetzl pressure cells. Section Code Ref no. Pressure 0/0215

Section	Code	Ref no	Medium	Rock struct type
0/02150, 10 o'clock	1SS00001	1	Concr/bent	
0/02150, 2 o'clock	1SS00002	2	"	
0/02150, 9 o'clock	1SS00003	3	"	
0/02150, 3 o'clock	1SS00004	4	"	
0/02150, 7 o'clock	1SS00005	5	"	
0/02150, 5 o'clock	1SS00006	6	"	
0/02175, 11 o'clock	2SS00001	7	Rock/bent	Pegmatite
0/02175, 1 o'clock	2SS00002	8	"	Fract-poor
0/02175 10 o'clock	2SS00003	9	"	Pegmatite
0/02175 2 o'clock	2SS00004	10	"	Pegmatite
0/02175 9 o'clock	2SS00005	11	"	Fract rock
0/02175 3 o'clock	2SS00006	12	"	Fract-poor
0/02175 7 o'clock	2SS00007	13	"	Fractured
0/02175 5 o'clock	2SS00008	14	"	Fractured
0/02200 10 o'clock	3SS00001	15	Sand/bent	
0/02200 2 o'clock	3SS00002	16	"	
0/02200 9 o'clock	3SS00003	17	"	
0/02200 3 o'clock	3SS00004	18	"	
0/02200 7 o'clock	3SS00005	19	"	
0/02200 5 o'clock	3SS00006	20	"	
0/02700 10 o'clock	4SS00001	21	Sand	
0/02700 2 o'clock	4SS00002	22	"	
0/02700 9 o'clock	4SS00003	23	"	
0/02700 3 o'clock	4SS00004	24	"	
0/02700 7 o'clock	4SS00005	25	"	
0/02700 5 o'clock	4SS00006	26	"	
0/02725 10 o'clock	5SS00001	27	Sand/bent	
0/02725 2 o'clock	5SS00002	28	"	
0/02725 9 o'clock	5SS00003	29	"	
0/02725 3 o'clock	5SS00004	30	"	
0/02725 7 o'clock	5SS00005	31	"	
0/02725 5 o'clock	5SS00006	32	"	
0/02725 11 o'clock	6SS00001	33	Rock/bent	Fract-poor
0/02725 1 o'clock	6SS00002	34	"	"
0/02725 10 o'clock	6SS00003	35	"	Fractured
0/02725 2 o'clock	6SS00004	36	"	"
0/02725 9 o'clock	6SS00005	37	"	"
0/02725 3 o'clock	6SS00006	38	"	Fract-poor
0/02725 7 o'clock	6SS00007	39	"	Fractured
0/02725 5 o'clock	6SS00008	40	"	"

Cont Table 2-2.

Section	Code	Ref no	Medium	Rock struct type
0/02750 10 o'clock	7SS00001	41	Concr/bent	
0/02750 2 o'clock	7SS00002	42	"	
0/02750 9 o'clock	7SS00003	43	"	
0/02750 3 o'clock	7SS00004	44	"	
0/02750 7 o'clock	7SS00005	45	"	
0/02750 5 o'clock	7SS00006	46	"	

Pore pressure recording

Eight oil-operated Gloetzl cells of stainless steel, type P4 SF40, were installed in the sand to measure the porewater pressure. The pressure interval for which these gauges had to be designed was 0-4 MPa but the low range 0-0.1 MPa, which prevailed in the first phase of pressurizing, was of primary interest. This was because it was assumed that incomplete saturation of the sandfill would be revealed by irregular pressure recordings. No such indications were obtained, however. The pore pressure gauges termed 47-54 were placed in two of the planes in the sand backfill that contained total pressure cells, i.e. Sections 0/02325 and 0/02575 (cf. Figs 2-26 and 2-28).

Measurements of the displacement of the bentonite/ sand interface

The water uptake by the highly compacted bentonite from the pressurized sandfill was expected to yield fast saturation of the bentonite close to the sand interface. This would in turn yield displacement of this interface which was found to be difficult to measure by remote techniques. The rate as well as the amount of movement were instead observed directly in plexiglass tubes (Texoton Co, Mölndal, Sweden) with an inner diameter of 60 mm and a wall thickness of 6 mm. The displacements could be directly viewed by use of ordinary borehole optics and TV inspection equipments. The tubes were located in steel casings equipped with flanges through the concrete walls (cf. Fig 2-30), and tight sealing between them was obtained using Tremco Dymeric two-component epoxy seal (Göta Kemi, Gothenburg, Sweden). Sealings were also applied in the joints between the outer casing components.

All components turned out to be perfectly tight but some of the plexiglass tubes were fractured by tension in the portion that was located in the bentonite. The tubes were designed to resist com-

pressive pressures of 8 MPa and the failure was probably caused by the complex stress situation of axial tension and radial compression caused by the expanding bentonite.

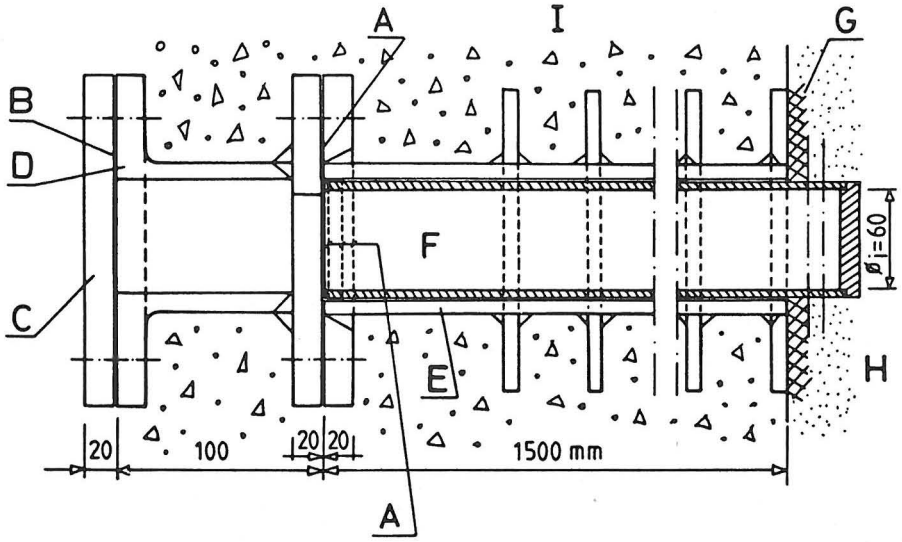

A Epoxy seal
B Rubber seal
C Lid
D Flange
E Steel casing (ϕ_{out}=102 mm)
F Plexiglass tube ϕ_{out}=72 mm)
G Bentonite
H Sand
I Concrete

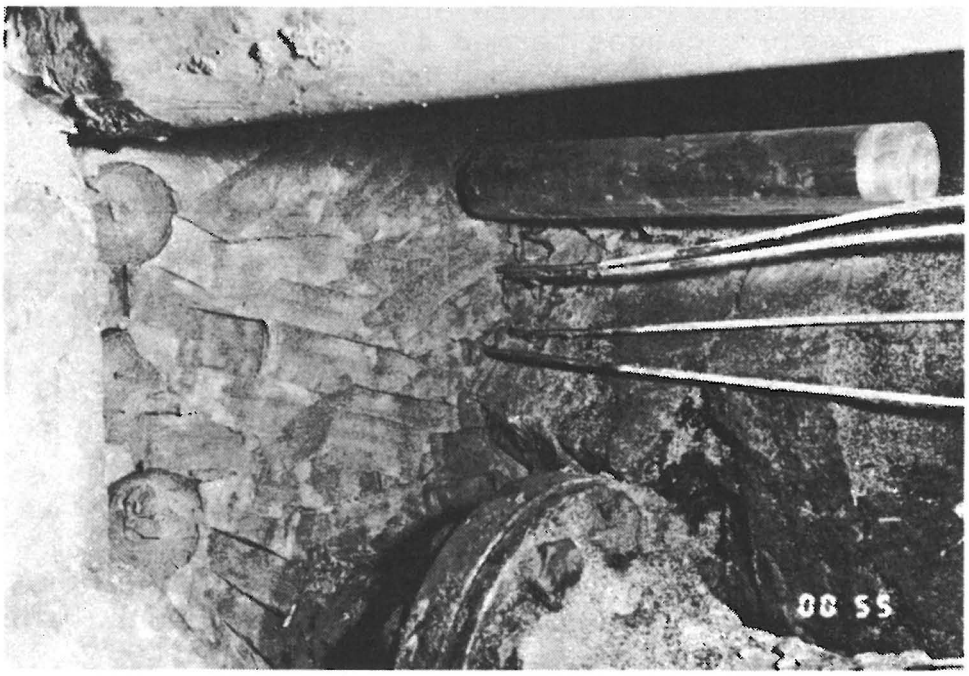

Figure 2-30. Steel casings with inspection tubes consisting of plexiglass extending through the concrete and bentonite into the sand. The lids were in position except at the inspections in order to eliminate the risk of leakage in case of breakage of the plexiglass tubes. The photograph shows one of the tubes as it appeared at the excavation after terminating the test

Extensometers for recording rock and plug strain

Although it was assumed that only moderate stresses would be transferred to the rock by pressure changes in the injection chamber, extensometers were installed to measure the axial strain of the casing and the displacement of the two concrete walls. For the latter purpose bolts were inserted in the concrete and in the rock about 1 m from the concrete plugs. The rock bolts, of which there were four in the southern and northern walls at each plug end, were taken to represent fixed points and the change in distance to the bolts in the concrete was therefore assumed to represent displacement of the concrete walls. The measurement was made with an accuracy of 0.01 mm by using an adjustable micrometer (CE Johansson, Eskilstuna,). This tool was used also for measuring the change in diameter of the casing.

2.4.7 Test program

The test was planned to comprise a stepwise increase in water pressure with concomitant measurement of the leakage from the injection chamber. The selection of pressure increments aimed at simulating the pressure build-up around a plugged tunnel section in a real repository. The experience is that it takes a considerable time for the piezometric heads to be re-established in the vicinity of tunnels and shafts that are sealed and for the present test 1 month was taken to be relevant for the first 0.5 MPa pressure interval. Another 3-4 months would probably be required under real conditions to reach about 1 MPa pressure, which was also the approximate period of time that passed from the start of the test to the onset of this pressure. Further steps were 2 and 3 MPa, which were applied relatively rapidly. The maximum pressure was set at 3 MPa and it was planned to be maintained for at least half a year in order to determine whether the sealing effect of the bentonite would also remain constant or be increased.

The swelling pressure developed by the bentonite was also planned to be measured, the rock/bentonite pressure being of major interest since it was expected to be a determinant of the rock-sealing effect of the bentonite. Recording of the rate of displacement of the sand/bentonite interface was considered to be of importance because it would offer a possibility of verifying an earlier developed physical model for expansion of unconfined bentonite. In connection with this process the possible penetration of clay into the voids of the sand backfill was of interest as well.

At the end of the test, the casing was to be cut open and the larger part of the sand excavated for a detailed study of the distribution of water in the bentonite, with special respect to the conditions at the pressure cells. This was expected to reveal how uniformly water was absorbed by the bentonite and to make it possible to relate the recorded swelling pressures to the degree of saturation. Also, the excavation was assumed to give evidence of how completely the sand had filled the injection chamber.

This initial general plan could be pursued and a test sequence was also added to check the hypothesis that pump power breakdowns had caused plug movements and associated temporary changes in leakage. This was investigated by lowering and increasing the injection pressure a few times at the end of the test.

The various activities are summarized in Table 2-3.

Table 2-3. Test program in condensed form

Item	Value etc	Period
1st Prestress. of tie-rods	200 t/tie-rod	Apr 1984
Injection step	100 kPa	Apr 10-15, 1984
"	200 kPa	Apr 15-May 15, 1984
"	500 kPa	May 15-31, 1984
"	750 kPa	May 31-Aug 15, 1984
2nd Prestress. of tie-rods	450 t/tie-rod	Oct 1984
Injection step	2.0 MPa	Oct 20-Nov 5, 1984
"	3.0 MPa	Nov 5 1984-- Aug 31 1985
Inj pressure release	250 kPa	Aug 31-Sep 10, 1985
Injection step	1.0 MPa	Sep 10-20, 1985
"	2.0 MPa	Sep 20-Oct 1, 1985
"	3.0 MPa	Oct 1-15, 1985
Inj pressure release	250 kPa	Oct 15-Nov 1, 1985
Injection step	1.0 MPa	Nov 1-10, 1985
"	2.0 MPa	Nov 10-Nov 20, 1985
"	3.0 MPa	Nov 20-Dec 1, 1985
Inj pressure release	250 kPa	Dec 1-31, 1985
Unloading of tie-rods		Jan 10-30, 1986
Excavation		Feb 10-Apr 30, 1986

3 TEST RESULTS

3.1 PREDICTIONS

3.1.1 Leakage

When the present test was planned, the Buffer Mass Test and the Borehole and Shaft Plugging Tests had not been evaluated yet, and predictions of the sealing function of the Tunnel Plug were therefore based on a simplified model of water flowing from the injection chamber through the fractured rock around the perimeter, the permeability of this rock zone being affected by the pressure exerted by the adjacent bentonite and by clay penetration into open fractures. The percolated rock zone was taken to extend to 1 m distance from the perimeter and to have an average hydraulic conductivity of 10^{-7}-10^{-8} m/s. For injection pressures up to 1 MPa no outflow through the rock was assumed to take place according to this model since the existing piezometric head in the rock was assumed to be on the same order. At higher pressures the outflow was estimated to be 50-500 l/hour at 2 MPa and 100-1000 l/hour at 3 MPa, i.e. at 1 and 2 MPa overpressure, respectively. Based on qualitative reasonings it was estimated that about 50 % of the leakage would take place through the major, steeply oriented fracture sets in the floor and in the southern wall at the outer end of the plug (cf. Fig 2-15), while the rest would be equally distributed through the pegmatite zone at the outer end of the plug and at the inner diabase dike as well as to various anonymous fractures. A rough guess was that 80-90 % of the leakage would take place at the outer plug end.

As to possible leakage through the bentonite it was believed that once this material had become saturated to within a few centimeters from the rock surface, thereby forming a tight contact with the rock, it would let no water through. Based on the experience from laboratory tests, it was assumed that such a matured contact would be fully developed a few days after the onset of the test. However, considerable leakage, possibly in conjunction with piping and washing out of bentonite through the joint at the concrete/rock interface, was predicted for the first 2-3 days after the first pressure step-up, i.e. when 100 kPa injection pressure was applied.

The successive saturation of a larger part of the bentonite was expected to yield a swelling pressure that was assumed to compress those fractures that are oriented more or less parallel to the plug axis. The major, potential water-bearing steep fractures in the tunnel floor and the pegmatite zone would not be affected by this, while a number of oblique fractures in the walls at the outer plug end would get their apertures reduced. To that comes the effect of bentonite penetrating into fractures that transport water along the bentonite/rock interface, and these two sealing effects were estimated to bring down the leakage through the rock significantly. Thus, at 3 MPa injection pressure, the assumed initial 100-1000 l/hour flow was assumed to be reduced by about 20-40 % after 1 year, the rate of the reduction being very much dependent on the saturation rate as described below. The minimum estimated leakage at the end of the 3 MPa pressure period was 60 l/hour, while the maximum was about 800 l/hour. Some intermediate value would be most probable as concluded from various sources.

3.1.2 Build-up of swelling pressures

The model applied for estimating the rate of saturation, and thereby the rate of build-up of swelling pressures, was based on a laboratory-derived law for water uptake in confined highly compacted bentonite specimens (5):

$$\frac{\delta w}{\delta t} = D\nabla^2 w \qquad (1)$$

where w = water content
t = time
D = "diffusion coefficient", the value of which can be set at 4×10^{-10} m^2/s (1)

It was assumed that no expansion takes place (x=o in Fig 3-1), which is plausible for early wetting stages and particularly acceptable when considering the inner part of the bentonite body. Here, water uptake stems from the rock/bentonite interface and the homogenization of the bentonite takes place under almost constant volume conditions. Here is actually also the part of the bentonite where the fracture-influencing swelling pressure would be produced. Eq. (1) and simple 2 D FEM technique (FEMTEMP, Chalmers University of Technology, Gothenburg) were applied in the calculations, taking the initial water content as 10 % and that at complete saturation as 20 %. Three wetting stages representing about 4, 11 and 20 month after onset of the test are shown in Fig 3-2. The boundary conditions with respect to the access to water were that surfaces A-B and B-C were taken to

be impermeable, while the rock/bentonite and sand/ bentonite interfaces represented boundaries with unlimited access to water.

The calculations demonstrated that the bentonite was not going to be completely or even largely saturated in the planned, approximately 20 months long test (Dec 1985 in Fig 3-2) except for an approximately 5 cm wide boundary zone at the wet interfaces. Applying the principle that the swelling pressure is directly proportional to the average degree of saturation (6), the average swelling pressure at the rock/ bentonite interface was estimated for three wetting stages. The calculations were based on the swelling pressure 14 MPa at complete saturation and this yielded the maximum values given in Table 3-1. Assuming the initially incomplete contact between the individual blocks to cause a substantial delay in the pressure build-up it was estimated that the pressures would only rise to about 50 % of the theoretically deduced values. These reduced values are also given in Table 3-1, the predicted pressures being assumed to fall in between these extremities.

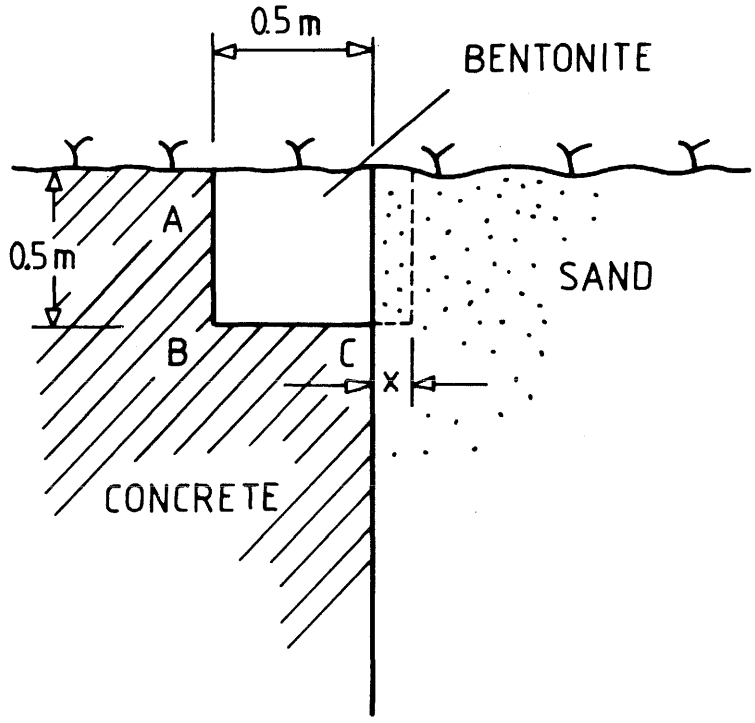

Figure 3-1. Geometry of the bentonite/concrete sealing

Table 3-1. Prediction of swelling pressures

Time after onset of first water injection, months	Expected swelling pressure at the rock/bentonite interface, MPa	
	Maximum	Minimum
5	4	2
15	6	3
20	7	3.5

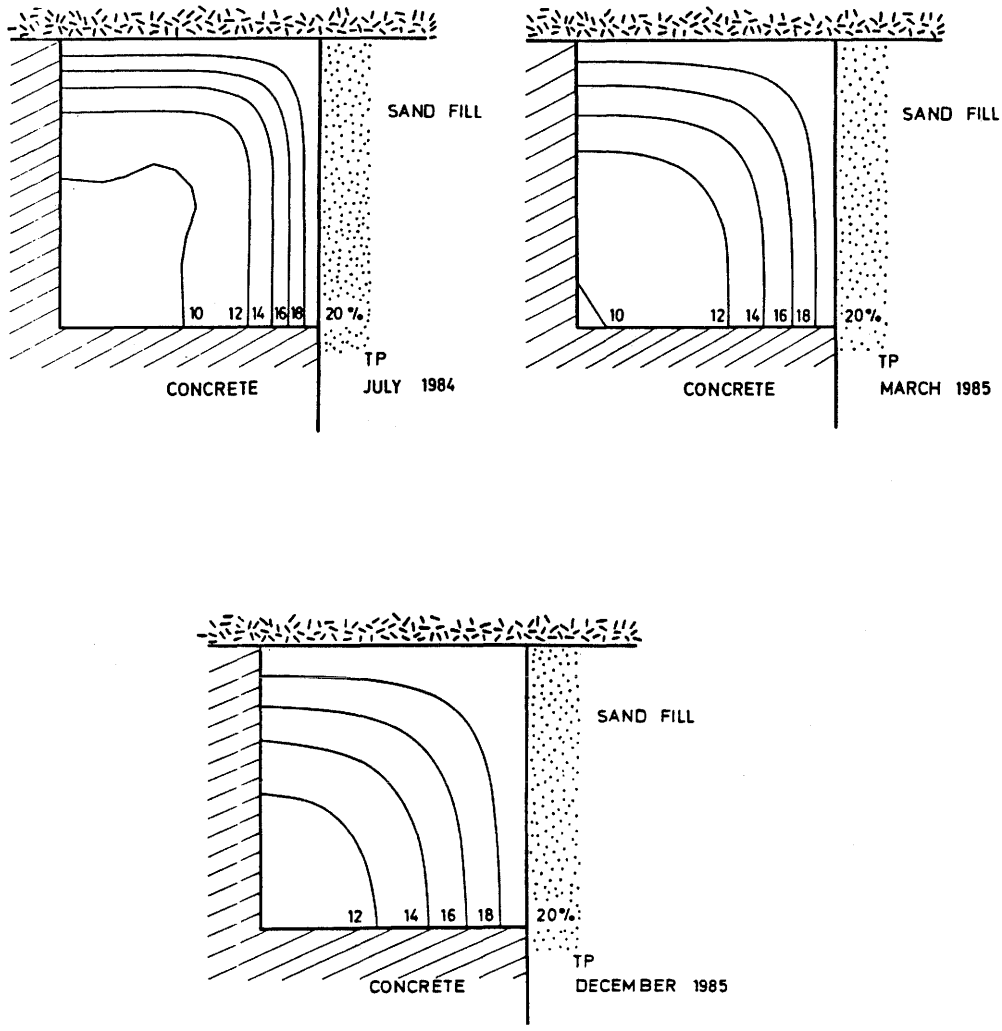

Figure 3-2. Three wetting stages of the bentonite assuming that no expansion takes place

The pressure at the sand/bentonite interface was expected to increase very slowly because of the compressibility of the sand, particularly in the upper part of the tunnel where the sand was known to have a low bulk density. Here, the swelling pressure was not expected to exceed about 100 kPa in the first 15-20 months, assuming isotropic conditions to prevail. The rate of water uptake at the sand boundary and the associated expansion of the bentonite is discussed in the subsequent chapter.

3.1.3 Displacement of the sand/bentonite interface

The displacement of the sand/bentonite interface was assumed to be developed without any significant increase in contact pressure because of the high compressibility of the sand. Thus, the pressure was expected to be approximately 100 kPa in the upper part of the tunnel and possibly twice as much in the lower part during the major part of the test.

The displacement was calculated stepwise, the first increment yielding such an expansion of a boundary element that its bulk density corresponds to a swelling pressure of 100 kPa. The next step implied expansion of a second, neighboring element with the same initial thickness as the first one so that it would get the same bulk density, etc. The average flow path length for water migrating from the successively displaced sand/bentonite interface to the inner, expanding element is accordingly increased and the swelling process therefore retarded. The calculation was thus almost identical to the procedure applied for estimating the rate of clay penetration into rock fractures from deposition holes with highly compacted bentonite (1). The time t for expansion of each element is defined as:

$$t = \frac{H^2}{k \cdot u} \qquad (2)$$

where H = total lateral extension of the expanded zone

k = average hydraulic conductivity of the expanded zone and the nonexpanded clay

u = negative pore pressure = $|p_s|$, where p_s = swelling pressure

The predicted rate of displacement of the sand/bentonite interface is shown in Fig 3-3. We see that the expansion of the bentonite was estimated to be about 10 cm in the upper part of the tunnel at the end of the test. The corresponding value would be slightly lower in the lower part because

of the higher density and thereby lower compressibility of the sand.

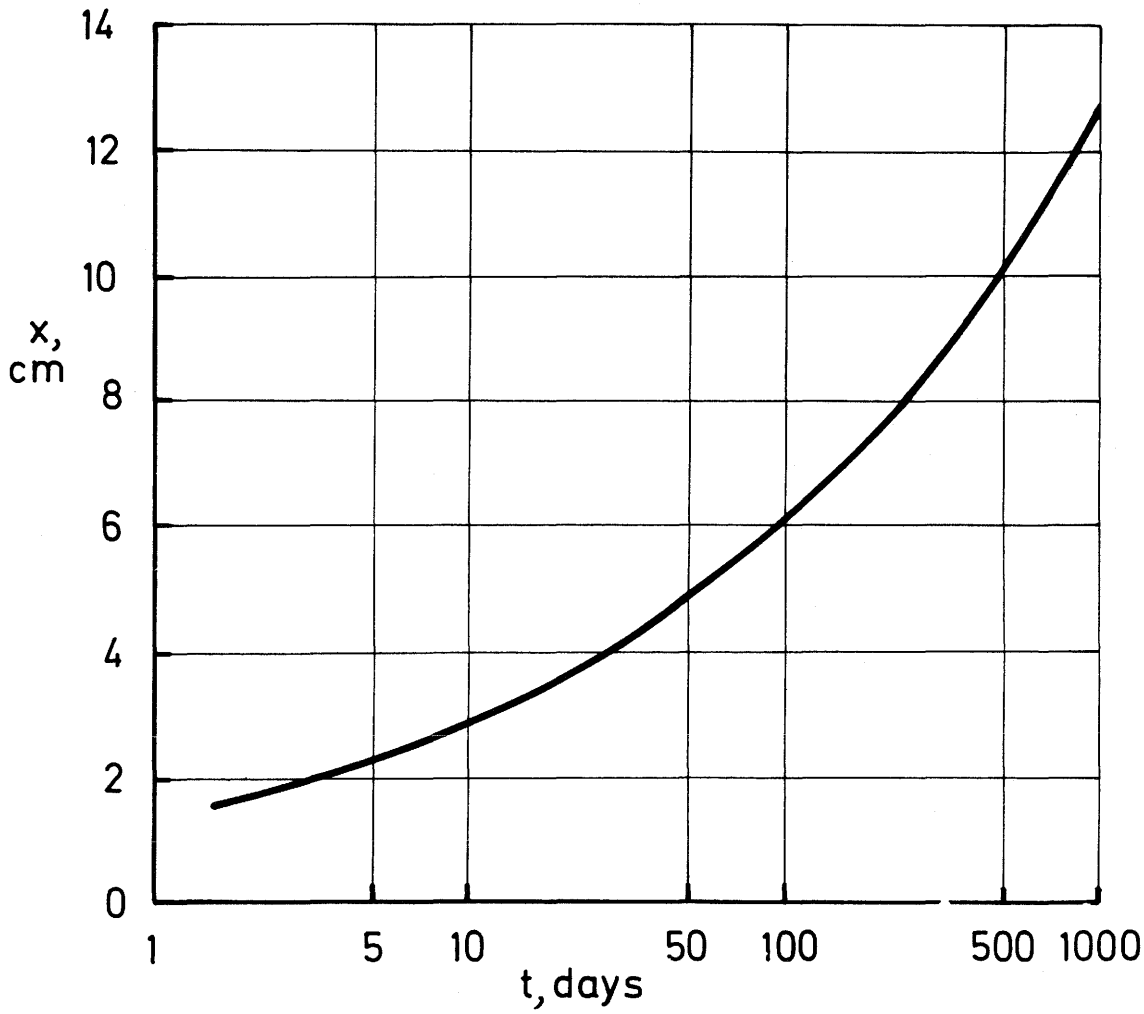

Figure 3-3. Calculated displacement of the sand/bentonite interface in the upper part of the tunnel

3.2 RECORDINGS

3.2.1 Construction work

As in the Borehole and Shaft Plugging Tests, the need for comprehensive instrumentation and special arrangements like the tie-rods, caused a much longer construction time than would be required under real repository conditions. The difference would be particularly obvious in full-face drilled shafts and tunnels in which a minimum of welding and formwork would be required on site. Under such circumstances the total construction time of a 10 m long plug of the type shown in Fig 1-1 would not be more than a few weeks. It should be pointed out that tie-rods are not required in practice since the pressure conditions will be quite different from those in the present test (cf. Fig 1-3).

While the initial plan was to let water spray from the injection pipe gallery when applying the bentonite blocks, in order to check the practicality of the whole operation, it was abandoned because it would create extremely uncomfortable conditions that were actually not relevant to the construction of a real plug.

The experience from the construction of the plug was that no real problems appeared and that this type of effective sealings can be produced by ordinary construction companies.

3.2.2 Sealing effect

3.2.2.1 Flow recording

The pressure-related decrease in water flux from the injection chamber was the only relevant parameter in evaluating the sealing effect of the bentonite. As mentioned in the preceding chapter, considerable leakage was expected to take place through the rock outside the radius of action that the bentonite was assumed to have on the rock, and the change in leakage at different time intervals after each pressure increase was taken as a true measure of the sealing power of the bentonite.

The most accurate value of the water flux was obtained through the flow meters which recorded the amount of injected water into the sand-filled chamber. Fig 3-4 shows the flux as a function of time, and it demonstrates several major phenomena:

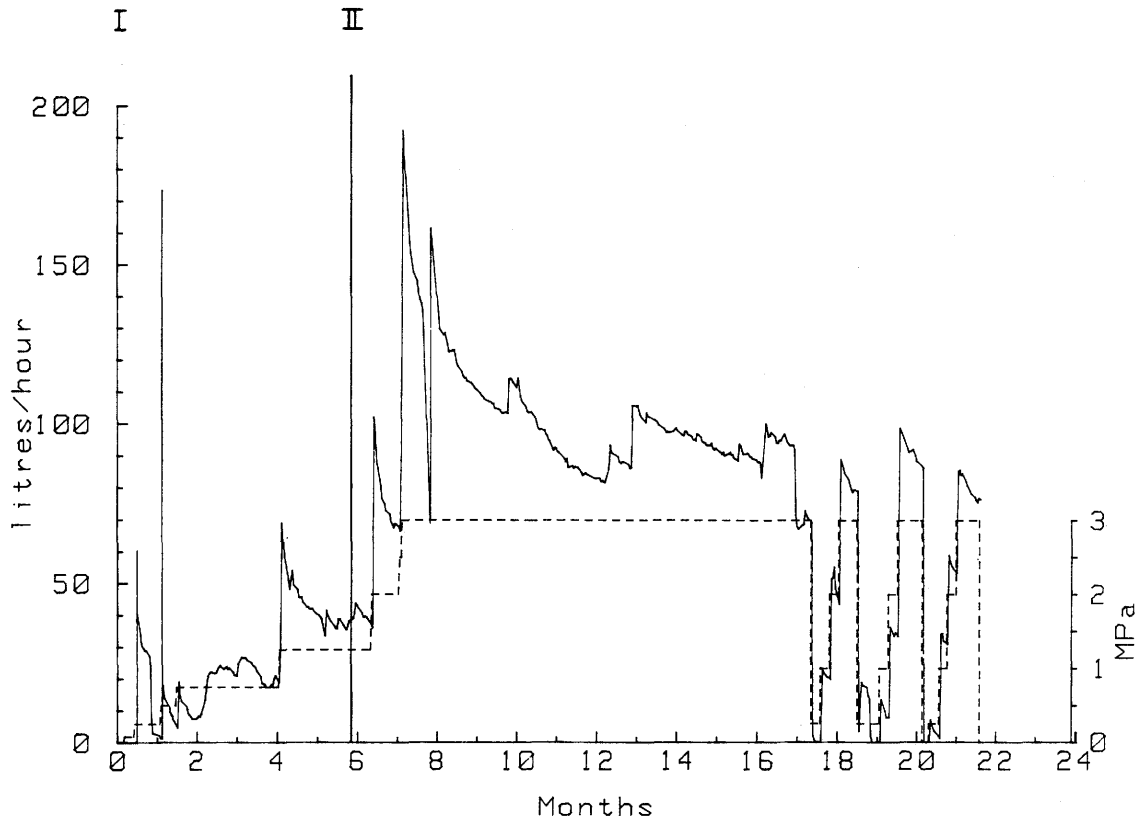

Figure 3-4. Flux of injected water. Zero time in this diagram and in those of Figs 3-6 to 3-9 represents mid April 1984, i.e. when the first prestressing took place (I). II represents the second prestressing

* At each pressure step a high peak value was obtained indicating rapid temporary inflow. The major reason for this is concluded to be compression of air-containing pores in the sand at the first pressure steps, and penetration of water into fractures that were expanded by the injection pressure when it reached higher values. At the lowest pressure steps strong leakage took place at the rock/bentonite interface for about 1 day.

* The flux tended to stabilize at values that were approximately proportional to the pressure up to 1.25 MPa, while it increased considerably at higher pressures. This suggests that the natural piezometric head at the rock/sandfill interface was on the order of 1-1.5 MPa.

* At the highest pressure, the flux tended to drop at a decreased rate from 200 l/hour to about 75 l/hour in the course of the test, and the larger part of this reduction is concluded to be caused by various sealing effects of the bentonite.

* During the 10 months long, 3 MPa pressure period four major irregularities appeared in the form of temporary peak values. It was suspected that these were caused by short pump power breakdowns that caused a pressure drop and shortening of the plug with concomitant displacement of the rock at the rock/concrete interface and thereby induced alteration of fracture apertures. To check this hypothesis the pressure was deliberatly dropped to 250 kPa in two sequences as shown in Fig 3-4. Thereby, the typical flow disturbances appeared, which thus supports the idea that rock deformation, caused by power breakdowns, produced the peaks.

* At the application of the 0.75 MPa injection pressure early in the test, the water flux became about 15 l/hour and then dropped to about half this figure in 2-3 weeks. During this period the air-drying units were in operation to determine the flow from the rock immediately outside the plug construction. This operation raised the air temperature to about 30°C which must have reduced the aperture of all fractures that were exposed at the rock surface. Accordingly, when these devices were removed, the flow increased to 20-25 l/hour in a few days.

The water collected outside the two ends of the plug construction gave a flux pattern that is illustrated by Fig 3-5 for the first 10 months. The diagram shows a striking similarity between the injected and collected amounts of water, which thus demonstrates that the outflow from the injection chamber mainly took place through the rock immediately outside the plug ends. The collection of outflowing water gave a possibility of determining how much of it that originated from the inner end. It turned out to be between 5 and 10 % throughout the test.

3.2.2.2 Direct observations

Immediately after finishing the plug construction the water pressure was raised to 100 kPa and strong leakage was observed at the rock/concrete interface all around the outer and inner plug ends. Air bubbles were seen in the leaking water in the first days, indicating that some air was contained in the upper part of the sand fill. A number of water samples were taken for investigating whether it contained clay eroded from the bentonite but there was no sign of clay.

It appeared that most of the visible flow from the rock initially came from the pegmatite zone just

above the outer plug and from a few steeply oriented fractures in the walls adjacent to this plug. These outflows decreased very much in the course of the test.

No outflow from the rock in the form of dripping etc could be seen after about 1 month at the inner plug.

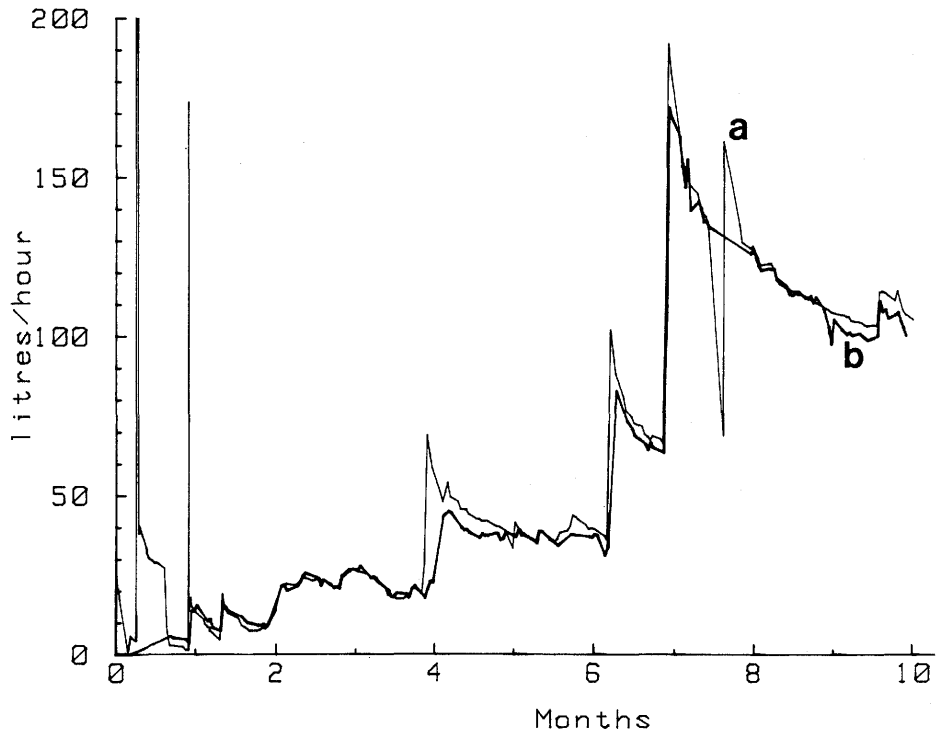

Figure 3-5. Recorded flow of injected water (a) and collected water (b)

3.2.2.3 Conclusions

A major conclusion is that the drop in leakage by 60 % that took place in the about 10 months long test period at maximum pressure, largely exceeded the expected reduction. The observation that the outflow decreased very much from the pegmatite zone and the steep fractures in the rock walls agrees with the prediction that the bentonite would be able to seal them effectively. Since its sealing power was expected to be insignificant in the steep fractures in the floor, it is concluded that the major part of the leakage took place through the last-mentioned passages in the late part of the test (Fig 2-15).

An additional conclusion is that while the bentonite sealing strongly reduced the leakage in the

course of the test, water rapidly passed through the joint between bentonite and rock for a few hours at the first pressure steps. The fact that no clay was washed out suggests that the bentonite initially formed a coherent but non-homogeneous clay gel at the rock/bentonite interface and that this gel soon became consolidated and integrated in the expanding clay mass. One possible sealing mechanism may have been that eroded clay aggregates from this gel were forced into the joint between the rock and the concrete and sealed this space.

A third conclusion is that a concrete plug construction with no bentonite sealings would have continued to leak at a rate indicated by the flow peak at the first water injection steps. At a pressure of 3 MPa the estimated leakage would have been more than 1000 l/hour.

3.2.3 Axial deformation of the plug construction

3.2.3.1 Measurement of displacements of the concrete plugs

The diagrams in Figs 3-6 and 3-7 show the measured displacements of the outer and inner ends of the plug construction. Both indicate the importance of the prestressing of the tie-rods and of the increased injection pressure although it is clear that the displacements were very small. The first prestressing caused an inward displacement of the outer plug end by about 0.75 mm from the initial position represented by the 0-value. One of the points (No 1) indicated less displacement than the others (Nos 2, 3 and 4) and, thus, torsion of the plug, but after the second prestressing almost uniform strain and straightening of the plug was developed. It is seen that the water pressure increase from 100 kPa to 0.75 MPa moved the outer plug out again by about 0.25 mm but it then returned to almost the same position as after the first tie-rod prestressing even when the water pressure had been raised to 1.25 MPa. The pressure increment from 2 to 3 MPa did not cause any noticeable displacement. An interesting fact is that the three pressure drops at about 18 and 19 months after test start moved the "movable corner" of the outer plug inwards by 0.25 mm, from the apparent equilibrium position that it had reached. The rest of the plug reacted much less, i.e. by about 0.1 mm.

Fig 3-7 shows that the inner plug moved towards the sandfill in approximately the same way as the outer one, but we see that the upper end of the plug was displaced significantly more than the lower. We also see a clear tendency of the upper end to be moved inwards by time at the highest water pressure.

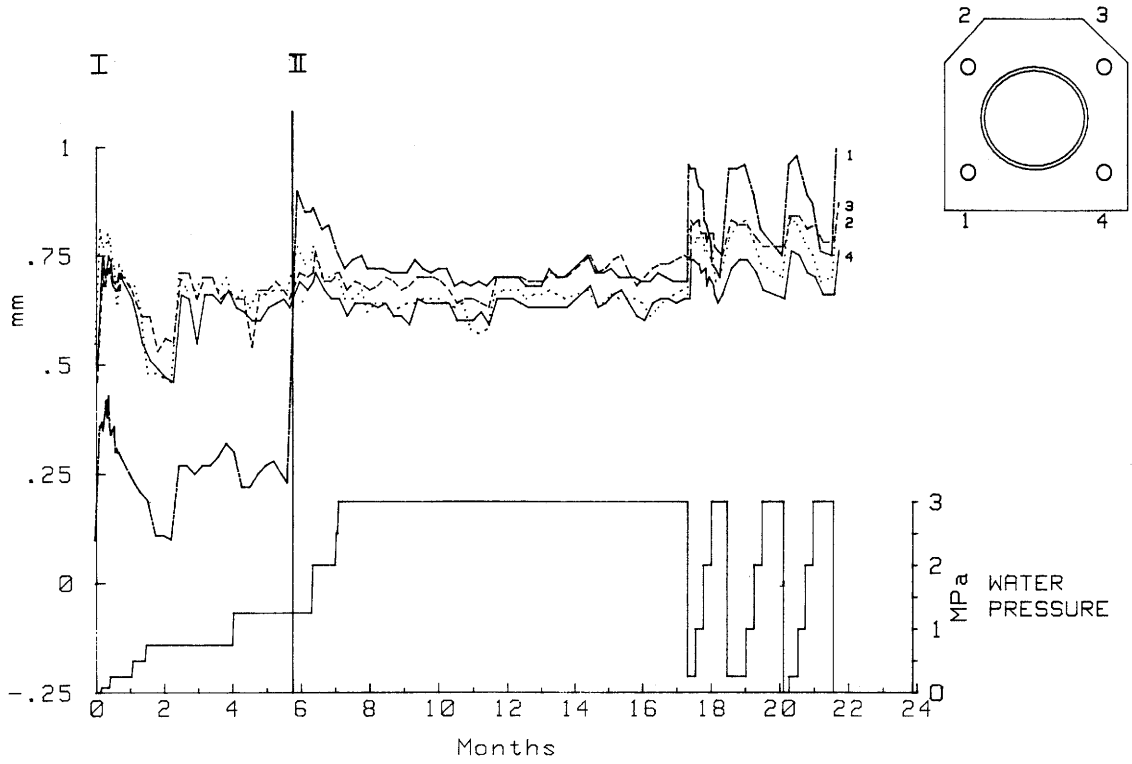

Figure 3-6. Displacement of the outer plug end. Plus sign indicates movement towards the inner plug. In the upper right figure the plug is viewed from the outer end of the drift

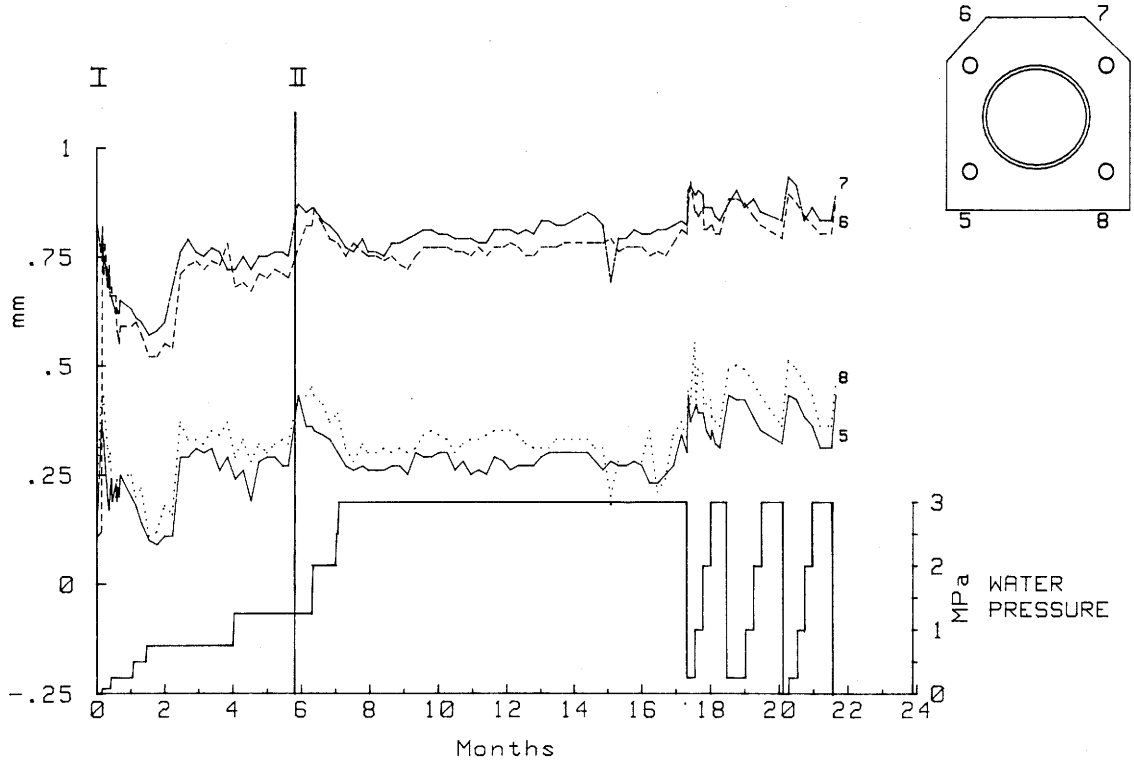

Figure 3-7. Displacement of the inner plug end. Plus sign indicates movement towards the outer plug. In the upper right figure the plug is viewed from the outer end of the drift

3.2.3.2 Deformation of the central casing

The extensometer measurements in the course of the test did not give a clear picture of the stress distribution in the plug construction. However, as shown by the diagram in Fig 3-8, some major features can be seen. Thus, the first prestressing caused an immediate shortening of the casing by about 0.5 mm and a further, delayed contraction by the same amount despite the successive increase in water pressure. The application of 0.75 MPa water pressure produced expansion to almost the initial length, while the second prestressing caused a shortening that was smaller than the first, probably due to the relatively high water pressure. The high water pressure steps 2 and 3 MPa brought it back again to nearly the same length and stress state as it had before the second prestressing. The series of cyclic changes in water pressure from 3 MPa to 250 kPa at the end of the test caused a corresponding change in length by about 0.4 mm. An interesting fact is that an abrupt expansion of the casing took place after about 15 months. It illustrates the complex force interaction between the plug components and does not seem to be related to a displacement of the concrete plugs relative to the rock.

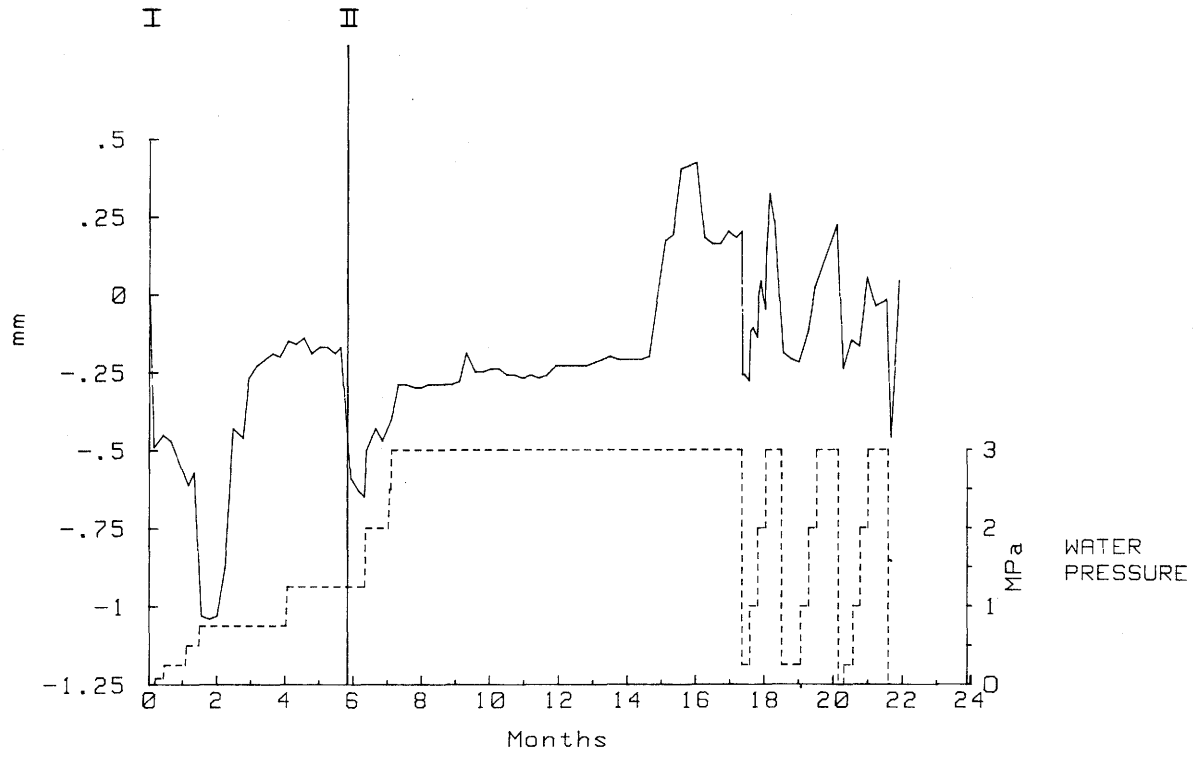

Fig 3-8. Axial deformation of the steel casing.
+ indicates expansion, - contraction

3.2.3.3 Conclusions

The measured displacements of the plug units were very much smaller than the expected ones, which clearly demonstrates that the rock interacted strongly with the plug. Thus, a large part of the loads induced by prestressing and water pressurizing must have been carried by the rock, which means that the predicted slip along the rock/plug interface was incorrect. The major reason for the good interaction is probably that the bentonite had formed an effective and tight contact with the rock, which would imply that it had maturated and filled up the recesses more rapidly than predicted.

The transfer of axial forces to the rock, which was very much feared in the planning of the test, did not have any significant effect on the leakage, except for a short period after the large drops in water pressure. At these instances the plugs moved 0.1-0.3 mm and if they interacted perfectly with the rock, the total rock deformation close to the plugs must have been on the same order of magnitude. This would have induced a change in fracture apertures that may well have caused the temporary, moderate increase in flow that was associated with the pressure changes.

The interaction between the various plug components and the rock appears to be very complex and largely determined by creep effects in the concrete.

3.2.4 Swelling pressure determinations

3.2.4.1 Measurements

The Gloetzl cells recorded the total pressure, which appeared to be built-up rather irregularly both with respect to time and location. A major problem was caused by compression of the return tubings at high water and swelling pressures. Reliable values were therefore not obtained at later stages in all cells. Fig 3-9 demonstrates that the pressures tended to reach a maximum at the end of the test period, but that large differences prevailed. This diagram also shows that the drop in injection pressure from 3 MPa to 250 kPa gave a drop in total pressure of 2.75 MPa which certifies that the swelling pressure is the difference between total pressure and pore pressure.

The evaluated swelling pressures are given in Table 3-3, the reference numbers being those used in Table 2-2, which specifies the location of the cells.

Table 3-3 does not comprise pressures recorded at the concrete/bentonite interface since they showed large anomalies. A few valuable observations were made, however, the major one being that 10 out of 12 of the cells did not react when the water pressure was increased to 1 MPa and that 5 showed pressures lower than the applied water pressure throughout the test. This shows that the bentonite block system, which must have been exposed to this pressure had not established a uniform contact with the concrete and cells due to largely incomplete saturation even at the end of the test. Swelling pressures, some of them clearly erroneous, were only exhibited by 4 cells in the later part of the test, the maximum value being estimated at about 1 MPa.

Table 3-3. Evaluated swelling pressures in MPa

Cell, Ref no	Time after test start, months 5	10	15	20	Remark
7	1.4	1.8	2.0	-	
8	0	0	1.0	-	
9	1.0	0.8	1.2	-	
10	0.9	1.5	-	-	Rock/bentonite
11	1.9	2.8	3.7	-	
12	0.9	2.3	3.8	-	
13	1.7	1.7	2.2	-	
14	0.8	0.6	1.2	-	
15	0	0	0.1	0.1	
16	0	0	0.1	0.1	
17	0.2	0.2	0.4	0.5	Sand/bentonite
18	0.1	0.2	0.2	0.2	
19	0	0.1	0.2	0.2	
20	0.2	0.2	0.4	0.3	
27	0	0	0.1	0.1	
28	0	0	0.1	0.1	
29	0.1	0.2	0.3	0.3	Sand/bentonite
30	0.1	0.3	0.5	0.5	
31	0	0.2	0.3	0.3	
32	0	0.2	0.3	0.3	
33	0	0	1.0	2.0	
34	0	0	0.5	0.8	
35	1.0	1.6	2.5	3.0	
36	0.2	0.6	1.3	2.1	Rock/bentonite
37	1.4	3.8	4.2	3.9	
38	0	2.8	5.1	5.1	
39	0.2	3.0	4.5	5.2	
40	0	1.0	2.2	4.7	

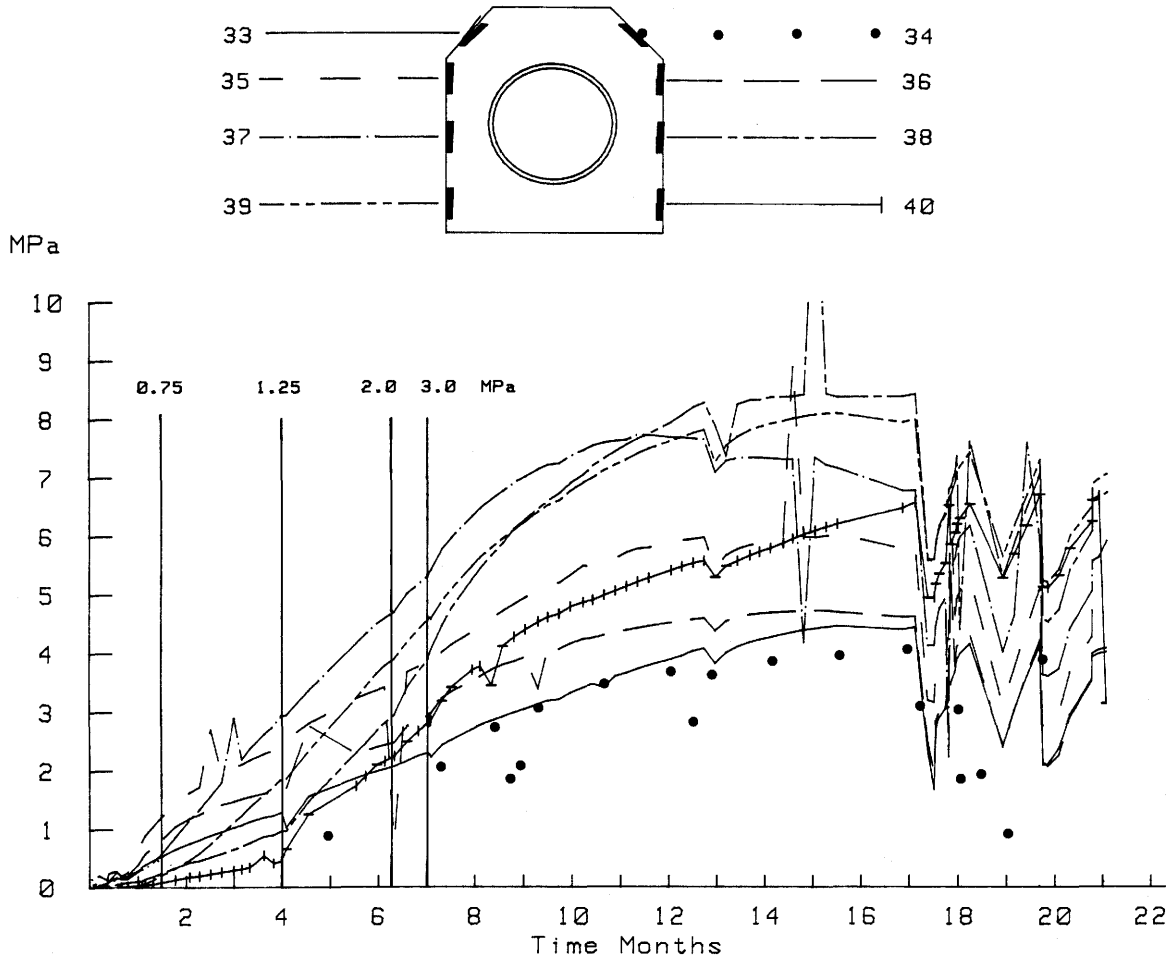

Figure 3-9. Recorded total pressures along the rock/bentonite interface at the inner plug

We see that the swelling pressure at the rock/bentonite interface ranged between 0.8 and 5.2 MPa at the end of the test, while the pressure at the sand/bentonite contact was substantially lower. No reliable pressure values were obtained from cells with reference numbers 7-14 after 20 months because of deformation and plugging of the return tubings.

Several conclusions can be drawn from the measurements:

* The majority of the swelling pressures recorded at the rock/bentonite interface were in the range of 0.2-1.4 MPa after 5 months and 1-2.5 MPa after 10 months, while most cells signalled pressures in the interval 1.5-3 MPa after 15 months. After 20 months, when all the cells except those at the front plug had reacted, the corresponding range was about 2-5 MPa. We find

that the recorded pressures were much lower than the predicted minimum values for 5 months testing time, while there was fair agreement between measured pressures and predicted minimum pressures for 15 months testing time. The values measured after 20 months generally ranged between the minimum and maximum predicted values.

* Except for the cell with Ref no 7, which was located at the wet pegmatite zone, all cells in the upper part of the plugs reacted slower and gave lower pressures than most of the cells in the lower part. The reason was very probably the reported difficulties in applying the bentonite blocks and fitting in bentonite powder in the upper parts. The associated higher porosity would explain the discrepancy in the rate of maturation and build-up of swelling pressures.

* The cells at the sand/bentonite interface all reacted at approximately the same rate. After 5 months only 50 % of the cells gave any pressure, while 70 % had reacted after 10 months, the values ranging between 0.1 and 0.2 MPa with one exception. After 15 months most values were still in the interval of 0.1-0.2 MPa, while the majority showed an increase to 0.2-0.3 MPa after 20 months. As expected, the slowest pressure build-up and the lowest pressures were recorded in the upper part of the plugs (Ref no 15, 16, 27 and 28). Here, the pressure did not exceed about 0.1 MPa, while the maximum value deeper down in the sand fill was 0.5 MPa at the end of the test.

* A close analysis of the recorded values at the rock/bentonite interface showed that the pressure build-up was very irregular. In some instances the pressure was rapidly developed and then dropped, after which it again increased, usually at a low rate. Several cells did not become activated until after almost a year and then indicated rapid and steady pressure build-up. This clearly demonstrated that the wetting and expansion was associated with fracturing and displacement of the bentonite blocks. The strong ability of the material to self-heal and become homogeneous would ultimately bring the pressure/time curves to merge into one narrow group. This latter process was probably about to begin when the test had to be terminated.

* The fact that the pressure build-up appeared to have stagnated after about 18 months indicates that the degree of saturation was rather high and that the maturation rate exceeded the predicted one.

3.2.5 Displacement of the sand/bentonite interface

A TV camera and a simple optical borehole inspection device were used a number of times to identify the displacement of the sand/bentonite interface. Since some adhesion of the clay to the plexiglass tubes was assumed to take place, no exact information of the displacement was expected. The measurements, which could be made with an accuracy of at least ±1 mm, gave the results in Table 3-4.

Table 3-4. Observed displacements of the sand/bentonite interface. Average of observations at each plug

Time after onset of test, months	Outer plug, cm	Inner plug, cm
5	3	3
10	5	4
15	6	5
20	7	5

The individual deviation from the average value at each time of observation turned out to be less than ±0.5 cm, which indicated that the expansion of the highly compacted bentonite was very uniform over the entire sand/bentonite interface.

3.3 MEASUREMENTS AT THE EXCAVATION

3.3.1 General

According to the original plans the central steel casing was going to be cut open at the termination of the test so that bentonite samples could be taken for determination of the actual water content distribution, and so that the exact displacement of the sand/bentonite interface could be measured. Also, a detailed investigation of the possible penetration of clay from the expanding bentonite into the voids of the sand fill was planned. This latter study was not conducted, however, since microscopic analyses of the interaction between the coarse sand type and the clay in the Shaft Plugging Test, that was terminated shortly before the present test, had clearly demonstrated that the penetration was totally negligible (1).

Access to the interior of the plug was obtained by cutting 3 m long and about 1 m high openings in the sides of the casing. The larger part of the sand fill could then be excavated so that the bentonite became available for sampling. The entire bentonite

front surface was exposed at the outer plug, while only its upper part was made available at the inner plug. The excavation was made stepwise so that the bentonite would not dry in the course of the almost 2 months long sampling operation. The lower, inner part of the sand fill was not removed since the clay sampling at the outer plug and at the upper part of the inner plug gave a sufficiently complete picture of the physical state of the bentonite.

A major observation at the sand excavation was that the sand completely filled the space between the plugs. Thus, no compaction of the loosely layered sand under its own weight had taken place.

3.3.2 Clay sampling

Once the sand had been removed from the upper part of the outer plug the sampling for water content determination was started. As in the Buffer Mass Test and Shaft Sealing Test systematic sampling was required and several techniques were used. A suitable way of taking somewhat larger samples than in these earlier tests was to make "core drilling" to about 5 cm depth and then break up the clay by a pneumatic spit so that the column-like clay cores could be removed without difficulty (cf. Figs 3-10 and 3-11).

The sampling was confined to the bentonite that surrounded the Gloetzl cells which were mounted onto the rock. Plane, vertical surfaces at about 7-10 cm mutual distance were exposed in the stepwise excavation for sampling of a total clay volume of about 0.15 m^3 at each cell. This generally gave 8 sampling levels and from each level 30 to 50 samples were taken, i.e. about 250 to 400 samples per cell. Sampling was made at all the cells of the outer plug and at 4 cells of the inner plug. For the sake of clarity only a fraction of the results will be presented here, namely those of the cells listed in Table 3-5. These cells were chosen because they represented largely different swelling pressures and rock conditions.

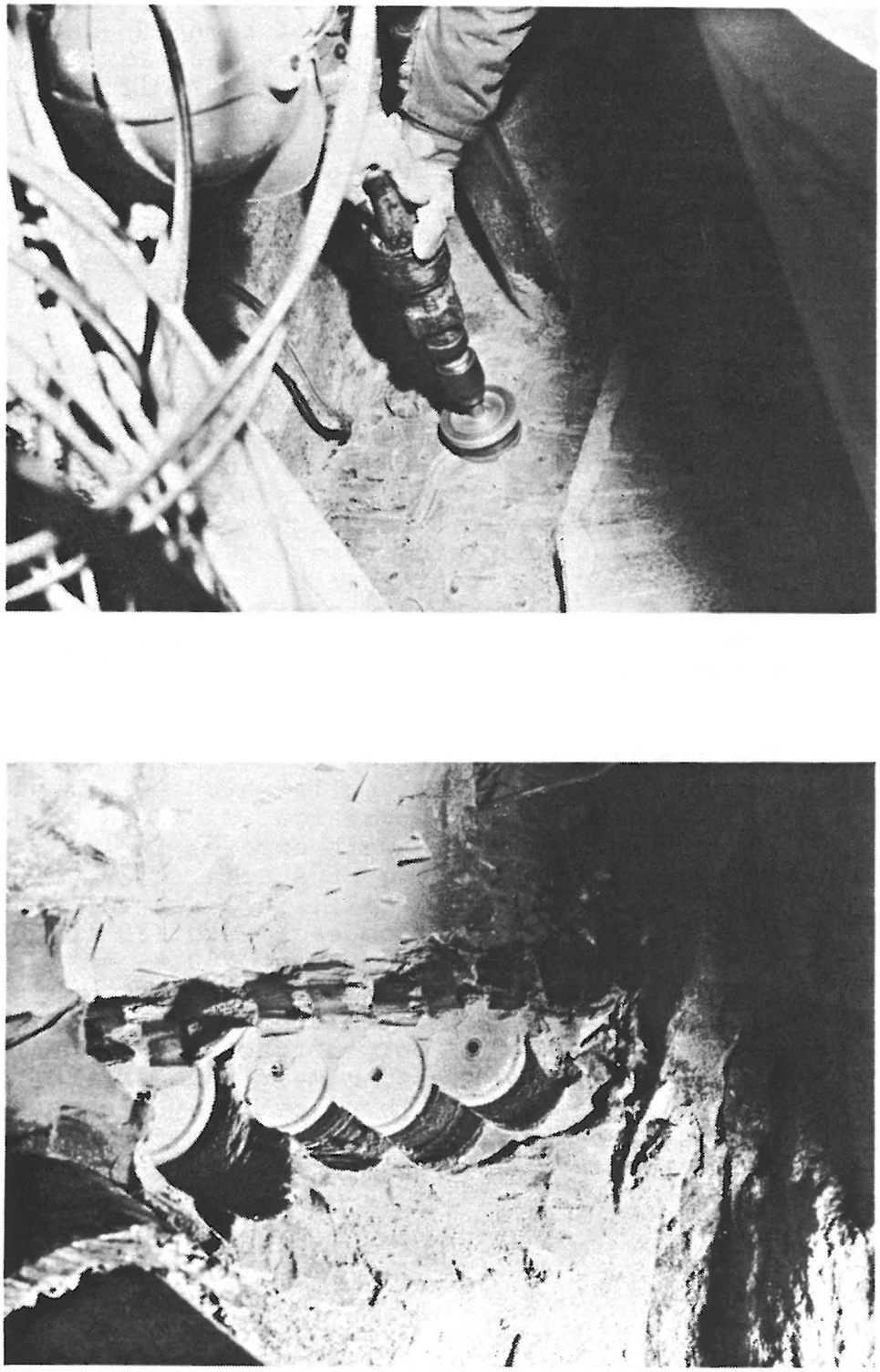

Figure 3-10. Clay sampling procedure. Upper picture shows the "core drilling", the lower exposed clay cores prepared for sampling

Figure 3-11. Excavation stages. Upper picture shows the clay surface before sampling, the lower removal of clay by use of a pneumatic spit. The latter technique was used also for taking samples

Table 3-5. Gloetzl cells at which excavation was conducted

Cell, Ref no	Maximum swelling pressure, MPa	Rock type
7	2.0	Pegmatite
8	1.0	Fracture-poor rock
9	1.2	Pegmatite
11	3.7	Fractured rock
12	3.8	Fracture-poor rock
34	0.8	Fracture-poor rock
35	3.0	Fractured rock

3.3.3 Water content distribution

3.3.3.4 Measurements

The water content values for each sampling level were plotted so that "isomoisture" curves could be derived as shown in Figs 3-12 to 3-26. These figures are representative examples of the evaluated moisture distributions, which will be discussed for each individual excavation site.

Cell no 7

For this cell 4 sections are shown. Fig 3-12 represents the conditions just beyond the sand/bentonite interface where the clay had absorbed much water and displaced the sand. As expected, the water content was high, ranging between about 70 and 120 %, which corresponds to a bulk density of approximately 1.4-1.6 t/m^3. The appearance of a stiffer, less wet region close to the rock is explained by wall friction, which prevented or delayed the expansion.

Fig 3-13 illustrates the wetting stage about 25 cm from the bentonite front. The clay contained a "dry" spot with a water content of about 25 %, the location of which indicates that wetting in general took place from three sources: 1) the sand fill, 2) the rock and 3) the concrete. At the rock there was a wet and soft zone of clay with a bulk density of only about 1.5 t/m^3. The soft consistency indicates that this space was not completely filled with bentonite blocks at the application, while a solid bentonite block was put in direct contact with the pad of the cell. It is clear that the cell (G) did not prevent water from migrating to this block, the bulk density of which had become about 1.85 t/m^3. This corresponds well to the recorded swelling pressure 2 MPa.

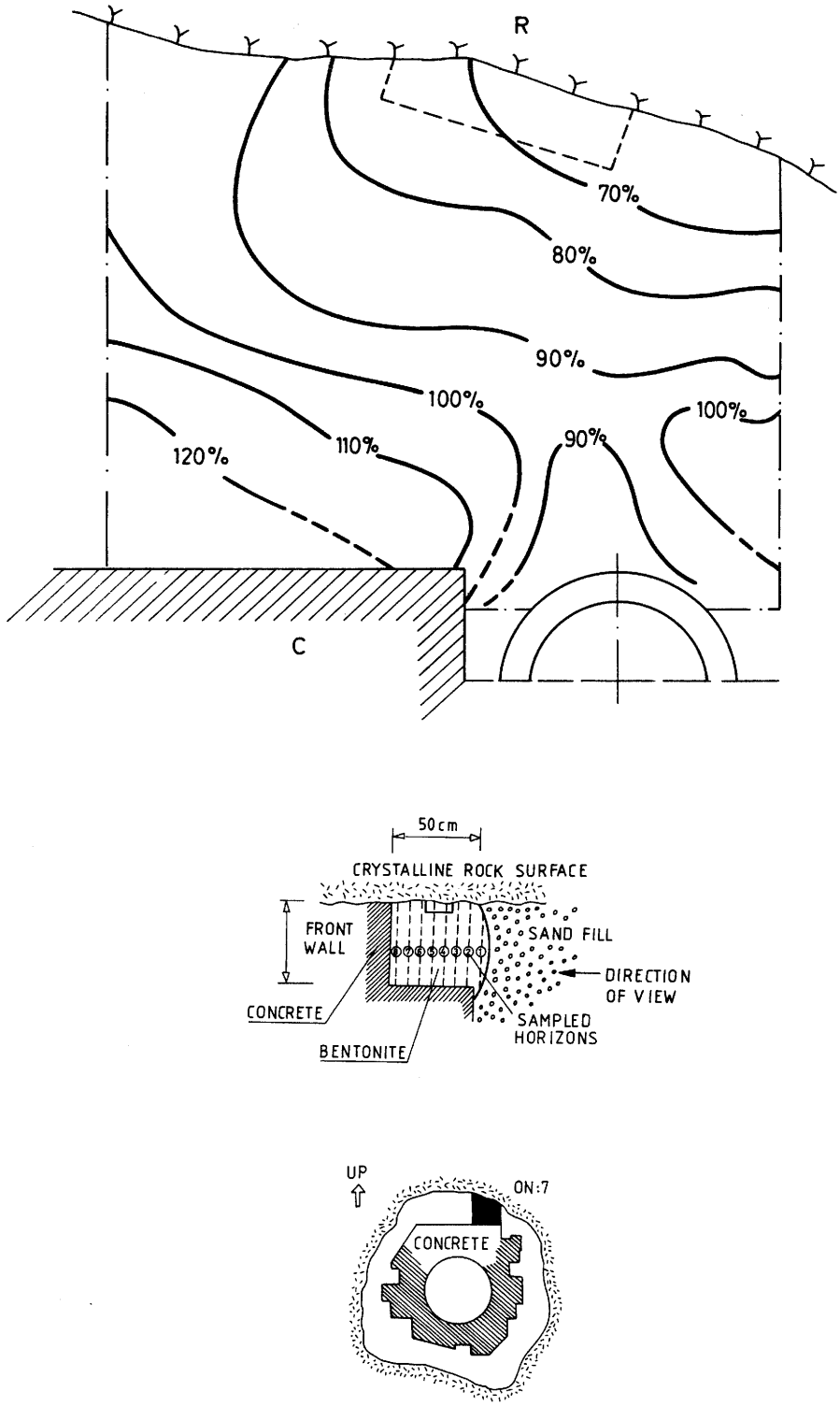

Figure 3-12. Water content distribution in a section perpendicular to the rock close to the sand/bentonite interface at Cell no 7

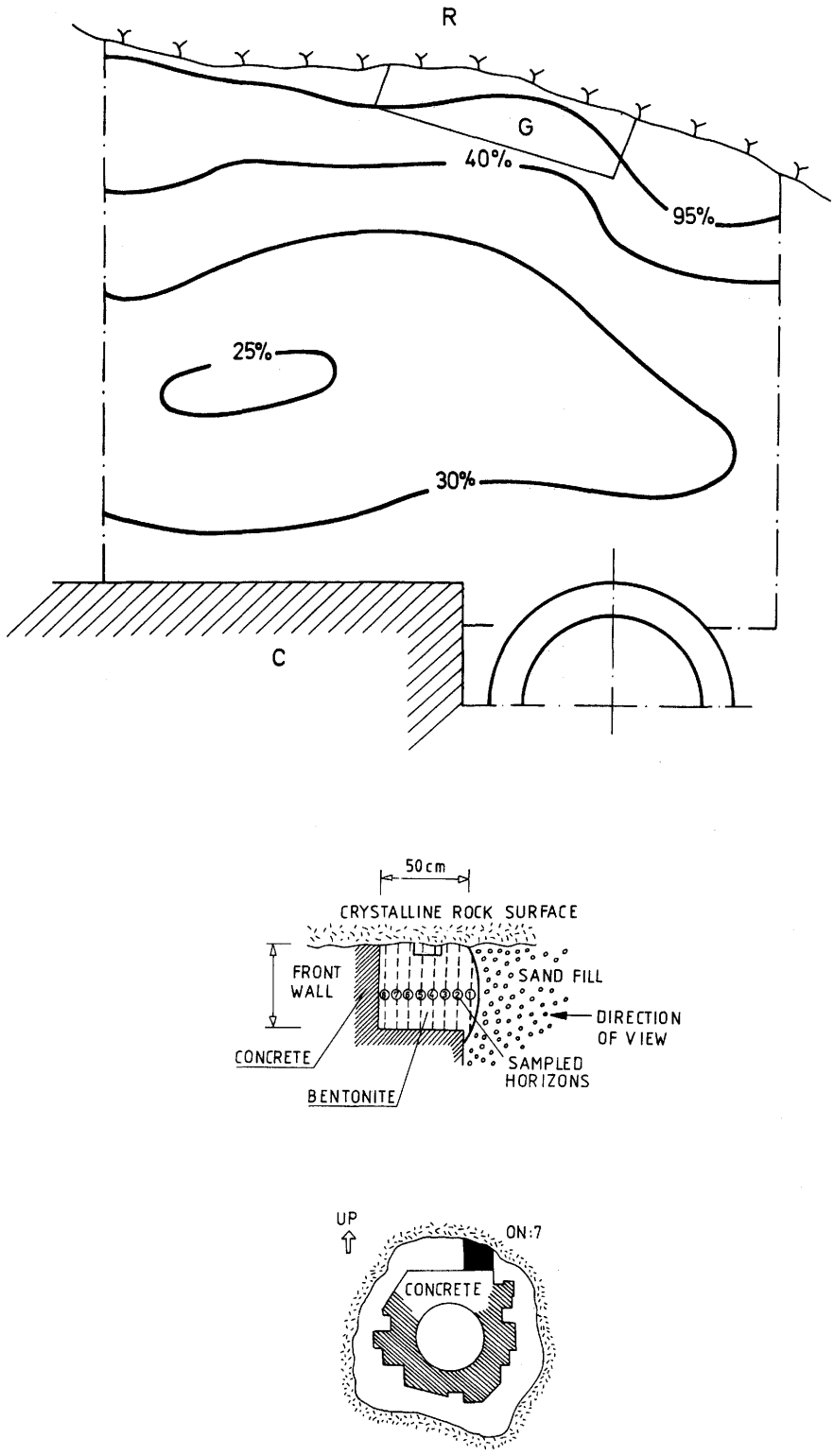

Figure 3-13. Water content distribution in a section perpendicular to the rock surface at Cell no 7

Fig 3-14 depicts the water content distribution about 40 cm from the bentonite front, i.e. just beyond the cell. Here, the bentonite was largely water saturated with a density of about 1.9 t/m^3, i.e. slightly less than the predicted density at complete water saturation. This stage was not expected to be reached at such an early stage, however, the discrepancy being explained by the fact that the concrete had served as a water source. No soft zone at the rock appeared here, which suggests that the initial degree of bentonite filling was high.

Fig 3-15 represents a section located about 10 cm from the inner end of the recess. The significant homogeneity and almost complete saturation demonstrates that the water absorption rate was much higher than predicted. The reason for this is that there were three wet boundaries, namely the rock as well as the end and side surfaces of the recess.

A general conclusion concerning the conditions at Cell no 7 is that the entire bentonite body had become largely saturated with a water content ranging between about 30 and 40 % in the larger part. This shows that the bulk density had become lower than expected which explains the relatively low swelling pressure 2.0 MPa. The low density was logically explained by the difficulty in filling the recess effectively with bentonite blocks at the installation. The bentonite had been effectively wetted from the water-bearing pegmatite as well as from the concrete.

Cell no 8

Fig 3-16 shows the water content distribution in the clay in a cross section through the cell. It is concluded that the clay was fully or largely saturated at the two wet boundaries, i.e. the rock and the concrete, while a large, central part of the bentonite had a degree of saturation of approximately 60-80 %. The slower wetting of the bentonite at this cell than at Cell no 7 may partly be explained by the very low frequency of fractures and fissures in the rock at Cell no 8. The low recorded swelling pressure 1.0 MPa is in accordance with the incomplete saturation.

Cell no 9

Fig 3-17 illustrates the distribution of the water content in the clay in a cross section through the cell. The pattern is very similar to that of Cell no 8 and is accordingly in good agreement with the low recorded swelling pressure 1.2 MPa. The reason for the low wetting rate is at least partly that

the pegmatite dike here is not at all as water-bearing as the one close to the crown of the drift.

Cell no 11

Fig 3-18 indicates that the bentonite was largely saturated and significantly homogeneous at Cell no 11 and that the bulk density was relatively high, i.e. about 1.95 t/m^3, which is also in fair agreement with the recorded, relatively high swelling pressure 3.7 MPa. The high density may be explained by the fact that the pad of the cell and the concrete surface were parallel, by which the bentonite blocks could be fitted together in a tight pattern. This yielded insignificant swelling and fast water uptake and development of reaction pressures, which resulted in the high swelling pressure. It is noticed that the concrete served as a water source in addition to the rock which was rich in fractures at this location. This contributed to the fast maturation of the bentonite.

Cell no 12

Fig 3-19 indicates that the bentonite was uniformly wetted and relatively homogeneous with a high degree of water saturation. The density was about 2.0 t/m^3, which corresponds well with the recorded swelling pressure 3.8 MPa. The reason for the high density is the geometry of the bentonite-filled space, as in the case of Cell no 11.

Cell no 34

Fig 3-20 demonstrates that the water content varied in approximately the same way as at Cell no 8, which would suggest a low swelling pressure. The very irregular shape of the concrete probably led to a porous and incomplete filling of bentonite blocks and fragments, which suggests that reaction pressures were mobilized at an even slower rate than at Cell no 8. This in agreement with the low swelling pressure 0.8 MPa.

Cell no 35

Fig 3-21 shows a water content pattern which is very similar to the uniform distribution at Cell no 12, although the present water content values are somewhat higher and the bulk density consequently lower. The degree of homogeneity was rather high, suggesting a fairly high swelling pressure, especially since the geometrical conditions offered a possibility of fitting in the bentonite blocks in a tight fashion as at Cells no 11 and 12. The recorded swelling pressure 3.0 MPa supports this hypothesis.

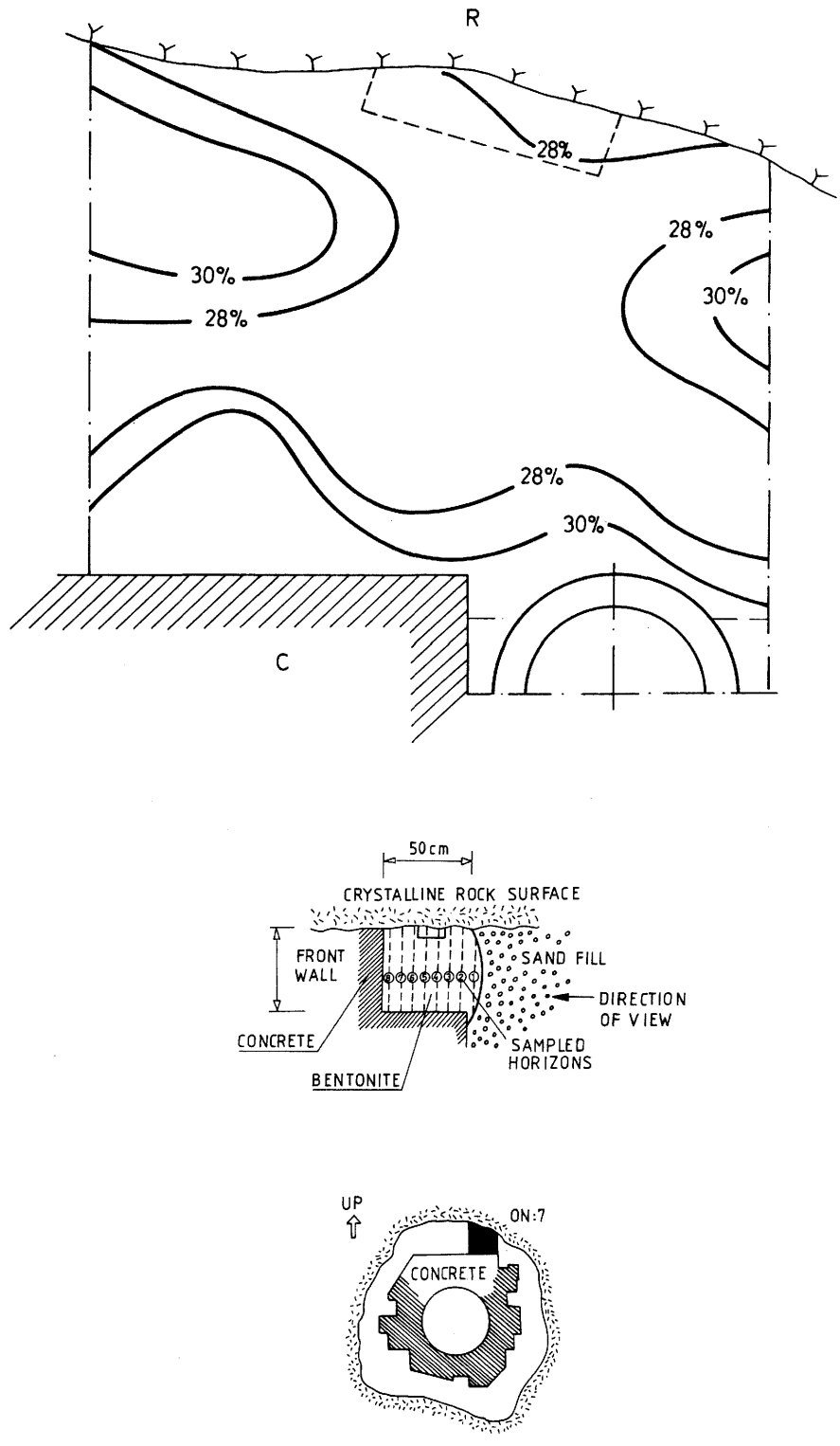

Figure 3-14. Water content distribution in a section perpendicular to the rock surface about 40 cm from the bentonite front at Cell no 7

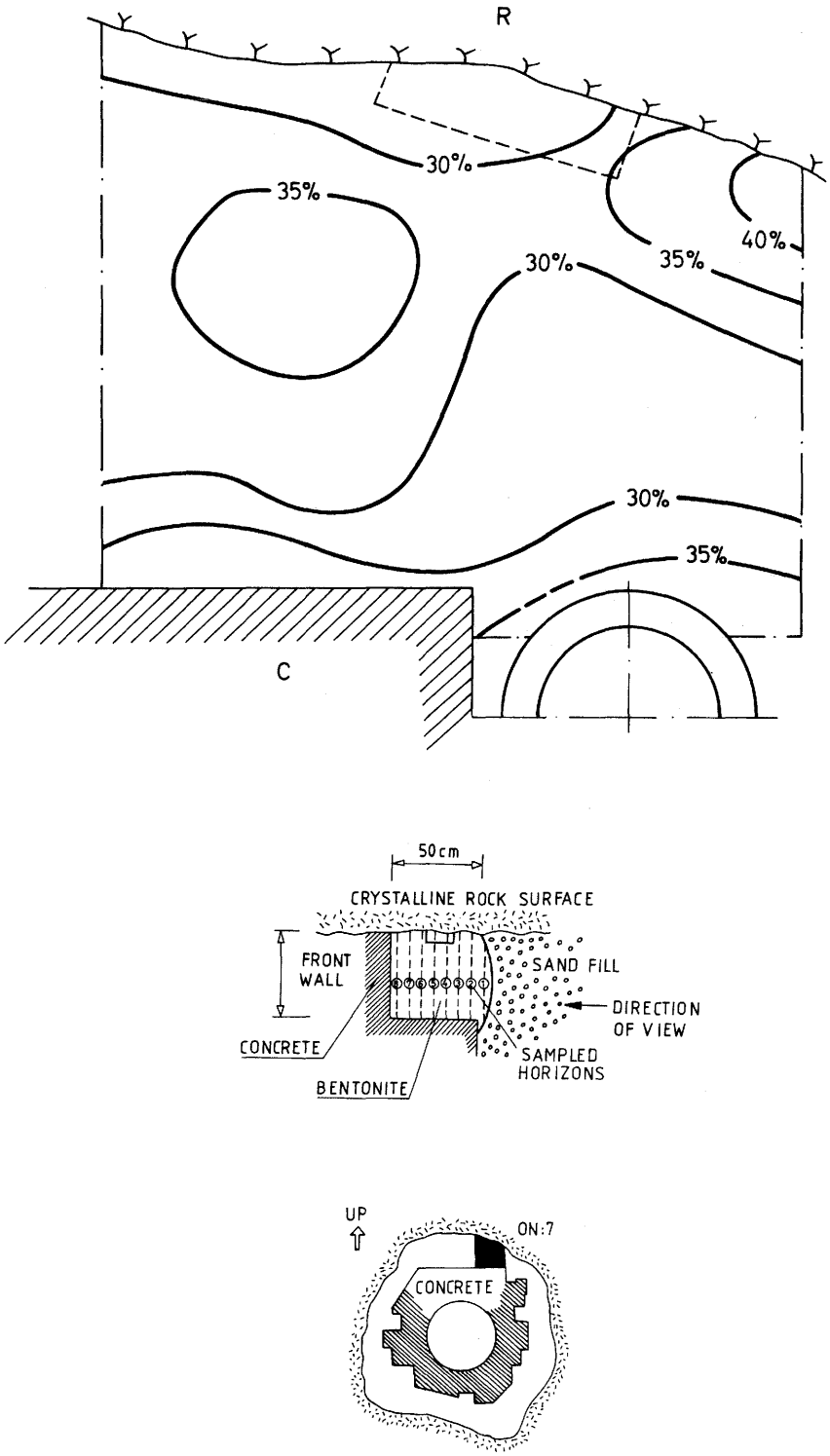

Figure 3-15. Water content distribution in a section perpendicular to the rock surface close to the inner end of the bentonite body at Cell no 7

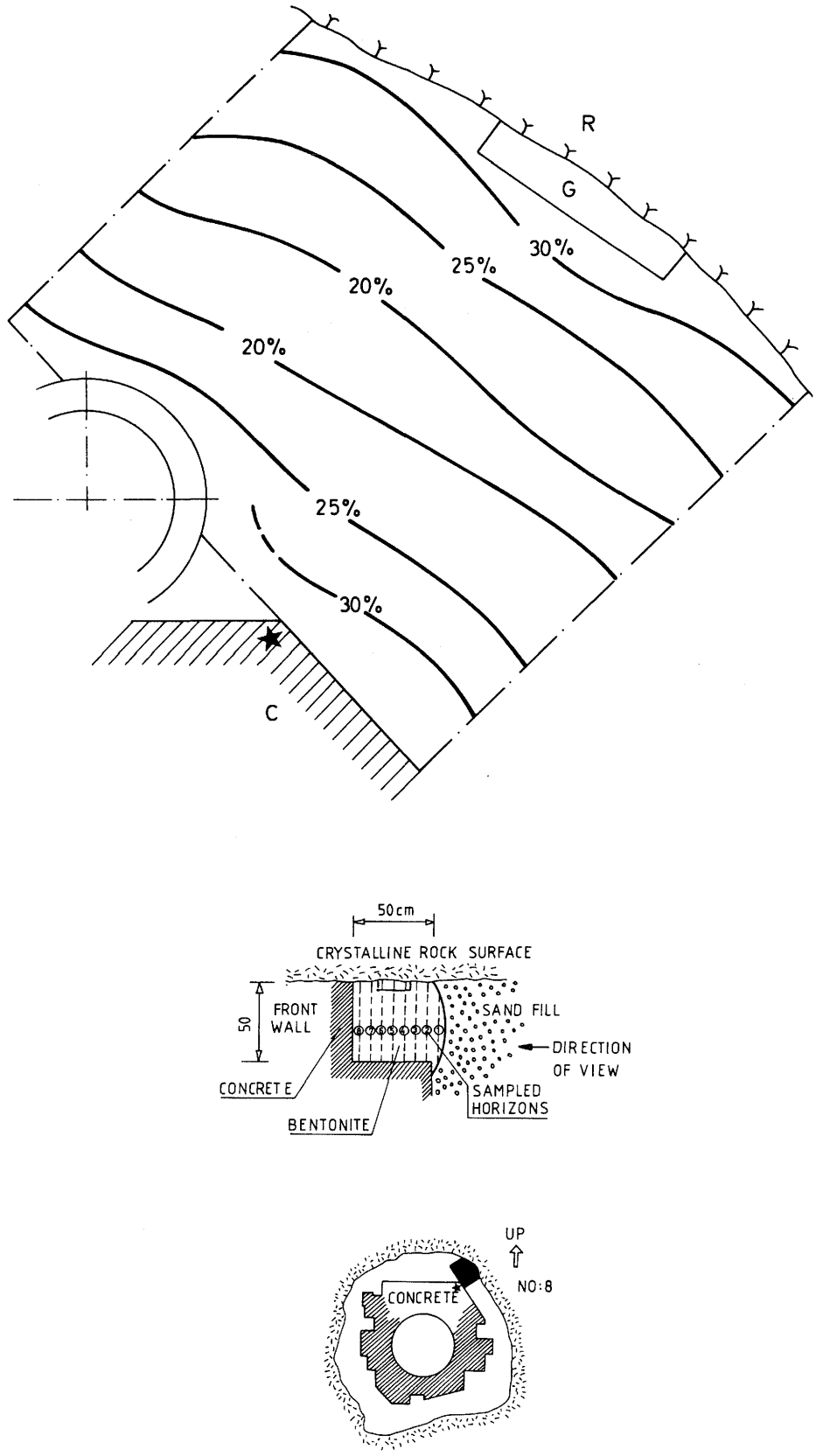

Figure 3-16. Water content distribution in a section perpendicular to the rock surface at Cell no 8

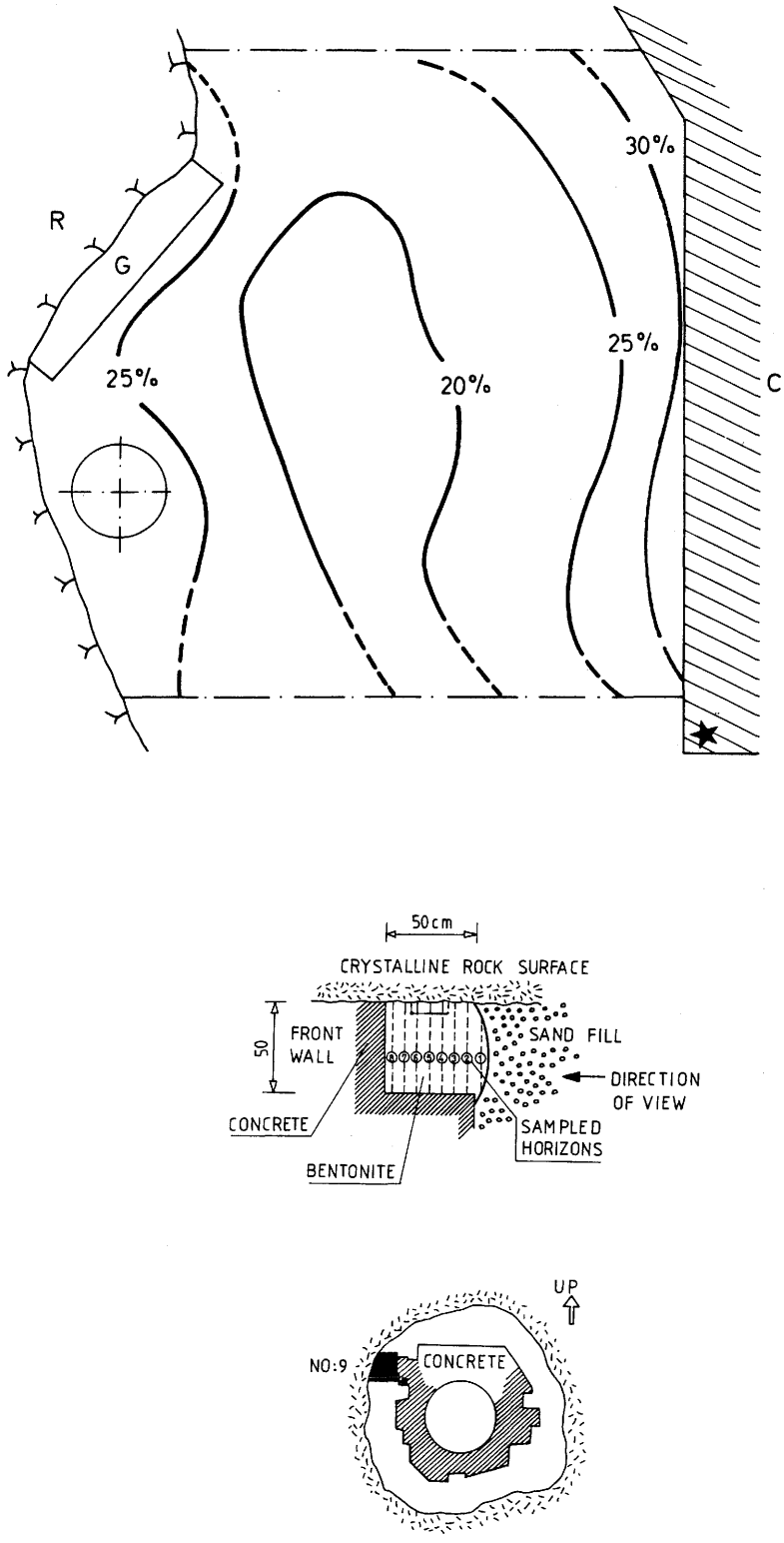

Figure 3-17. Water content distribution in a section perpendicular to the rock surface at Cell no 9

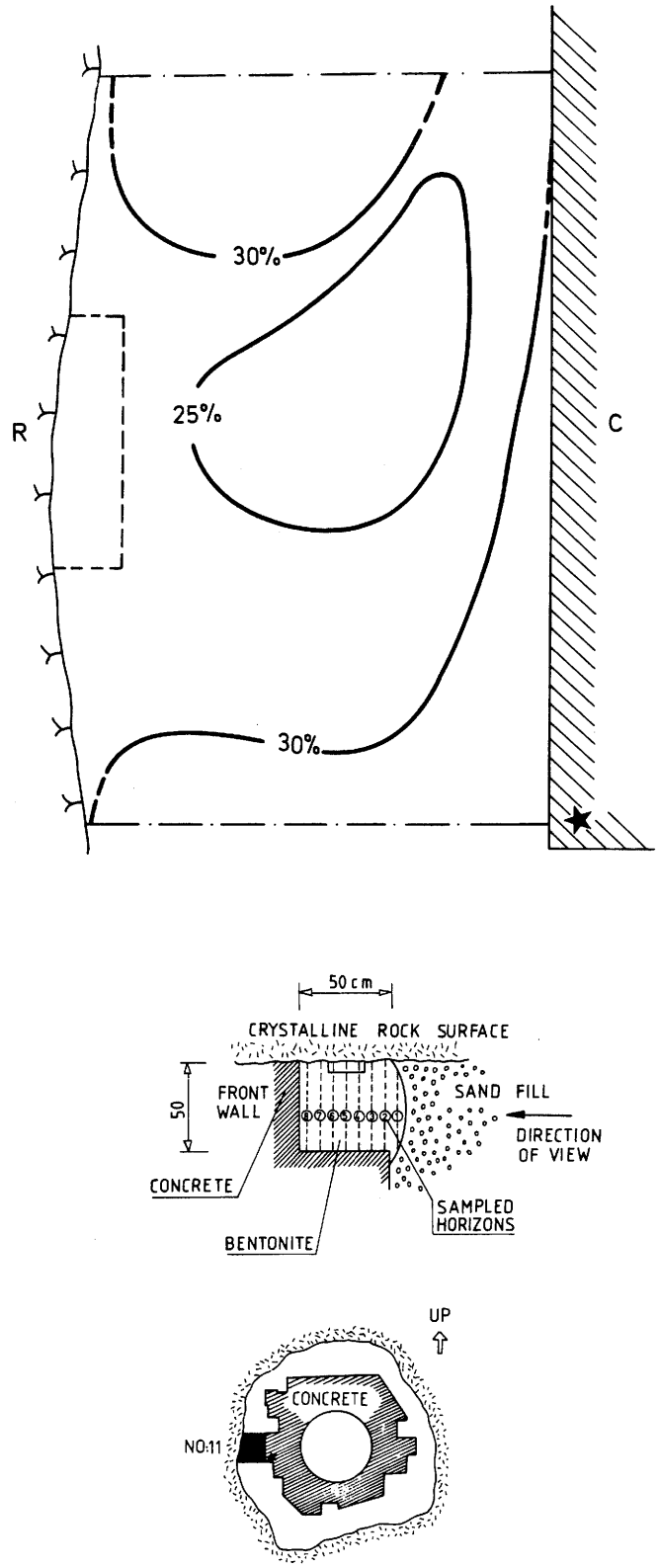

Figure 3-18. Water content distribution in a section perpendicular to the rock surface at Cell no 11

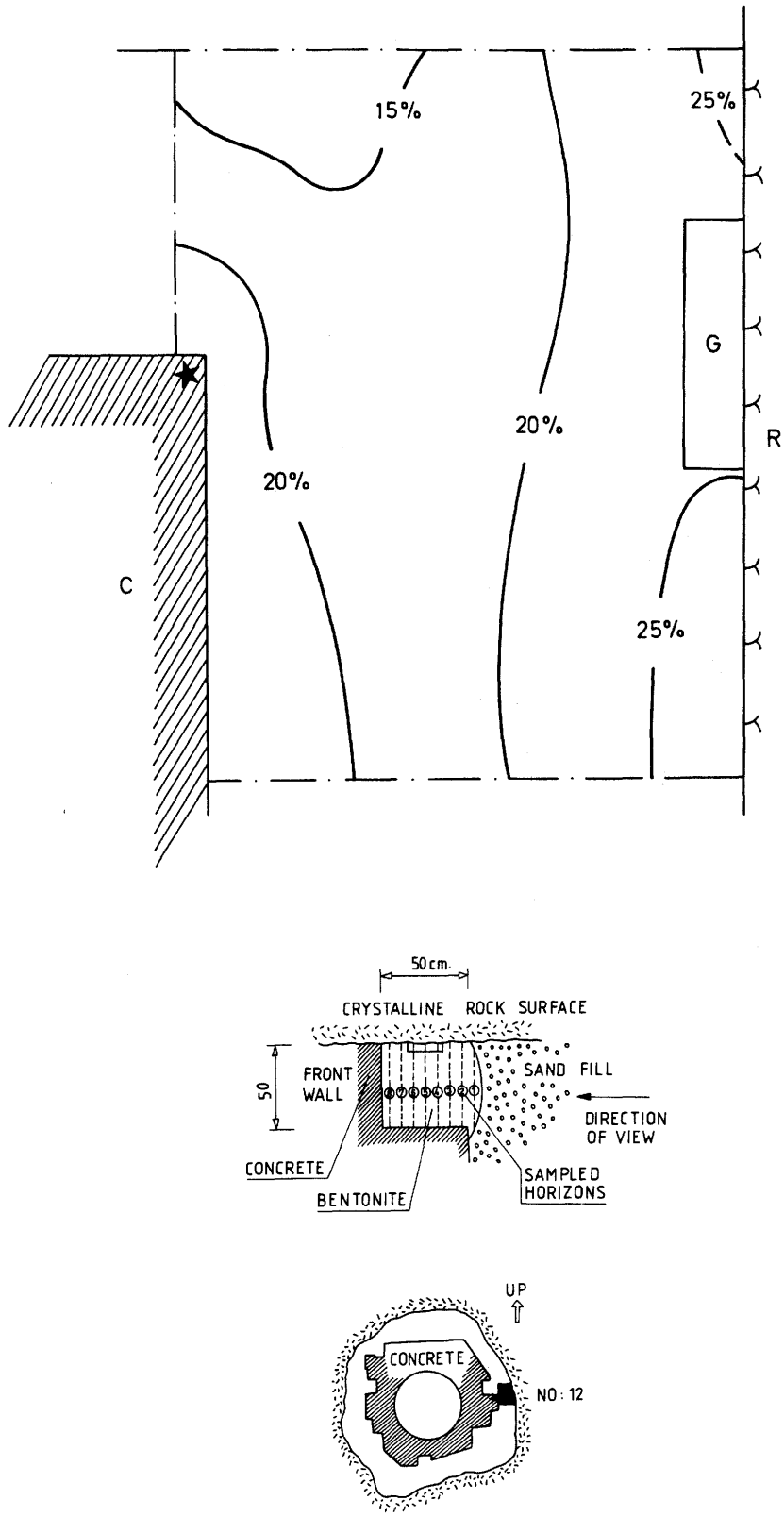

Figure 3-19. Water content distribution in a section perpendicular to the rock surface at Cell no 12

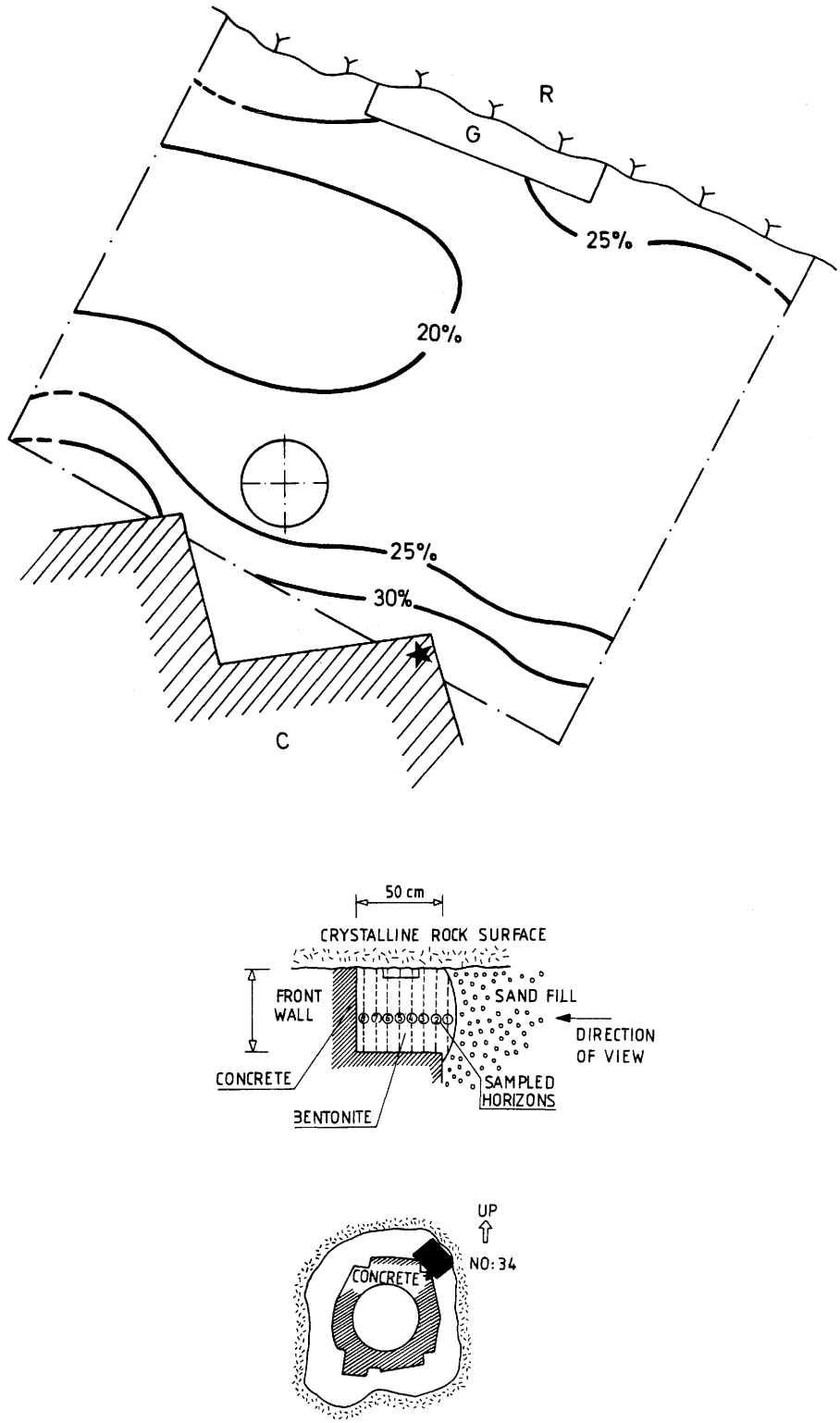

Figure 3-20. Water content distribution in a section perpendicular to the rock surface at Cell no 34

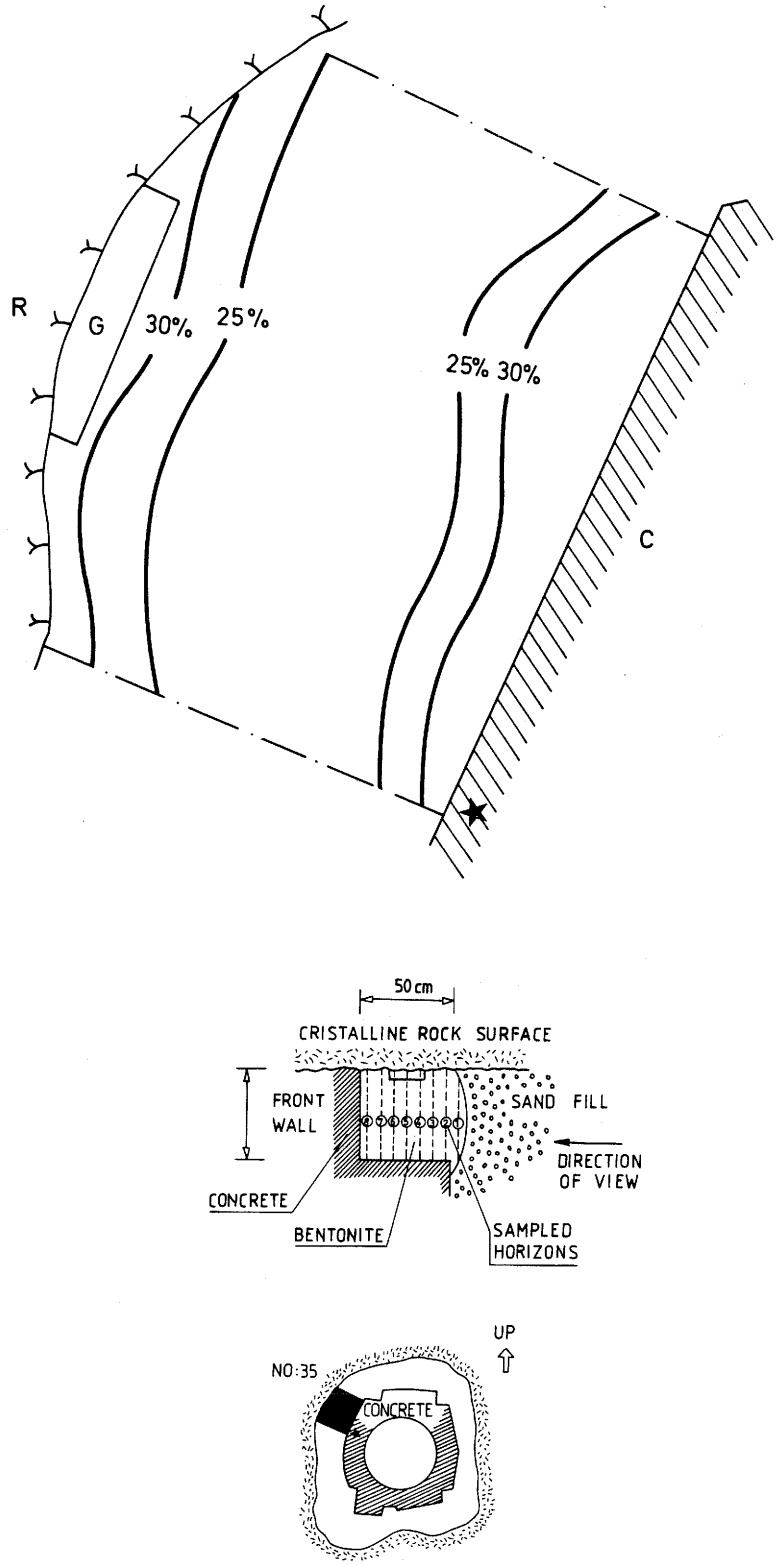

Figure 3-21. Water content distribution in a section perpendicular to the rock surface at Cell no 35

3.3.3.5 Conclusions

While the swelling pressures appeared to vary in a largely random way at a first glance, a detailed analysis showed that the varying pattern is explained by the different conditions at each cell:

* The degree of filling of the recess with bentonite blocks and fragments is the major determinant of the swelling pressure because it controls the bulk density. Thus, a complex geometry makes it difficult to fit in blocks in a tight pattern and this yields a high porosity and low net bulk density, while a simple space with parallel boundaries allows for a high degree of filling.

* It appears that water migration was considerably delayed in bentonite block fillings that contained irregular, large voids and wide joints. In well fitting block systems like those at Cell no 11, 12 and 35, the water uptake is governed by the diffusion model, while the large swelling of loosely arranged bentonite blocks or fragments that is required to yield continuity in the system is time-consuming and retards the wetting, as in the case of Cells no 8, 9 and 34

* The frequency of fractures in the rock is not a major factor for the rate of wetting when the rock water pressure is high and when the clay is effectively confined by the rock. However, for porous bentonite fillings a faster wetting by richly inflowing water from fractures will increase the maturation rate

* In most cases, the water uptake process was not disturbed by the pressure cells but in a few instances it can be seen that they served as shields and caused a slightly slower maturation of the bentonite adjacent to the pads than around them

* It was a surprise that the concrete served as an effective water source for the clay since its permeability and water retention capability are usually considered to be similar to those of moderately dense bentonite. The fact that the concrete still behaved as a wet boundary suggests that even high quality concrete has a significant hydraulic conductivity. Possibly, stress-induced fissuring and fracturing can have taken place in the concrete, by which passages for water may have been formed

* The experimentally determined high degree of saturation of the bentonite is in good agreement with the earlier conclusion that the swelling

pressures appeared to approach a maximum value. No further significant improvement in the sealing ability of the bentonite could therefore be expected even if the test had been extended over a long period of time.

3.3.4 Displacement of the sand/bentonite interface

The displacement of the bentonite front was found to be very uniform. It amounted to 10-12 cm in the upper part of the outer plug and to 8-10 cm in the lower part (Fig 3-22), which is in excellent agreement with the predictions. The excavation also showed that the expansion of the bentonite had not only moved the sand/bentonite front forwards, it had also displaced the sand laterally, "round the corner" as shown in Fig 3-23. This fabulous behavior is a good indication of the property of dense highly compacted Na bentonite to expand isotropically.

Figure 3-22. Appearance of the expanded bentonite. Some sand grains stick to the clay surface

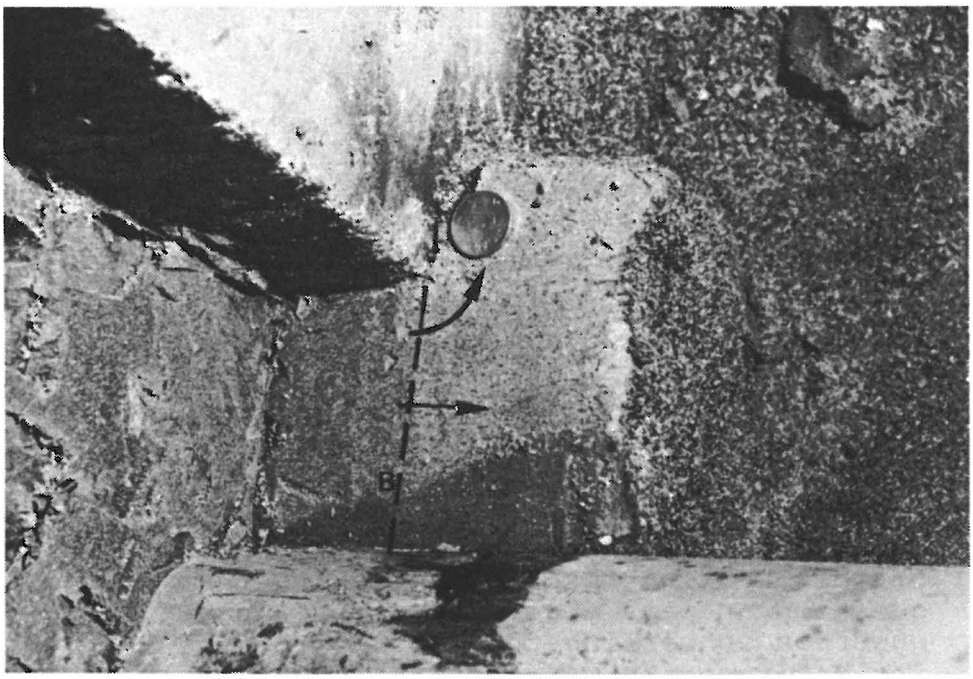

Figure 3-23. Example of expansion "round the corner" of the bentonite as observed in the course of the clay sampling. Arrows indicate swelling directions, B represents the initial sand/bentonite interface

4 DISCUSSION AND CONCLUSIONS

4.1 GENERAL ASPECTS

The strong sealing ability of highly compacted bentonite was obvious in the Borehole and Shaft Sealing Tests, which involved application of rather carefully prepared bentonite blocks that were arranged in a tight fashion. The practical difficulties in getting the same well-fitting block arrangement in the Tunnel Sealing Test resulted in strong local variations in density but the sealing power of the bentonite was still very substantial. This demonstrates the usefulness and practicality of this sealing technique, meaning that the first question on page 6 got a positive answer. The question concerning the validity of the BMT model for water uptake was certainly answered positively, and that concerning piping and erosion of the clay got the answer that no such effects appeared. This means that only the points concerning the sealing effect of swelling pressures and penetration of clay into fractures remain to be answered and they will be considered in this chapter. It has an introduction which is pertinent to the whole project, namely a short description of the detailed hydration and expansion processes, which yield matured clay of various density that has been found to serve as a very effective seal in all the Stripa tests.

4.2 HYDRATION AND SWELLING

4.2.1 Smectite/water association

The exact nature of the uptake of water by the smectite mineral montmorillonite is still not completely understood since this process is very much dependent on the crystal lattice constitution of this mineral, of which there are two possible versions (Fig 4-1). The hydration of the Edelman & Favejee structure has been explained by Forslind et al (7) as the formation of an ice-like water lattice that grows from the protruding hydroxyls of the basal planes when the interlamellar cations are monovalent and small (Li and Na) and when the temperature is below about 100°C. A number of metastable and stable states of the H-bonded lattice may thereby be established. This model, which has received considerable support in recent years, offers an explanation also of the chemical

changes that are associated with heating ("beidellitization"). This latter matter has been treated in some detail in the final BMT report (8).

The wetting of the Hofmann, Endell & Wilm structure, which is conventionally referred to, is associated with the hydration of interlamellar cations. When wetting is initiated, water is first assumed to be distributed over external surfaces of stacks of lamellae ("domains") and then to yield successive hydration of the interlamellar space.

Like in the case of the Edelman & Favejee model, interlamellar water lattices may be established on wetting of the Hofmann, Endell & Wilm structure but the spatial arrangement of the water molecules is largely determined by the position of interlamellar exchangeable cations, which in turn depends on the location of the deficit of positive clay lattice charge. The orientation and mutual interaction of the water molecules as well as their association with the interlamellar cations and the crystal lattice are altered in the successive build-up of interlamellar hydrates, the expected degree of ordering being low, particularly of the second and third hydrates. The Hofmann, Endell & Wilm structure is assumed to be valid at temperatures exceeding about 100°C. Thus, a temperature increase in a repository from a few centigrades to 100°C is expected to yield a contraction of the montmorillonite stacks and an associated growth of voids, whereby the hydraulic conductivity and creep rate of the clay increase significantly.

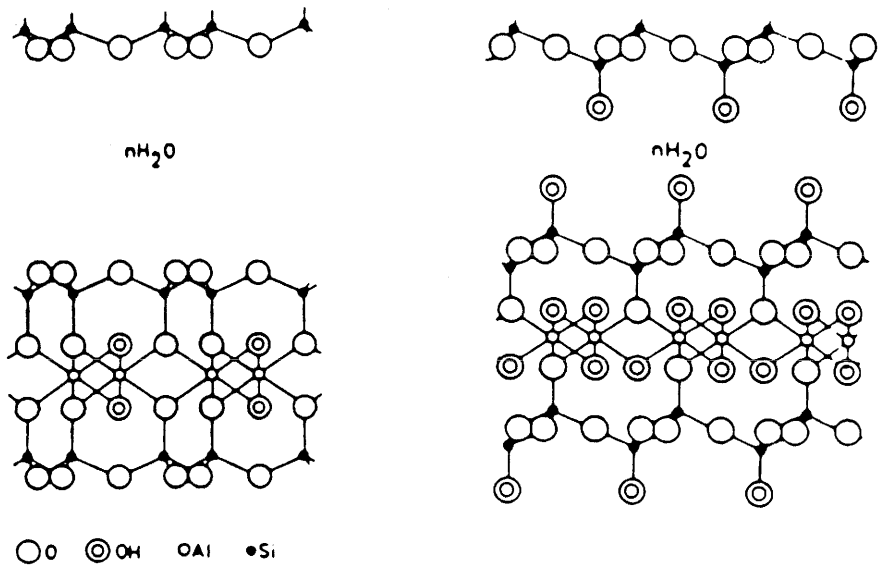

Figure 4-1. The two montmorillonite versions
Left: The Hofmann, Endell & Wilm structure
Right: The Edelman & Favejee structure

Recent investigations indicate that expansion from a condensed state of the montmorillonite stacks, like that of the air-dry highly compacted blocks of MX-80 bentonite, proceeds to a maximum interlamellar distance corresponding to three water molecule layers, and that further swelling is produced by separation of the expanded stacks by which double-layer interaction takes place at their interfaces (Fig 4-2). This leads to reorientation and partial splitting of the stacks and growth of pores so that the swelling clay forms a very soft gel, which is the character of the front part of the bentonite that penetrates into fractures (Fig 4-3). The latter figure demonstrates that the groups of flakes form a regular honeycomb-like pattern with no large pores, which explains why the hydraulic conductivity under fresh-water conditions is relatively low, i.e. 10^{-6}-10^{-8} m/s even when the density is as low as 1.1-1.3 t/m^3. We conclude from this, that fractures into which Na montmorillonite has penetrated, as in the various Stripa sealing tests, become virtually impermeable even if the gel density is very low. Detailed, recent analyses of the physical state of Na montmorillonite pore-water are given in (9).

As to the hydration and homogenization of blocks of highly compacted bentonite which are confined, the dense granules consisting of aligned smectite flakes expand and yield a largely homogeneous microstructure with only very few wide continuous pores. The general pattern of stacks of parallel flakes is preserved as long as the bulk density does not drop below about 1.8-1.9 t/m^3 (Fig 4-4).

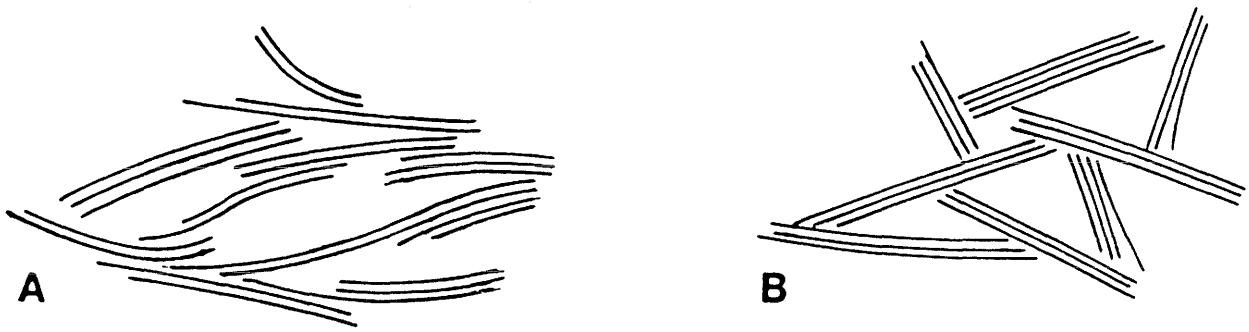

Figure 4-2. Microstructure of Na smectite clay at low bulk densities. State A is assumed to result from expansion from denser states, while state B is most probable for sediments formed by successive association of discrete particles

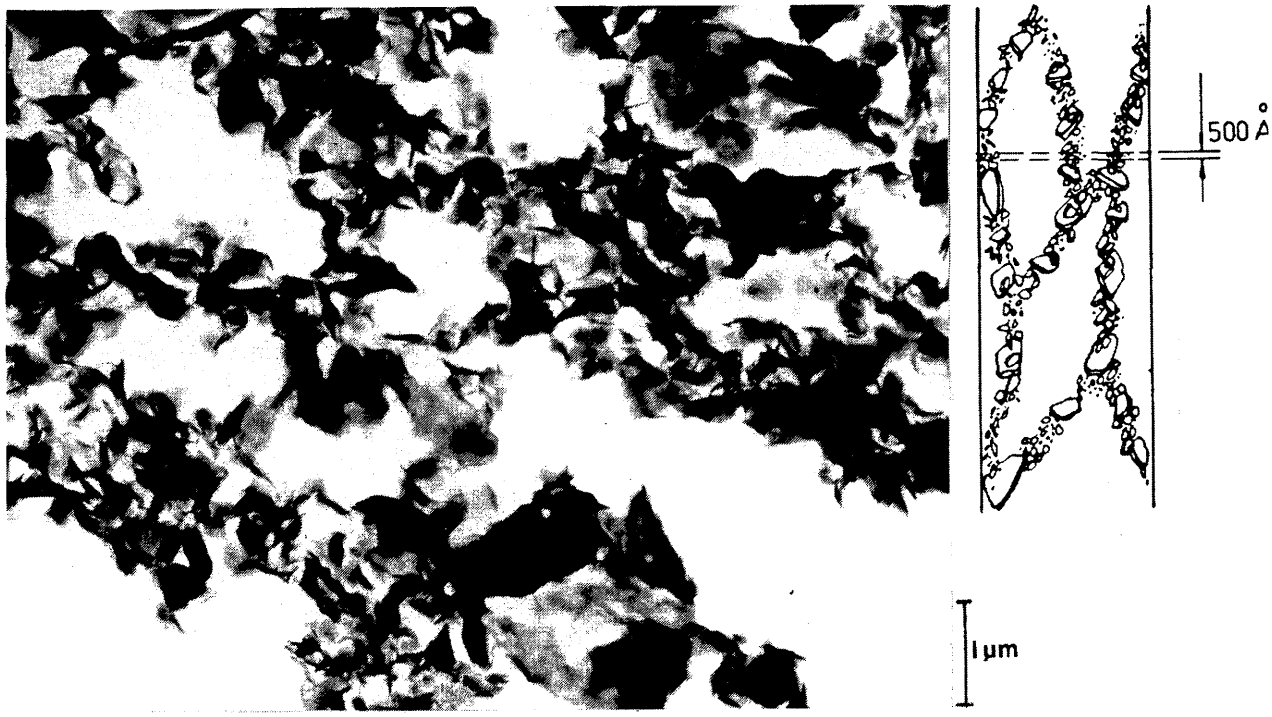

Figure 4-3. Transmission electron micrograph of ultrathin section of commercial sodium bentonite (GEKO/QI) expanded to a density of about 1.3 t/m^3 in water saturated state. The section is illustrated in the tactoid-type structure suggested for water-rich clays (10)

Figure 4-4. Schematic particle arrangement in highly compacted Na bentonite granules. Left picture: powder grains in air-dry state. Right picture: "homogeneous" state after saturation and particle redistribution

A=particle aggregate, a=large interparticle void, b=small interparticle void, c=interlamellar space

4.2.2 Clay/rock interaction

4.2.2.1 Processes at the rock/bentonite interface

In all the sealing tests in Stripa, blocks of highly compacted Na bentonite were applied relatively close to but usually not in direct contact with the rock. The general physical model of water uptake and swelling for such constellations, which was derived in the evaluation of the Buffer Mass Test, has the following main features: Water initially flowing from fractures causes rapid local swelling of the bentonite which blocks the inflow openings and force water to follow "second order" fissures. They in turn become sealed by which water is directed to flow through the finest passages like fine fissures and incomplete crystal contacts.

The detailed process is that shown in Fig 4-5. The first stage is the imbibition of water and growth of a soft clay gel that fills up the space between the rock and the yet not wetted, dense bentonite. The second stage is the migration of water from the rock through the soft gel into the dense bentonite in which a high porewater tension is set up. The bentonite expands successively and exerts an increased pressure on the soft gel which consolidates. Ultimately, a homogeneous and fully saturated dense clay mass is formed.

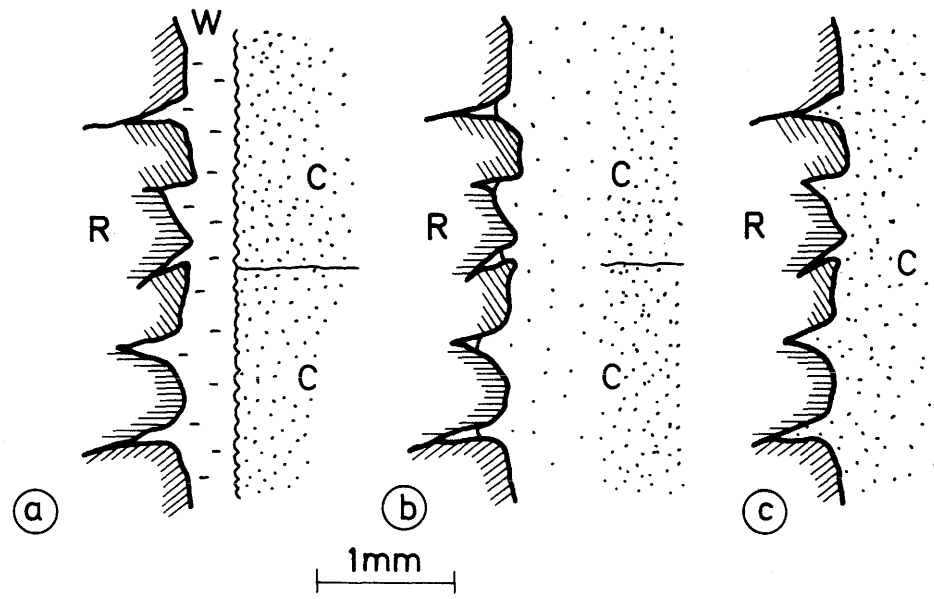

Figure 4-5. Schematic picture of clay penetration into the rock matrix and formation of a tight clay/rock contact. a) Clay blocks in position, starting point. b) Early stage of expansion. c) Final stage with integrated clay (c) and crystal matrix (R). W represents water, C bentonite, and R rock

When the initial rock/bentonite fitting is relatively good, as in the case of borehole plugs and plugs in raise-drilled shafts, the initial stage lasts for a short time only. This is illustrated by the Buffer Mass Test which indicated that swelling pressures built up by initiation of the consolidation process were significant already a few weeks after the onset of the wetting, the free space between the rock and clay blocks being about 10 mm. The fit between the rock and the bentonite blocks and fragments was not at all as good in the Tunnel Plugging Test and the consolidation of the soft boundary zone was therefore slower at several cells, the most obvious example being Cell no 7 (Fig 3-13).

Even where there were still significant differences in water content and hence incomplete homogenization at the excavation, the initial joints between the individual bentonite blocks could not be seen. Fig 4-6, which was taken at the rock/bentonite interface in the upper part of the tunnel, illustrates the absence of discontinuities and it also shows how completely the expanded bentonite contacts the rock, leaving no openings at the interface.

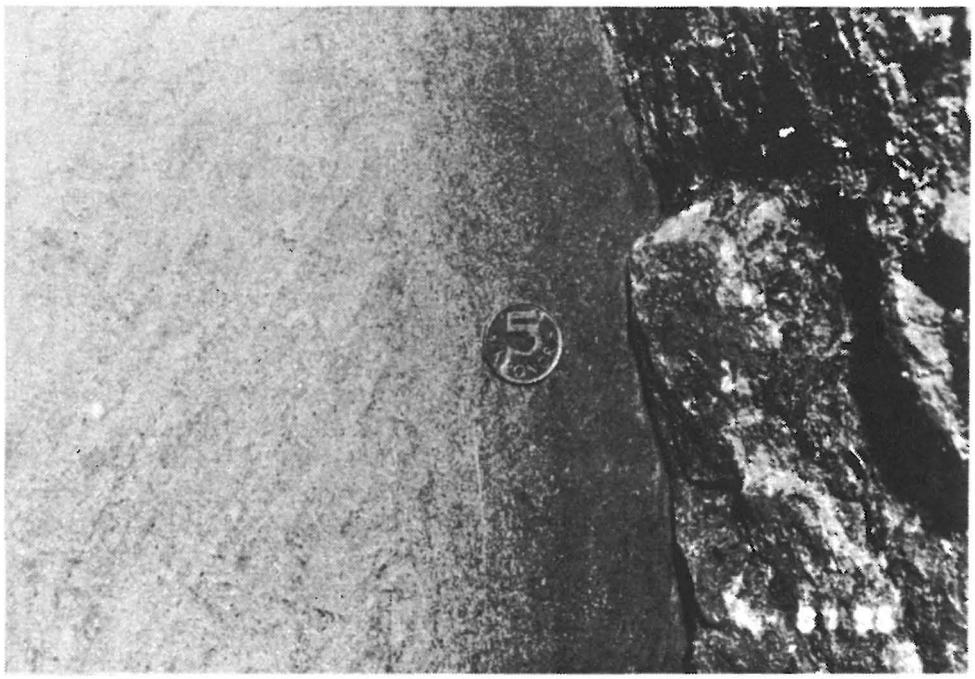

Figure 4-6. Typical appearance of the rock/bentonite interface at the end of the test. The contact is complete and no joints or discontinuities can be seen

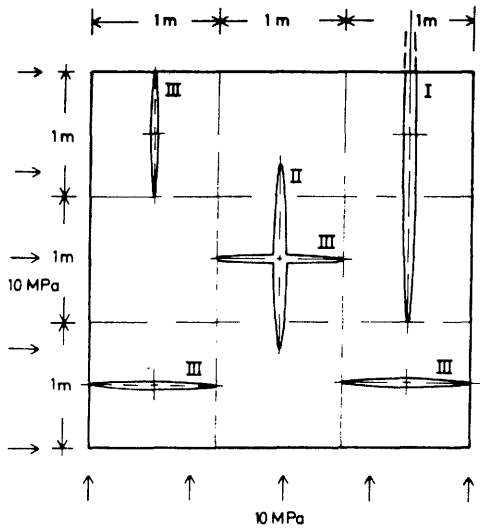

Fracture sets:	I	II	III
Long diameter	a=3.0 m (truncated)	a=1.5 m	a=1.0 m
Short diameter	c=1.5x10^{-4} m	c=1.5x10^{-4} m	c=10^{-4} m

Figure 4-7. Schematic cross section through rock model with stochastically varied fracture geometry (11). Example with isotropically loaded element

4.2.3 Effect of swelling pressure on the hydraulic conductivity of the rock

There is no generally accepted theory or model for calculating the influence of the normal stress on the permeability of rock fractures, and the matter is continuously worked on in many countries. Preliminary calculations have been made using a simple model of ellipsoid-type voids simulating natural fractures (Fig 4-7 and 4-8) and literature-derived relationships between normal pressure and fracture aperture (10). As concluded from Chapter 2.3.3 and Fig 2-15 it is obvious that mainly the steep fracture termed I and equally oriented ones in the northern and southern tunnel walls at the outer plug can be affected by a swelling pressure exerted on the rock. Taking the swelling pressure to be 2.7 MPa as an average (Cells no 9, 10, 11, 12 and 13) and assuming that complete release of the normal stress had been caused by the excavation process, we find by applying the afore-mentioned model that the aperture would be reduced by about 10-30 % and the conductivity by at least 50 % due to the swelling pressure. According to the predictions, the total leakage through the steeply oriented fractures in the tunnel walls and tunnel floor amounts

to about 50 % of the total leakage. Assuming that the steep fractures in the tunnel walls are responsible for half of this leakage we then find that the pressure-induced reduction by 50 % reduces the total leakage by only 10-15 %. This suggests that the large part of the 60 % reduction of the total leakage was caused by the sealing of the pegmatite zone. The deductions in the subsequent chapter illustrate that this may well have been the case.

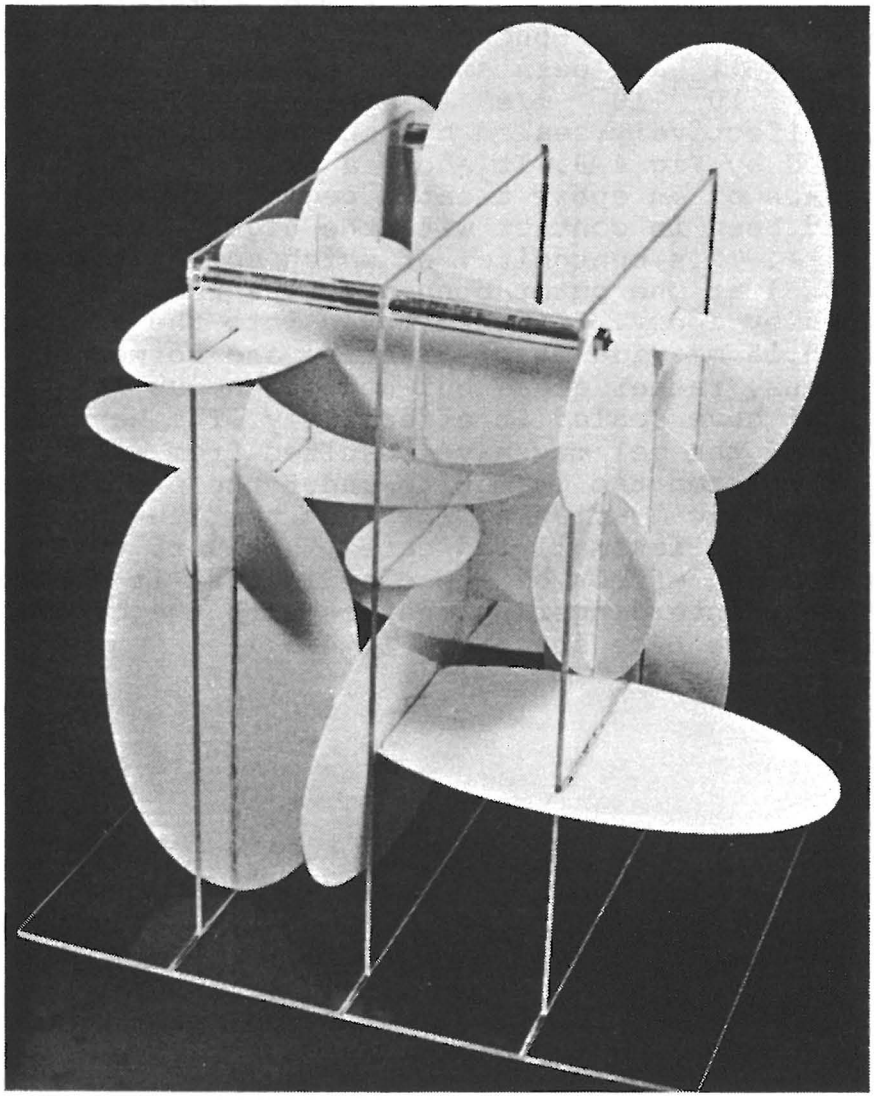

Figure 4-8. Photograph illustrating the fractue connectivity of the 3D model

4.2.4 Effect of clay penetration into fractures and pores in the rock

Laboratory tests as well as the Buffer Mass Test and the Borehole and Shaft plugging tests have shown that Na bentonite penetrates fractures which are wider than about 0.1 mm. The clay penetration depth is very small in such narrow fractures and the rate of migration retards rapidly, while fractures which are wider than a few tenths of a millimeter get filled with a rather dense clay gel to a depth of several centimeters in a year. A number of steep and subhorizontal natural fractures including the upper pegmatite zone had their apertures widened by the blasting so that they effectively let water through in the early part of the test. This was particularly obvious for the pegmatite where crystals could easily be removed from the loose matrix, the depth of the most severe disintegration probably being only a few centimeters. The estimated hydraulic conductivity of this disturbed zone may well have been similar to that of sandy silt, i.e. 10^{-4}-10^{-5} m/s. It appeared to have been rather effectively sealed by penetrating clay as evidenced by Fig 4-9. It shows a thin section micrograph of an epoxy-treated pegmatite sample that had been in contact with the highly compacted bentonite. This bentonite, of which some traces are seen (HCB) at the outer boundary, was removed and replaced by epoxy. Clay had moved into the approximately 0.15 mm wide major fracture and formed a continuous, rather dense but heterogeneous gel (B) that must have sealed it effectively. The heterogeneity of the gel may have resulted from water that percolated the pegmatite under the prevailing high hydraulic gradients. The fact that the penetration depth is small indicates, however, that the major sealing effect of the clay is that it creates a perfect, interfingering contact with the crystal matrix of the type shown in Fig 4-5.

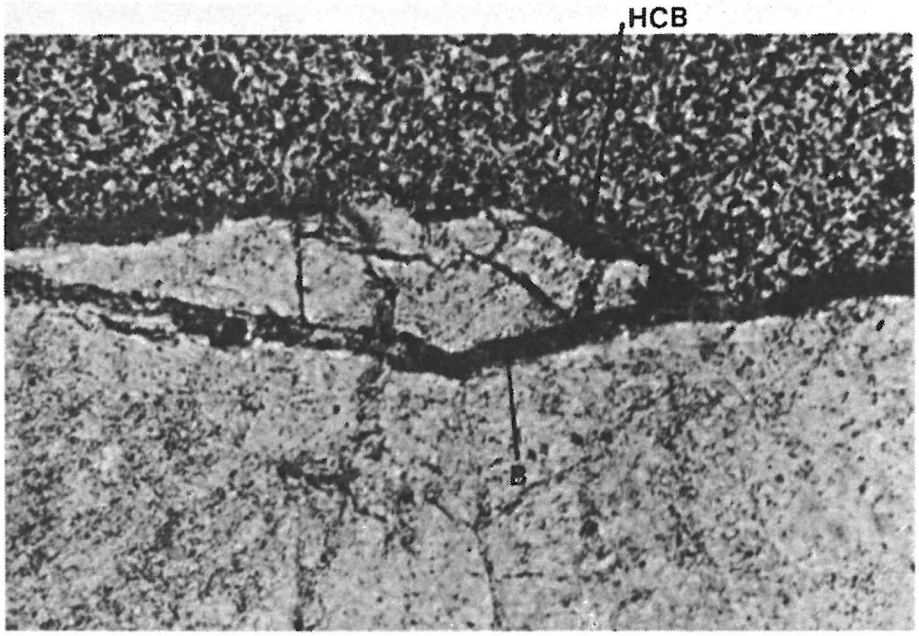

Figure 4-9. Micrograph of 30 µm thin section of epoxy-embedded pegmatite sample. The light-grey parts are quartz crystals while the speckled upper part is the epoxy. The black fillings are clay. Polarized light, 40x magnification. Photo by Mikael Erlström, SGAB, Lund

4.3 FURTHER IMPROVEMENT OF PLUG FUNCTION

4.3.1 Additional sealing effects

The experience from the Shaft Plugging Test offers a natural way of improving the sealing power of a plug of the presently investigated type. Thus, particularly if the tunnel is excavated by full-face drilling technique an efficient additional sealing effect would be obtained by cutting a slot around the perimeter and filling it with blocks of highly compacted bentonite. This would cut off fractures that are subparallel to the tunnel axis and that may tend to be expanded in a highly anisotropic primary stress field (Fig 4-10). Clay injection can be made radially from the slots as shown by the same figure. The function of the slots and the groutings is to truncate shallow, axially oriented fractures in the rock and thereby make the water flow through less permeable and more tortuous passages deeper in the rock.

The individual steps in the construction of such a plug would be analoguous to those described in Fig 1-3. Thus, a general procedure would be as shown in Fig 4-11.

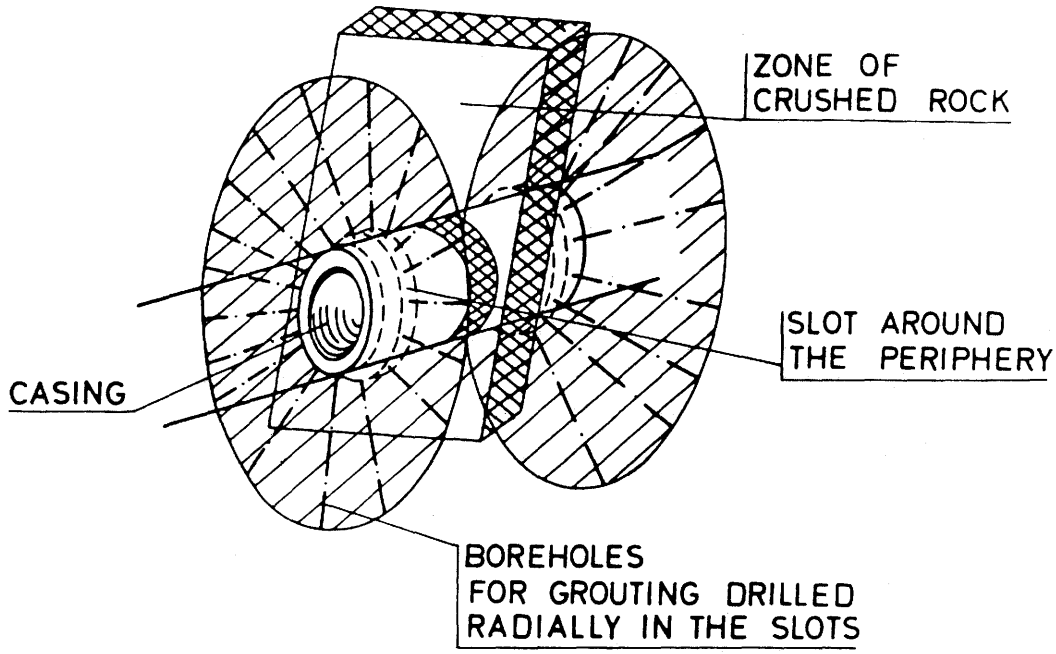

Figure 4-10. Schematic picture of casing equipped with bentonite plugs in slots at the ends to prevent water inflow from strongly water-bearing rock zone. Pre-grouting in spoke-type distributed boreholes extending from the slots

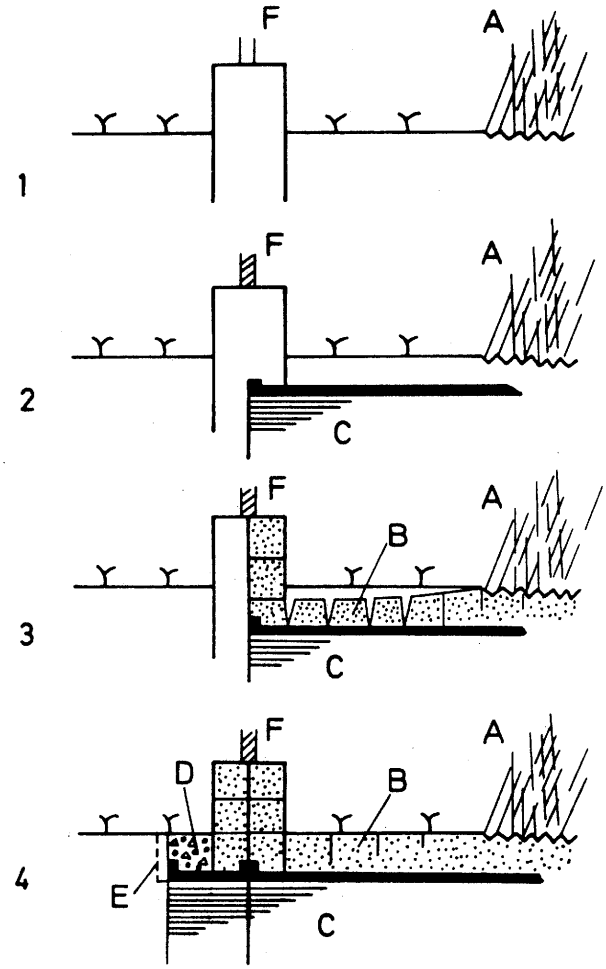

Procedure:

1 Slot is cut and holes drilled for grouting

2 Grouting is made and casing installed

3 Bentonite blocks, fragments and powder are applied between casing and rock (rapid swelling at the water-bearing zone)

4 Extension of casing, completion of slot-filling and casting of concrete support

Figure 4-11. Axial section of tunnel illustration possible arrangements and procedures in plugging tunnels so that passage-through is allowed for. A) Pervious rock-zone, B) Bentonite blocks, C) Steel casing, D) Concrete, E) Temporary steel form, F) Boreholes for grouting

4.3.2 Grouting of selected fractures

The conclusion in Chapter 3.2.2.3 that the major part of the leakage in the latest stage of the test took place through the steeply oriented sets of fractures in the tunnel floor suggests that a significant reduction in leakage would be obtained if these fractures were sealed. This hypothesis was tested after terminating the high-pressure test sequence but immediately before the casing was cut open for the sampling.

The sealing was made by applying a simple version of a grouting technique, "dynamic injection", that has been developed within the SKB research program (12). The grouting was made with Li-converted bentonite with a water content of about 500 %, the location of the boreholes and intended spread of grout being illustrated in Fig 4-12.

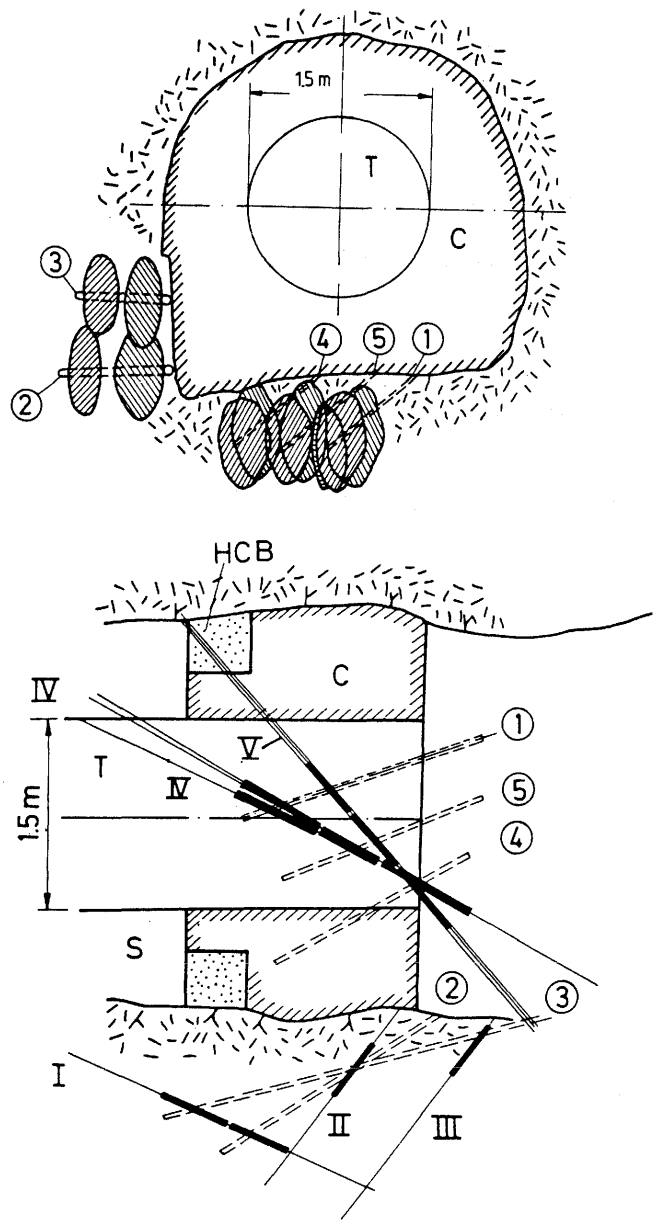

Figure 4-12. Schematic picture of sealing of major rock fractures I-V. Holes 1-5 were drilled for grouting, the thick black zones indicating the expected spread of the injected grout

After grouting, the water pressure was increased stepwise from 250 kPa, which had been maintained during the treatment, to 3 MPa and the leakage measured and compared to what it was just before the grouting. It was thereby observed that the leakage was reduced by more than 50 % at pressures lower than 2 MPa, while the sealing effect was lower at higher pressures. If we consider that the leakage was approximately 30-40 l/h at 0.75-1.25 MPa pressure early in the major test (cf. Fig 3-4) and that this flow dropped to about 20 l/h at 1 MPa pressure just before the grouting, we see that the net leakage of about 7 l/h after the grouting implies that this treatment had been successful. A major conclusion from the entire field study is therefore that if suitable techniques can be developed to identify and effectively seal discrete, water-bearing fractures in the rock adjacent to dense Na bentonite plugs, their sealing function can be extended to cover a large rock volume. Such development would be a natural goal for the planned third phase of the Stripa project.

5 ACKNOWLEDGEMENTS

The authors like to express their sincere gratitude to the construction company Gustafsson & Ericsson, Storå, for the excellent quality of the plug construction and, above all, for the great flexibility in conducting the work so that test activities could be made intermittently.

Also, deep-felt thanks are extended to Jeanette Stenelo who made the typing and to Birgitta Hellström who was responsible for the drawings.

6 REFERENCES

1. Pusch, R., Börgesson, L. & Ramqvist, G., 1986. Final Report of the Borehole, Shaft and Tunnel Sealing Test - Volume II: Shaft Plugging. Stripa Project, in press

2. Pusch, R., Nilsson, J. & Ramqvist, G., 1985. Final Report of the Buffer Mass Test - Volume I: Scope, preparation, field work, and test arrangement. Stripa Project, Technical Report 85-11.

3. Pusch, R., Börgesson, L. & Ramqvist, G., 1986. Final Report of the Borehole, Shaft and Tunnel Sealing Test - Volume I: Borehole Plugging. Stripa Project, in press

4. Hagvall, B., 1982. Buffer Mass Test - Data Acquisition and Data Processing Systems. Stripa Project, Internal Report 82-02

5. Börgesson, L., 1982. Buffer Mass Test - Predictions of the Behavior of the Bentonite-based Buffer Materials. Stripa Project, Internal Report 82-08

6. Pusch, R., Börgesson, L. & Ramqvist, G., 1985. Final Report of the Buffer Mass Test - Volume II: Test Results. Stripa Project, Technical Report 85-12

7. Forslind, E. & Jacobsson, A., 1972. Water, a Comprehensive Treatise (Ed. Franks), Ch 4:173-248 Clay-Water Systems. Plenum, New York

8. Pusch, R., 1985. Final Report of the Buffer Mass Test - Volume III: Chemical and Physical Stability of the Buffer Materials. Stripa Project, Technical Report 85-12.

9. Pusch, R. & Karnland, O., 1986. Aspects of the Physical State of Smectite-adsorbed Water. SKB Technical Report, in press

10. Pusch, R. & Karlsson, R., 1967. Shear Strength Parameters and Microstructure Characteristics of a Quick Clay of Extremely High Water Content. Proc. Eur. Geot. Conf. Oslo

11. Pusch, R., 1985. A Multi-purpose Rock Fracture Model. Internal SGAB Report, IRAP 85502, March 3

12. Pusch, R., Erlström, M. & Börgesson, L., 1985. Sealing of Rock Fractures. A Survey of Potentially Useful Methods and Substances. SKB Technical Report 85-17

7 APPENDICES

Comment

Photographic copies of a set of major drawings prepared for the construction work are given here. The text has not been translated from Swedish since possible practical use in countries other than USA, Canada and Great Britain will probably require translation to the respective language.

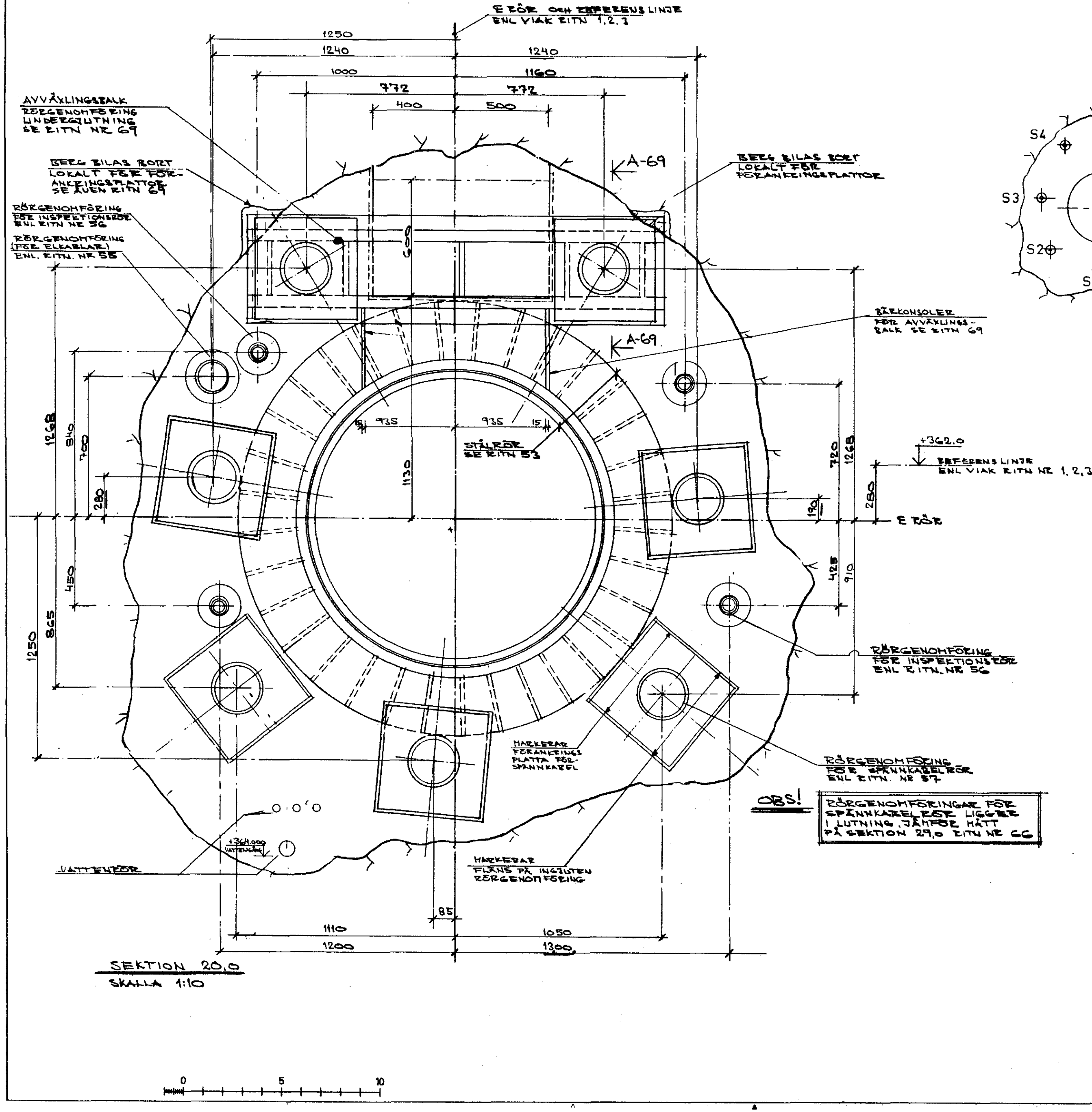

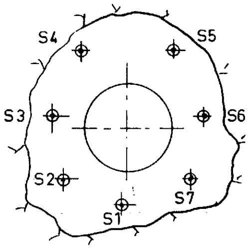

Fördelningslista		
Ritn. utsänd den		
GBE BYGG AB		
GÄVLE VARV		
STRIPA		
J&W LULEÅ		

FÖRESKRIFTER

SPÄNNKABLAR NR S1 - S7 AV FABRIKAT VSL (STABILATOR) TYP E 6-37-272 KN ELLER LIKVÄRDIG.

LITTERA S4 OCH S5 MED TEORETISK NETTO-LÄNGD = 9000 + 80 + 550 + 32 + 20 = 9682 EXKLUSIVE FÖRDELNINGSPLATTANS TJOCKLEK.

ÖVRIGA LITTERA S1-S3, S6, S7 MED NETTO-LÄNGD = 9000 + 20 + 20 = 9040 EXKLUSIVE FÖRDELNINGSPLATTANS TJOCKLEK.

UPPSPÄNNING: BETONGKONSTRUKTIONEN BÖR VATTENHÄRDA I MIN. 3 VECKOR FÖRE UPPSPÄNNING. KABLARNA FÖRSPÄNNES SUCCESIVT TILL TOTALT 7 x 4,45 MN PER STYCK I 10 STEG FÖRSLAGSVIS I ORDNING S1, S5, S4, S2, S7, S3, S6. SAMTIDIGT KONTROLLERAS SPÄNNING OCH SAMMANTRYCKNING AV STÅLRÖRET, SOM ANTAGES BLI 193 MPa RESP. 6,9 MM. OM DESSA VÄRDEN EJ UPPNÅS (P.G.A. ATT BETONGEN LASTAR AV MOT BERGVÄGGEN) SKALL KONSTRUKTÖREN UNDERRÄTTAS OM UPPMÄTTA VÄRDEN.

SLUTSTADIUM: DÅ VATTENTRYCKET MELLAN TUNNELPROPPARNA SENARE TILLKOPPLAS MED (3MPa) OCH BENTONITTRYCKET SUCCESIVT ÖKAR TILL (5 MPa) BERÄKNAS DEN TOTALA KRAFTEN PÅ PROPPARNA BLI 53,5 MN, VARVID STÅLRÖRET BERÄKNAS TA 14,3 MN OCH 7 ST KABLAR TOTALT 7 x 5,6 = 39,2 MN.

ÖVRIG ARMERING Ks 40, DÄR EJ ANNAT ANGES

BETONG: BTG K400 SÅ KALLAD MIKROBETONG MED MAX STENSTORLEK 8 MM OCH FLYTTILLSATS. EBJ KAN BISTÅ MED PROPORTIONERING OM ERFORDERLIGT.
BETONGGJUTNING SKALL SKE MED STÖRSTA OMSORG SÅ ATT ALLA RÖR, STOPPFLÄNSAR ETC. BLIR KRINGGJUTNA.
VATTENHÄRDNING SKALL UTFÖRAS SÅ ATT SPRICKBILDNING ELIMINERAS

UTRYMMESBEHOV FÖR DOMKRAFTER (FÖR SPÄNNKABLAR) PARALLELLT MED SPÄNNKABLARNA UTANFÖR FÖRANKRINGSPLATTORNA ∅700 x 2000.

APPENDIX 1

Arbetsritning	VZ	810430
Rev Ant Ändring/ändringsorder	Sign	Datum

KBS STRIPA PROJECT

J&W AB Jacobson & Widmark
Civil and Structural Engineering, Soil Mechanics

STRIPA PROJECT PHASE 2
TUNNELPLUGGNING
SEKTION 20,0
MÅTT

Skala 1:10 | Datum 1983-06-30 | Ritn nr 3054101-61
Handläggare H R

APPENDIX 2

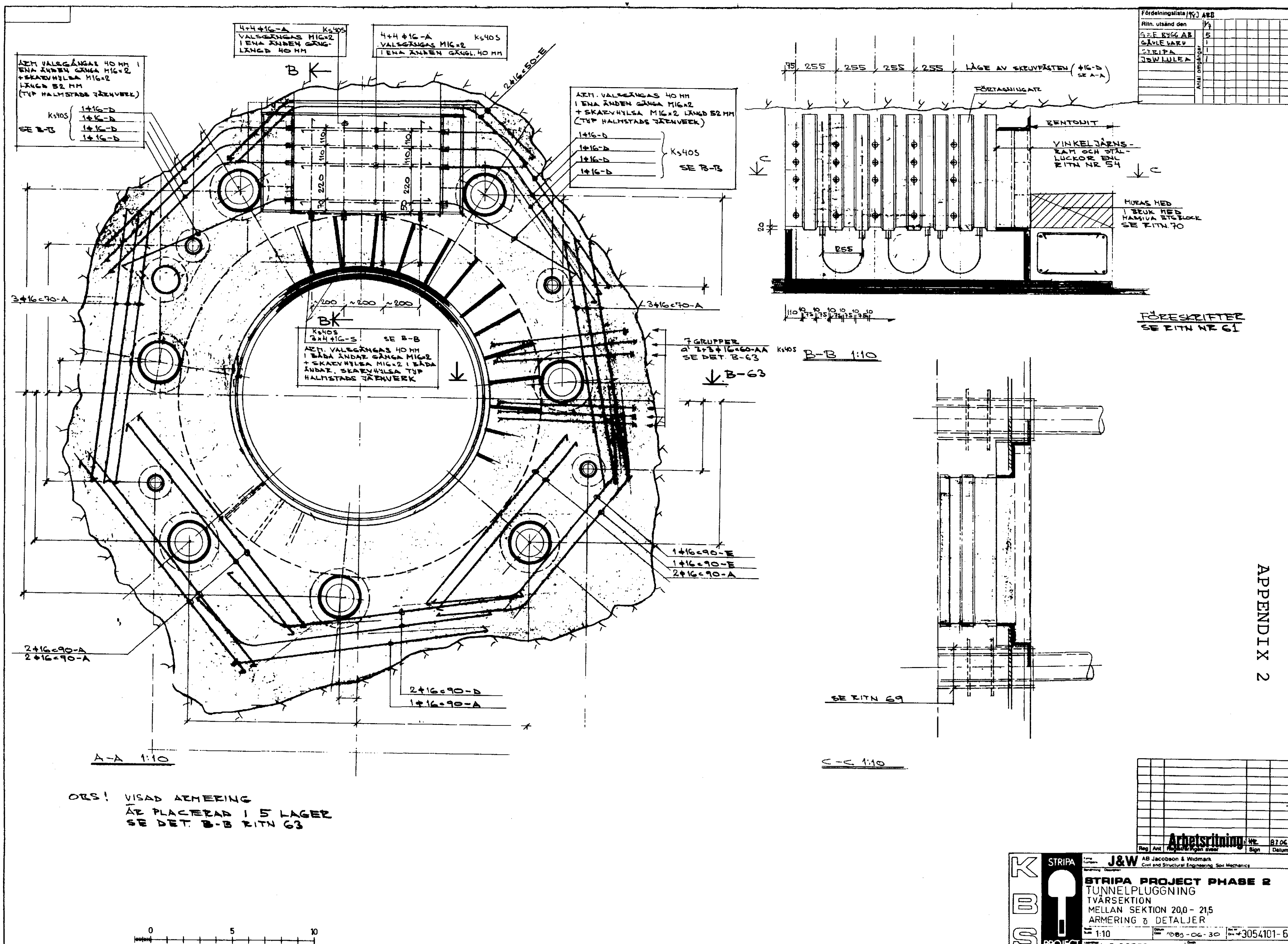

A-A 1:10
B-B 1:10
C-C 1:10
ARM. VALSGÄNGAS 40 MM I ENA ÄNDEN GÄNGA M16×2 + SKARVHYLSA M16×2 LÄNGD 52 MM (TYP HALMSTADS JÄRNVERK)
4+4 φ16-A Ks40S VALSGÄNGAS M16×2 I ENA ÄNDEN GÄNGLÄNGD 40 MM
1φ16-D
Ks40S
SE B-B
3φ16c70-A
2φ16c50-E
7 GRUPPER
SE DET. B-63
1φ16c90-E
2φ16c90-A
2φ16c90-D
1φ16c90-A
2φ16c90-A
LÄGE AV SKRUVFÄSTEN (φ16-D SE A-A)
FÖRTAGNINGAR
BENTONIT
VINKELJÄRNS-RAM OCH STÅL-LUCKOR ENL RITN NR 54
MURAS MED I BRUK MED HALVA BTG BLOCK SE RITN 70
FÖRESKRIFTER SE RITN NR 61
SE RITN 69
OBS! VISAD ARMERING ÄR PLACERAD I 5 LAGER SE DET. B-B RITN 63
255
Arbetsritning
J&W AB Jacobson & Widmark Civil and Structural Engineering Soil Mechanics
KBS
STRIPA PROJECT
STRIPA PROJECT PHASE 2
TUNNELPLUGGNING
TVÄRSEKTION
MELLAN SEKTION 20,0 – 21,5
ARMERING & DETALJER
1:10
H RYDBERG
3054101-64

Fördelningslista	1993	1/2
Riln. utsänd den		
G & E BYGG AB	Antal omgångar	5
GAULE HAPU		1
STRIPA		1
J & W LUND		1

FÖRESKRIFTER
SE RITN NR G1

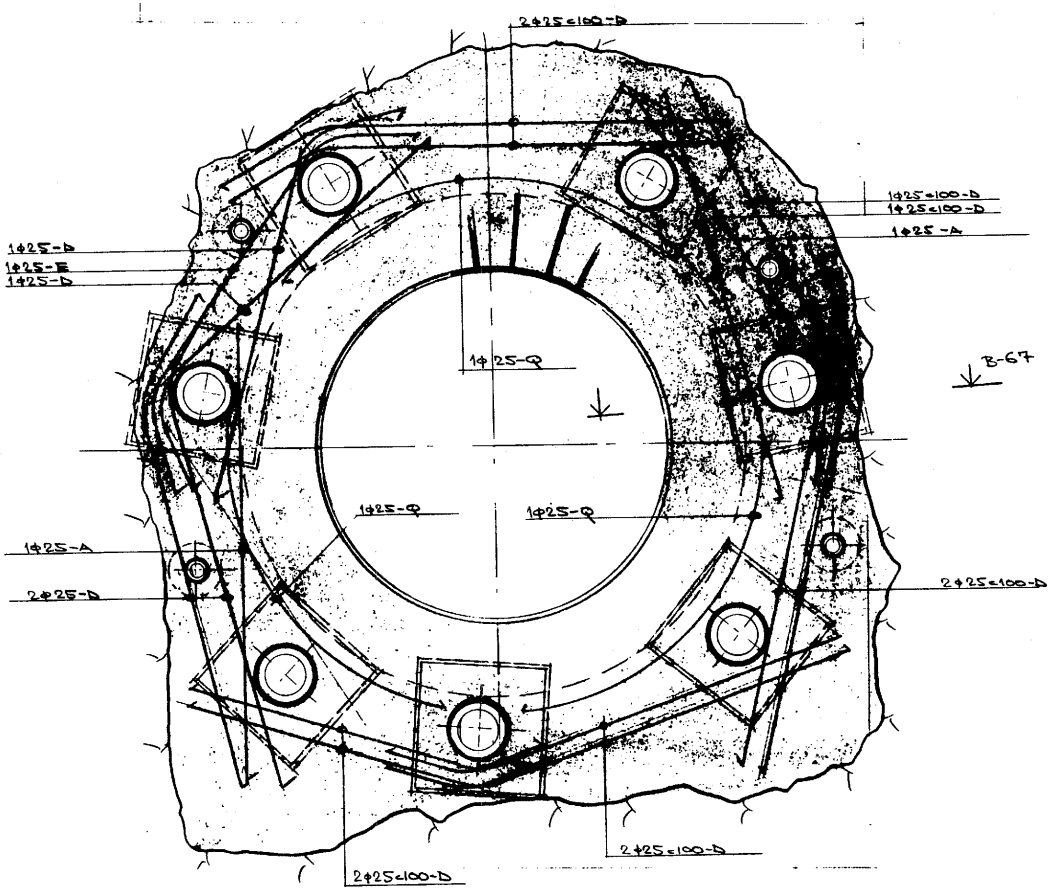

A-A 1:10
SEKTION 29.0
1:10

0 5 10

APPENDIX 3

Rev	Ant	Ändringar	Sign	Datum
		Arbetsritning	NE	910630

K B S | STRIPA PROJECT

J&W AB Jacobson & Widmark
Civil and Structural Engineering Soil Mechanics

STRIPA PROJECT PHASE 2
TUNNELPLUGGNING
TVÄRSEKTION 29.0
ARMERING

Skala 1:10 | Datum 1993-06-30 | Ritn.nr 3054101-68
Granskad HR | Godkänd

Fördelningslista	ARB	
Ritn. utsänd den	13/6	
GÄVLE VARV	6	
J&W LULEÅ	1	
GZE BYGG AB		2
STRIPA	1	

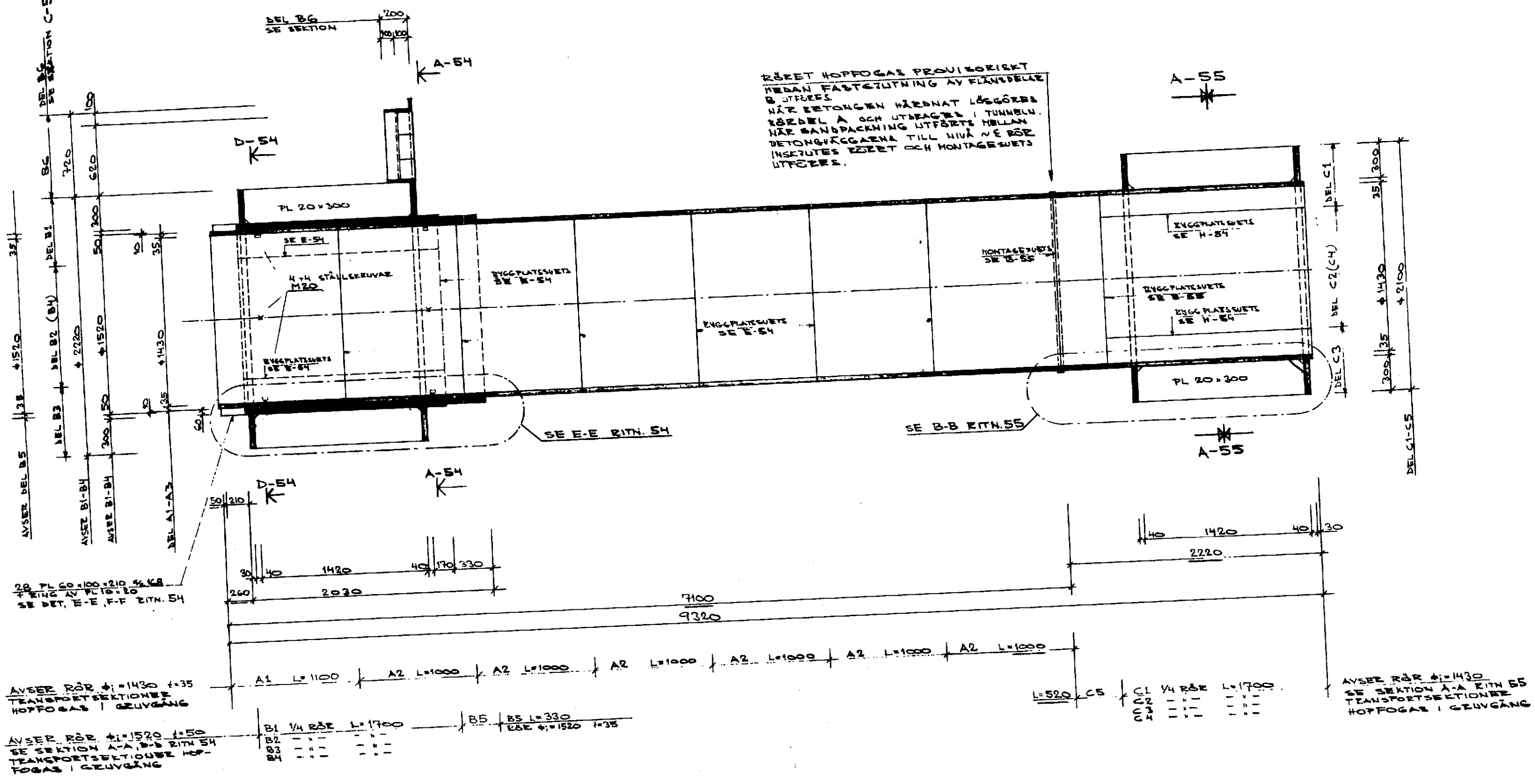

FÖRESKRIFTER

MATERIAL SS2132
SKÄRKLASS SK1
SVETSKLASS Sv1
TOLERANSER: SE BYGGNADSBESKRIVNING

SVETS MED BETECKNINGEN TÄT SKALL DESSUTOM VARA TÄTSVETSAR (VARA VATTENTÄTA VID 8 MPa (80 kp/cm²) ÖVERTRYCK)

HÄNVISNINGAR

DETALJER RITN NR -54, -55

APPENDIX 4

TRANSPORTVIKTER		
DEL	VIKT kg/ST	ANTAL
DEL A1	1423 kg/ST	1
A2	1288	6
B1	1689	1
B2	1689	1
B3	1689	1
B4	1689	1
B5	451	1
BG	350	1
C1	1382	1
C2	1382	1
C3	1382	1
C4	1382	1
C5	554	1

A Arbetsritning 830613
Reg | Ant | Registreringen avser | Sign | Datum

KBS STRIPA PROJECT

J&W AB Jacobson & Widmark Civil and Structural Engineering, Soil Mechanics.

STRIPA PROJECT PHASE 2
TUNNELPUGGNING
STÅLRÖR LÅNGDSEKTION

Skala 1:20 | Datum 1983-04-26 | Ritn nr 3054101-53
Handläggare H.RYDBERG | A